REPUBLIQUE ALGERIENNE DEMOCRATIQUE ET POPULAIRE
MINISTERE DE L'ENSEIGNEMENT SUPERIEUR ET DE LA RECHERCHE SCIENTIFIQUE

UNIVERSITE ABOU-BEKR BELKAID - TLEMCEN

DISSERTATION

Submitted to:

THE FACULTY OF SCIENCE – DEPARTMENT OF CHEMISTRY

In partial fulfillment of the requirements for:

MASTER'S DEGREE IN

Macromolecular Chemistry

by:

Ms OULD MEZIANE Chahla Fatima Zohra

Ms GOURMALA Feryel Nesrine

On the subject of

Advanced functional bio-based hydrogels: preparation, characterization and applications

---

Defended publicly on 25 June 2025, at Tlemcen, before an academic jury composed of:

Mr BOURAS Brahim	Professor	University of Tlemcen	President
Mr HOCINE Tayeb	Lecturer A	University of Tlemcen	Supervisor
Ms DJAMAI Wissam	Lecturer B	University of Tlemcen	Examiner

Academic year : 2024 ~ 2025

Dedication

***F**irst and foremost, I dedicate this work to my beloved parents. Your prayers throughout every step of my journey have been my greatest strength. You have surrounded me with love that knows no limits. Every success I achieve is built on the sacrifices you've made and the values you instilled in me. I owe you everything, and no words will ever fully express how deeply grateful I am. I love you more than life itself.*

***T**o my dear brothers, Reda and Oussama, thank you for your support and for always being there in your own special ways. Life gave me the best brothers, and for that, I am truly blessed.*

***T**o my wonderful sister-in-law, Wafaa the sister from another mother, thank you for your warmth, your kindness, and always being there for me .*

***T**o my precious nephew, Iyed your smile brightens even the darkest days. You are the joy of my life. I'm so lucky to be your aunt.*

***T**o my fiancé your love, passion, and unwavering support have been a cornerstone of my journey. Thank you for standing beside me with patience and faith, and for being my calm in every storm. To his family, thank you for encouraging me every step of the way.*

***T**o my incredible partner Feryel, not just a brilliant collaborator but also my soul sister and closest friend. Your energy and compassion transformed this experience into something truly unforgettable. Thank you for being exactly who you are.*

***T**o my soul sisters Souaad, my canım sağ kolum, your quiet strength and unconditional support have made you my safe place and most trusted confidante; Imene, my suç ortağım, you bring laughter to my days and comfort to my heart; and Amira, the keeper of our memories and a piece of my soul, your friendship is one of the greatest treasures of my life. Thank you all for being sisters in spirit.*

***T**o my besties, Sarra and Chaimaa. Your laughter and unwavering presence have brought me comfort in difficult times and shared joy in moments of celebration. Life is sweeter with you both in it.*

***T**o all my beloved family you are the roots from which I grow, and your presence in my life is a blessing I never take for granted. And to every person who has touched my life in ways big or small this achievement is also yours.*

Chahla Fatima Zohra

Dedication

***T**o those whose presence has been the invisible ink of these pages.*

***T**o my father, in your silence, I found strength. Your gaze and your simple gestures have been my compass. Thank you for your example and your quiet love. I love you deeply. To my mother, you carried me well beyond nine months. Your love guided, supported and encouraged me. This memoir is the fruit of your courage. I owe you everything.*

***T**o my twin sister, Inès, we grew up together, we're moving forward together. Two memories, one heart. I'm proud of you and grateful to have you by my side.*

***T**o my big brother, Omar, you inspire me and protect me without saying a word. Thank you for your kind eyes and quiet strength. I love you very much.*

***T**o my little brother, Rassim, you're growing up fast, but you'll always be my little brother. I'm proud of your heart and your sense of humor. I'll always be there for you.*

***T**o my sister-in-law, Hanane, thank you for your kindness and the gentle warmth you've brought into our lives.*

***T**o Salim, the little star that will soon light up our world.*

***T**o my grandfather, Rachid Boukli Hacene, your absence is a deep void, but your memory stays with me. This work is dedicated to you with all my love and eternal gratitude.*

***T**o my grandmothers, Mami and Mima, thank you for your discreet love and the quiet strength you passed on to me. You are my roots.*

***T**o my uncle Rafik Boukli Hacene, thank you for your wise and constant support, always present in your discretion.*

***T**o my partner and dear friend, Ould Meziane Chahla, your presence, support and patience have marked every step. This work bears your imprint. Thank you for everything.*

***T**o Chaïmaa, Sarra, Loubna, Fadia and Hidayet, Thank you for your words, your smiles, and your friendship. I carry you in my heart.*

***T**o Kader and Waga, thank you for everything that goes beyond theater: your humanity, your trust, your light.*

***T**o ChemClub, my second family, thank you for the joy, energy and strength you have given me. You have meant more than words can say.*

***T**o all those who have supported me from near and far - family, friends, teachers - thank you from the bottom of my heart. Thank you from the bottom of my heart. This memoir contains a part of each and every one of you.*

Feryel Nesrine

Acknowledgments

First and foremost, we humbly offer our deepest gratitude to the Almighty God, whose grace and mercy provided us with the strength, patience, and resilience to overcome every obstacle and bring this work to fruition. Without His divine guidance, this achievement would not have been possible.

This research was carried out within the Laboratory of Organic Electrolytes and Polyelectrolyte's Applications (LAEPO) at ABOU BAKR BELKAID University of TLEMCEN. We are profoundly thankful for the opportunity to work in such an enriching and stimulating academic environment, which played a vital role in shaping the success of this dissertation.

We extend our sincere thanks to Professor BOURAS Brahim, Director of LAEPO, for his leadership and generosity. His acceptance to serve as president of our thesis jury is a great honor, and we are profoundly grateful for his valuable presence and support.

We are equally grateful to Dr. DJAMAI Wissam, Lecturer B at the University of TLEMCEN, who kindly accepted to be our examiner. Her presence on our jury added tremendous value to our work.

Our heartfelt appreciation goes to our supervisor, Dr. HOCINE Tayeb, Lecturer A at the University of TLEMCEN. From the initial suggestion of our topic to the final stages of this dissertation, his unwavering support, intellectual guidance, and kind mentorship were indispensable. His dedication, availability, and belief in our potential greatly inspired and empowered us throughout this journey.

We would also like to express sincere thanks to all the teachers of macromolecular chemistry, whose courses laid the foundation of our understanding in this field. Their clarity, dedication, and passion for teaching have had a lasting impact on our academic path and were instrumental in the development of this work.

We are equally thankful to all members of the LAEPO staff. Their cooperation, professionalism, and technical assistance created a welcoming and supportive environment that allowed us to move forward with confidence and clarity.

A special and warm thank you goes to Professor SELLES Chaouki, whose continuous encouragement and generosity of spirit meant so much to us. His presence and support will always be remembered with deep respect and appreciation.

We are also deeply thankful to Mrs. MOKHTARI Nassima , Dean of the Faculty of SNV, for her unfailing kindness, steady support, and constant availability whenever assistance was needed.

Our sincere gratitude goes to Mrs. S. BOUAYAD AGHA, engineer at the LAEPO laboratory, whose patience, kindness, and technical guidance were invaluable. Her consistent willingness to assist and support us made a real difference in the daily progress of our research.

We also wish to express our appreciation to Mrs. KAHOUADJI Chaimaa, PhD researcher, for her thoughtful advice and generous guidance. We are equally thankful to Mr. BELAID A and Mr. BOURAS O, PhD researchers at the University of TLEMCEN, for their shared knowledge.

Finally, and with all our hearts, we would like to express our warmest thanks and affection to our beloved classmates and cherished colleagues. Your camaraderie, encouragement, and shared struggles made this path so much more meaningful and joyful. The memories we created, the support we exchanged, and the laughter we shared have turned this academic journey into an unforgettable adventure. You have truly become more than colleagues, some of you lifelong friends. We are forever grateful for the bond we built and the way you helped transform this experience into something extraordinary.

List of Content

Part 2: Study of bio hydrogels

List of Figures

Chapter I Literature Review

Chapter II Materials and Methods

Chapter III Results and Discussion

List of Tables

Chapter I Literature Review

Chapter II Materials and Methods

Chapter III Results and Discussion

List of Symbols and Abbreviations

PVA: Polyvinyl Alcohol

St: Starch

SA: Sodium Alginate

IPN: Interpenetrating Polymer Network

PEG: Polyethylene Glycol

PAA: Poly(acrylic acid)

PNIPAAm: Poly(N-isopropylacrylamide)

PHEMA: Poly(2-hydroxyethyl methacrylate)

E401: Sodium Alginate (E-number).Food additive

PVAc: Polyvinyl Acetate

VC: Vitamin C, known as ascorbic acid

ROS: Reactive Oxygen Species

RNS: Reactive Nitrogen Species

E300: Ascorbic Acid (Vitamin C, E-number)

SVCT1: Sodium-dependent Vitamin C Transporter 1, Transports vitamin C across intestinal and kidney membranes

SVCT2: Sodium-dependent Vitamin C Transporter 2, Transports vitamin C into organs (brain, placenta)

API: Active Pharmaceutical Ingredient

GFS: Simulated Gastric Fluid

IFS: Simulated Intestinal Fluid

RT: Room Temperature

F/T: freezing thaw

Sr: Swelling rate

LE: Loading effeciency

(PVA/SA)Ca3, (PVA/SA)Ca1: Polyvinyl Alcohol / Sodium Alginate crosslinked with 3% and 1% $CaCl_2$

(St/SA)Ca3, (St/SA)Ca1: Starch / Sodium Alginate crosslinked with 3% and 1% $CaCl_2$

F(St/SA)Ca1: Film of Starch / Sodium Alginate crosslinked with 1% $CaCl_2$

F/T (PVA/SA)Ca3, F/T (St/SA)Ca3: Freeze–Thaw Treated Polyvinyl Alcohol / Sodium Alginate and Freeze–Thaw Treated Starch / Sodium Alginate crosslinked with 3% $CaCl_2$

PVA Load: biohydrogels the (PVA/SA)Ca3 loaded with VC

St Load: biohydrogels the (St/SA)Ca1 loaded with VC

PVAMR, PVAXMR: biohydrogels the (PVA/SA)Ca3 encapsulating VC prepared with Reflux and without Reflux setup

StMR, StXMR: biohydrogels the (St/SA)Ca1 encapsulating VC prepared with Reflux and without Reflux setup

INTRODUCTION

Introduction

In recent years, bio-based hydrogels have emerged as an important category of functional materials due to their wide range of applications, particularly in the biomedical and pharmaceutical fields. Thanks to their high-water content, biocompatibility, biodegradability, and responsiveness to environmental stimuli such as pH, these flexible polymer networks offer promising potential in the development of controlled drug delivery systems [1].

However, while many natural and synthetic hydrogels have shown promise, they still face several limitations. Conventional hydrogels often lack sufficient mechanical strength, stability under physiological conditions, or the ability to deliver active compounds in a targeted and sustained manner. Moreover, their limited antioxidant capacity may reduce their protective effect on sensitive bioactive molecules during storage or gastrointestinal transit. These shortcomings highlight the need to develop smarter, more responsive hydrogel systems that can adapt to their environment while ensuring efficient therapeutic performance.

Within this context, natural and semi-synthetic polymers offer a valuable platform for innovation. Materials such as starch, poly(vinyl alcohol) (PVA), and sodium alginate (SA) are renewable, non-toxic, and capable of forming hydrophilic polymer networks suitable for biomedical use. When combined strategically and reinforced through ionic crosslinking, these polymers can form biohydrogels with enhanced functional characteristics.

The prepared hydrogels were characterized using various analytical techniques, including UV-visible spectroscopy (for absorbance measurements and calibration curves), FTIR (to identify functional groups and interactions), XRD (to examine crystallinity), and XRF (to determine elemental composition) [2].

The main objective of this study is to develop and evaluate smart, pH-responsive biohydrogels based on starch/SA and PVA/SA polymer networks. These hydrogels are designed to improve the stability and controlled release of antioxidant compounds, with potential application in oral drug delivery systems. By addressing the limitations of traditional hydrogels, this research aims to contribute to the development of multifunctional biomaterials that are both effective and environmentally sustainable [3].

The current work is organized into three chapters:

- Chapter 1 presents a review of the literature on hydrogels, certain biopolymers (PVA, starch, sodium alginate), ascorbic acid, and drug delivery systems.
- Chapter 2 details the materials, experimental procedures, and characterization techniques used in this study.
- Chapter 3 presents the results obtained, organized into three sections: hydrogel preparation, physicochemical and antioxidant analysis, and evaluation of drug delivery potential

References

[1] N. H. Thang, T. B. Chien, et D. X. Cuong, « Polymer-Based Hydrogels Applied in Drug Delivery: An Overview », *Gels*, vol. 9, nº 7, p. 523, 2023, doi: 10.3390/gels9070523.

[2] B. R. Denzer, R. J. Kulchar, R. B. Huang, et J. Patterson, « Advanced Methods for the Characterization of Supramolecular Hydrogels », *Gels*, vol. 7, nº 4, p. 158, 2021, doi: 10.3390/gels7040158.

[3] M. Kędzierska *et al.*, « Enhanced Hydrogel Materials: Incorporating Vitamin C and Plant Extracts for Biomedical Applications », *Molecules*, vol. 29, nº 11, p. 2633, 2024, doi: 10.3390/molecules29112633.

LITERATURE REVIEW

I.1 Hydrogels

I.1.1 Definition of Hydrogels

Hydrogels constitute three-dimensional hydrophilic polymeric networks characterized by their exceptional capacity for aqueous fluid absorption and retention, simultaneously preserving structural coherence through their crosslinked molecular architecture [1].

These exceptional materials may be synthesized from naturally derived polymeric substances (including alginate, chitosan, starch, or collagen), artificially produced polymers (such as polyvinyl alcohol (PVA), polyacrylamide, or polyethylene glycol), or composite formulations, thereby providing tunable mechanical, chemical, and physical properties contingent upon their compositional structure and crosslinking techniques [2].

Hydrogels are classified as either physical (reversible) gels generated through non-covalent interactions, or chemical (irreversible) gels established via covalent bonding mechanisms. The reticulated architecture of hydrogels is characterized by crosslinking junctions formed through robust chemical bonds (such as covalent linkages) or persistent/transient physical associations (including hydrogen bonding interactions) [3].

Their distinctive characteristics, encompassing elevated aqueous content, biocompatibility, and sensitivity to environmental parameters (pH, temperature, electromagnetic radiation, electric fields, or specific biomolecules), have facilitated extensive utilization across multifarious disciplines [2,3].

These applications span biomedical sectors (wound management, controlled drug release systems, tissue regeneration scaffolds), environmental remediation (water treatment, contaminant adsorption), agricultural uses (soil enhancement, controlled nutrient delivery), and industrial implementations (biosensors, soft actuators, food technology) [2,3].

I.1.2 Properties of Hydrogels

a) **Water retention capacity:** The capacity of hydrogels to absorb and maintain substantial quantities of aqueous solution within their three-dimensional networked architecture without undergoing dissolution. This characteristic is quantified through swelling ratio or equilibrium hydration content and is governed

by crosslinking density, polymeric composition, and environmental parameters (pH, temperature, ionic concentration) [1].

b) **Crosslinking:** Crosslinking density directly influences mechanical properties, diffusion characteristics, degradation kinetics, and aqueous retention capacity of the hydrogel matrix [3].

c) **Biocompatibility:** The capacity of hydrogels to perform with an appropriate host response in specific applications, including non-toxicity, non-immunogenicity, and integration with surrounding tissues, and compatibility with biological systems [1,4].

d) **Biodegradability:** is the ability of a substance to break down through natural biological processes into simpler, non-toxic components [4].

I.1.3 Classification of Polymer-Based Hydrogels by Physical Appearance

Polymer-based hydrogels can be systematically classified according to their morphological characteristics and structural architecture. The principal classifications encompass:

a) **Matrix (Bulk) Hydrogels:** These represent three-dimensional hydrogel systems characterized by homogeneous internal architecture. Formation occurs through monomer polymerization or pre-polymer cross-linking processes, resulting in hydrophilic networks capable of substantial aqueous swelling [5].

b) **Film (Thin-Film) Hydrogels:** These constitute two-dimensional hydrogel architectures exhibiting planar, sheet-like configurations. The structures demonstrate controlled thickness parameters and customizable mechanical characteristics, typically manifesting as thin, flexible, and conformable materials [5].

c) **Microsphere Hydrogels:** These hydrogel systems comprise discrete spherical entities microspheres. Particle dimensions range from several micrometers to hundreds of micrometers in diameter. The internal architecture exhibits porosity characteristics with elevated surface area-to-volume ratios attributed to their spherical geometry [5].

d) **Nanoparticle-Embedded Hydrogels:** These represent composite hydrogel systems incorporating nanoparticulate components (both organic and inorganic) within their network structure [5].

e) **Hydrogel Beads:** These consist of discrete spherical particles synthesized through suspension polymerization or emulsion polymerization techniques, resulting in uniform bead morphologies with controlled size distributions [5].

I.1.4 Categories of Hydrogels

I.1.4.1 Based on the physical structure of the network

a) **Amorphous:** These hydrogel systems exhibit polymer chains distributed in random, non-ordered configurations without crystalline structural regions [6].
b) **Crystalline:** These hydrogel networks demonstrate highly organized architectures characterized by uniform intermolecular interactions [6].
c) **Semi-crystalline:** These hydrogels incorporate both non-ordered amorphous phases and crystalline domains wherein polymer chains exhibit regular, repeating arrangement patterns [6].

I.1.4.2 Based on the nature of the polymer

a) **Homopolymeric hydrogels:** These networks originate from single monomer species [5,6].
b) **Copolymeric hydrogels:** These systems are formed from two or more distinct monomer varieties units [5,6].
c) **Interpenetrating Polymer Network (IPN) Hydrogels**: These structures comprise two or more interlaced polymer networks that undergo independent cross-linking without covalent interconnection [5,6].

I.1.5 Types of Hydrogels

I.1.5.1 Based on composition

a) **Natural hydrogels:** Polymer networks derived from naturally occurring biomacromolecules. These include polysaccharide-based hydrogels (alginate, chitosan, hyaluronic acid, cellulose derivatives), protein-based hydrogels (collagen, gelatin, silk fibroin, elastin), and DNA-based hydrogels [2].
b) **Synthetic hydrogels:** Polymer networks created from chemically synthesized monomers or polymers through controlled polymerization and crosslinking reactions. Common examples include poly (ethylene glycol) (PEG), poly(vinyl

alcohol) (PVA), poly(acrylic acid) (PAA), poly(N-isopropylacrylamide) (PNIPAAm), and poly(hydroxyethyl methacrylate) (PHEMA) [2].

c) **Hybrid hydrogels:** Multi-component polymer architectures that integrate natural and synthetic polymeric components to exploit the beneficial characteristics of both systems. These can be fabricated through diverse methodologies including interpenetrating networks, semi-interpenetrating networks, or direct chemical conjugation between natural and synthetic constituents[2].

I.1.5.2 Based on crosslinking method

a) **Physically cross-linked hydrogels:**

Three-dimensional networks formed through non-covalent interactions between polymer chains. These interactions encompass:

- **Ionic interactions:** Electrostatic attractions between oppositely charged [3].
- **Hydrogen bonding:** Hydrogen bond establishment between polymer chains [3].
- **Crystallization (Freezing–thawing):** The freezing–thawing methodology involves subjecting hydrogel precursors to freezing and thawing cycles. During the freezing phase, ice crystal formation occurs, , the polymers come closer and form crosslinks. Upon thawing, polymers approach and establish cross-links, stabilizing the hydrogel architecture [3].
- **Protein interactions:** Secondary structures like coiled-coils or β-sheets that form physical junctions [3].
- **Hydrophobic interactions:** Hydrophobic interactions constitute non-covalent forces occurring when non-polar molecular entities or groups aggregate in aqueous environments to minimize water exposure [3].

b) **Chemically cross-linked hydrogels**

Networks established through covalent bonding between polymer chains, generating permanent junction sites. Representative methodologies include:

- **Covalent crosslinking using bifunctional/monofunctional agents:** Polymers can undergo covalent cross-linking utilizing small molecular agents or through functional group modification for in situ hydrogel formation [3].
- **Photopolymerization: :** Light-activated formation of covalent bonds, often using photo initiators [7].

- **Enzymatic crosslinking:** Enzyme-catalyzed formation of covalent bonds [3].
- **Condensation reactions:** Formation of covalent bonds with elimination of small molecules [8].
- **Radiation crosslinking:** Use of high-energy radiation to generate free radicals that form crosslinks [3].

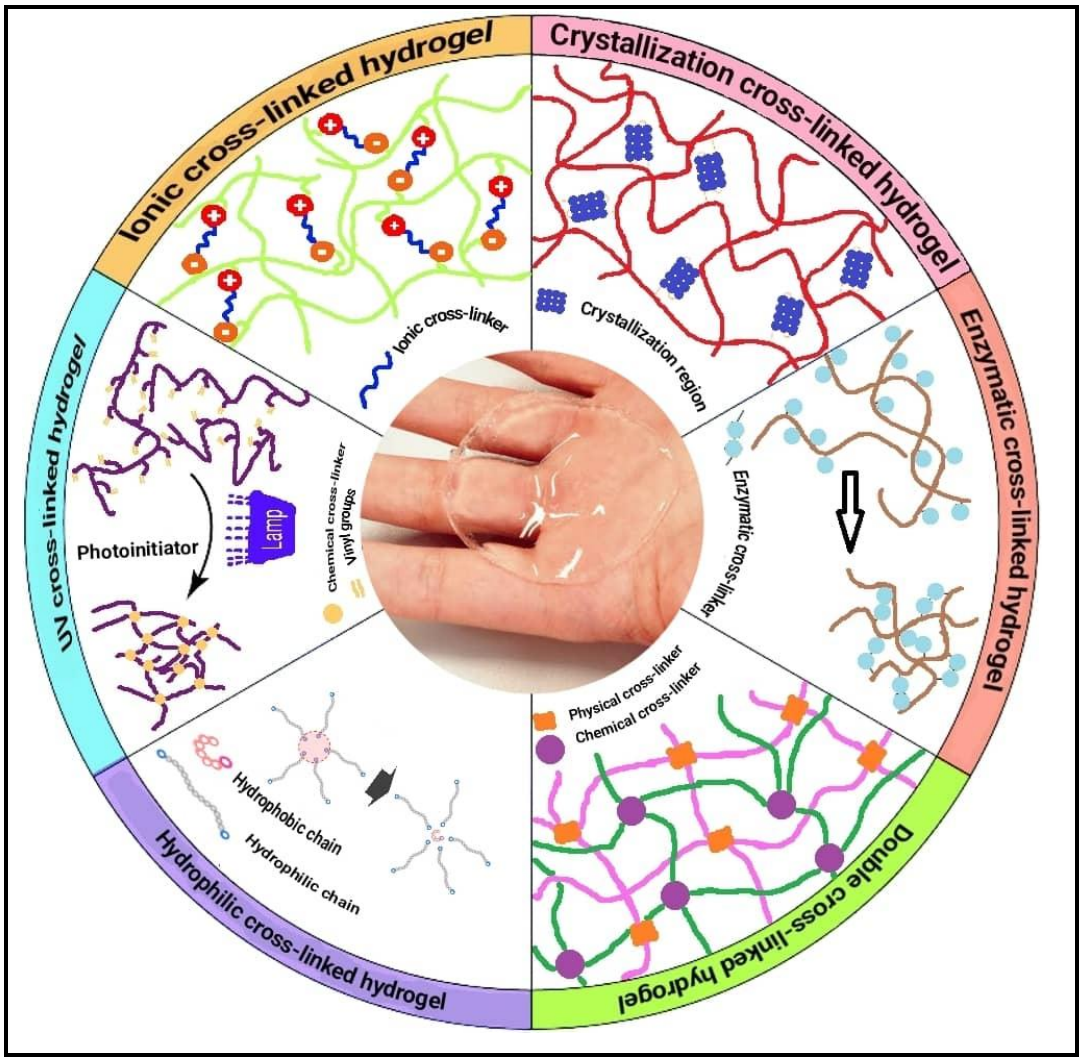

Figure I.1.5.1: Various types of crosslinked hydrogel

I.1.6 Hydrogel Applications

I.1.6.1 Biomedical Applications

a) **Drug Delivery:** Hydrogel systems function as controlled release platforms for pharmaceutical agents, enabling sustained therapeutic delivery over extended periods. These materials can be designed to exhibit stimulus-responsive behavior, such as pH or temperature sensitivity, to optimize drug release kinetics [6,9].

b) **Tissue Engineering:** Hydrogel matrices serve as scaffolding structures for tissue regeneration applications by providing supportive frameworks that facilitate cellular proliferation and differentiation processes [6,9].
c) **Wound Dressings:** Hydrogel-based dressing materials establish moist healing environments that promote wound recovery, absorb wound exudates, and minimize secondary trauma through reduced adherence to wound surfaces [6,9].
d) **3D Cell Cultures:** Hydrogel systems are employed as three-dimensional culture matrices, enabling researchers to investigate cellular behavior under conditions that replicate in vivo physiological environments [6].
e) **Anti-Bacterial Applications of Hydrogels:** These hydrogel systems are investigated for their antimicrobial characteristics, providing sustained antibacterial efficacy through incorporation of antimicrobial compounds [9].
f) **Hydrogels in Contact Lens:** Hydrogel materials are utilized in contact lens applications due to their oxygen permeability characteristics, hydrophilic properties, and biocompatible nature [9].

I.1.6.2 Environmental Applications

Wastewater Treatment: Hydrogel materials are being investigated for wastewater treatment applications based on their capacity to absorb and retain substantial volumes of aqueous solutions [10].

I.1.6.3 Food Industry Applications

a) **Food Texture Perception:** Hydrogel systems can alter food textural properties, enhancing consumer sensory experience [11].
b) **Food Packaging:** Hydrogel materials are incorporated into food packaging systems to improve moisture preservation and product freshness maintenance [11].

I.1.6.4 Agricultural Applications

Agricultural Uses: Hydrogel systems are implemented in agricultural practices to enhance soil moisture retention capacity, thereby reducing irrigation frequency requirements [11].

I.2 Starch

I.2.1 Definition of Starch

Starch constitutes a polysaccharide composed of D-glucose units interconnected through α-1,4 and α-1,6 glycosidic linkages, synthesized primarily within plant tissues as an energy storage carbohydrate . It occurs naturally in granular configurations, exhibiting variations in dimensions, morphology, and crystalline characteristics dependent upon botanical origin . As an extensively available and biodegradable biopolymeric material, starch finds widespread application across food and industrial sectors, encompassing pharmaceutical, textile, paper manufacturing, and bioplastic applications [12]. The first systematic scientific study of starch began in 1716 when Antonie van Leeuwenhoek observed it microscopically as discrete granules. This marked the beginning of three centuries of research into understanding starch's molecular structure and properties [13].

Starch comprises two principal constituents: amylose, characterized by linear architecture, and amylopectin, distinguished by extensive branching. The relative proportions of these components influence starch's physicochemical and functional characteristics, including viscosity behavior, gelatinization phenomena, and retrogradation processes. Its extensive utilization stems from its renewable characteristics, economic viability, and processing versatility [14].

Within plant cellular structures, starch undergoes synthesis and storage as semi-crystalline granular entities with varied morphologies and dimensions according to botanical source [14]. It demonstrates insolubility in ambient temperature water but undergoes gelatinization upon heating, disrupting crystalline architecture and enhancing viscosity [15].

In hydrogel applications, starch and its derivative compounds function as natural polymeric foundations, providing biodegradability, renewability, and economic efficiency. Starch derived hydrogel systems can undergo modification through processes including oxidation, hydroxypropylation, carboxymethylation, or grafting with synthetic polymeric materials to enhance characteristics such as aqueous absorption capacity, mechanical performance, and stimulus-responsive behavior [16].

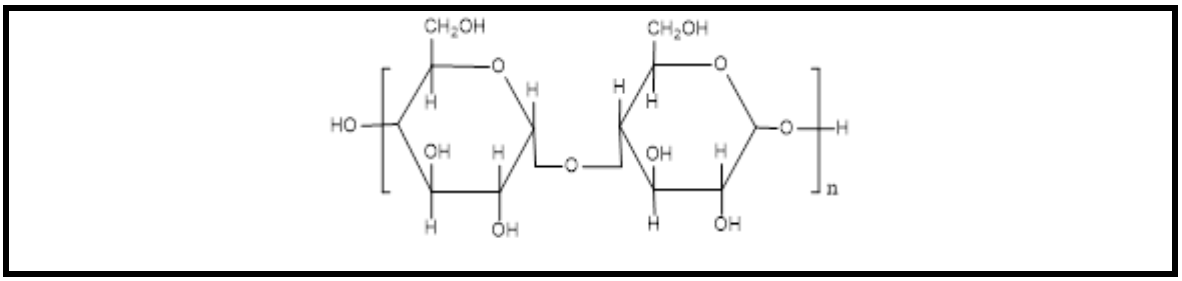

Figure I.2.1.1: Chemical structure of starch

I.2.2 Classification of Starch

I.2.2.1Classification by Botanical Source

a) **Cereal Starches:** These encompass maize, rice, and wheat starches, they are known for their moderate viscosity characteristics and stable gelatinization behavior [17].
b) **Tuber/Root Starches:** Comprise potato, cassava, and yam starches. These starch varieties characteristically exhibit elevated swelling capacity and transparency properties [17].
c) **Legume Starches:** These originate from leguminous sources including peas, beans, and lentils. They demonstrate limited conventional usage but possess specialized applications based on their distinctive functional characteristics [17].

I.2.2.2 Classification by Molecular Structure:

a) **Normal Starch:** A proportionally balanced composition of amylose and amylopectin. It represents the most prevalent starch form and demonstrates utilization across diverse applications. This type of starch has moderate solubility characteristics [18].
b) **Waxy Starch:** Composed predominantly of amylopectin, characterized by elevated viscosity and solution clarity. This composition makes waxy starch highly soluble and creates clear, stable solutions when heated in water [18,19].
c) **High-Amylose Starch:** Contains amylose concentrations exceeding 50%. This type has reduced solubility compared to normal and waxy starches. The high proportion of linear amylose chains creates strong intermolecular hydrogen bonding. It demonstrates utilization for strong gel formation capabilities and as a resistant starch source [19].

I.2.3 Molecular Composition of Starch

Starch consists of two primary polymeric components amylose and amylopectin.

a) **Amylose:** Constitutes a linear polymeric structure comprising α-D-glucose units interconnected predominantly through α-1,4 glycosidic bonds. Typically, amylose represents 15–30% of starch composition in most sources, though this proportion varies according to botanical origin [19].

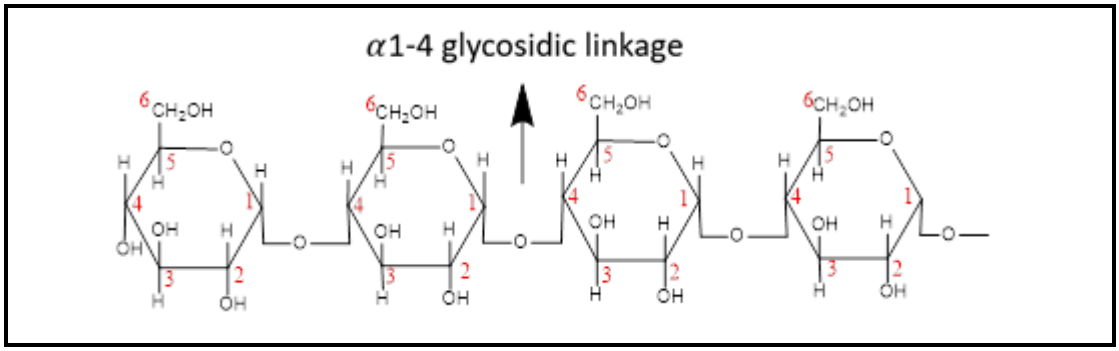

Figure I.2.3.1: Chemical structure of amylose

b) **Amylopectin:** Represents a highly branched polymeric structure, with glucose units linked through both α-1,4 and α-1,6 glycosidic bonds. It exhibits significantly higher molecular weight compared to amylose [19]. Amylopectin comprises 70–85% of starch composition, depending on source material [12].

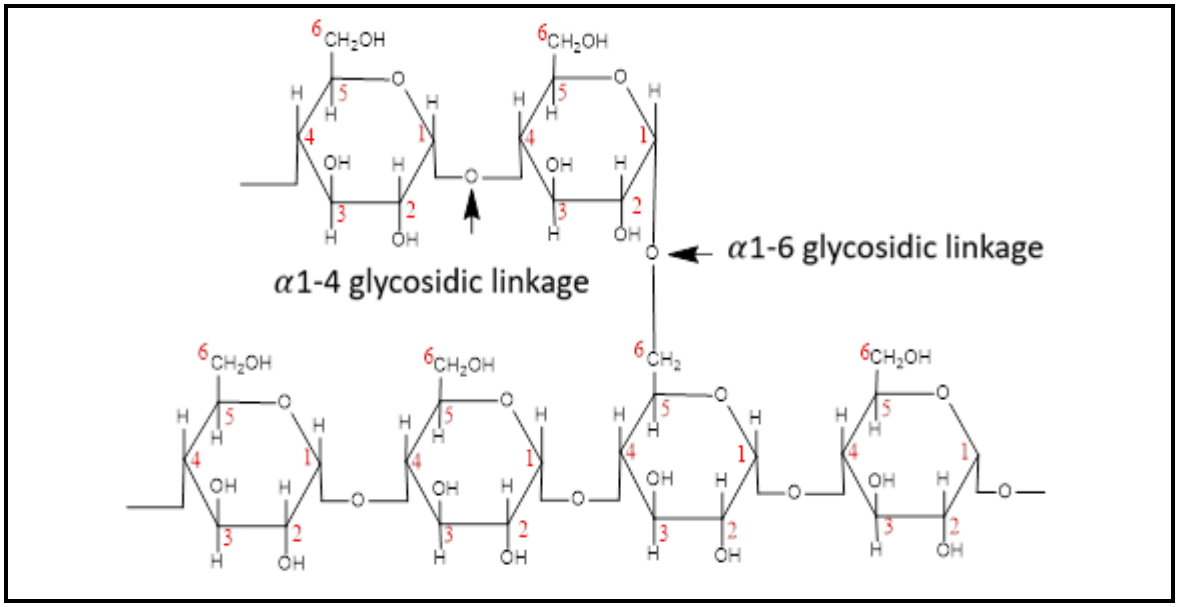

Figure I.2.3.2: Chemical structure of amylopectin

I.2.4 Mechanical Properties of Starch

a) **Tensile Strength:** Starch films, particularly those containing elevated amylose content, demonstrate moderate tensile strength characteristics. However, these films tend toward brittleness due to Amylose's crystalline nature [20].
b) **Elastic Modulus and Toughness:** Starch-derived materials frequently exhibit limited elasticity and toughness unless subjected to modification. Through adjustment of amylose-to-amylopectin ratios or addition of plasticizers and other biopolymeric components [14].

I.2.5 Physicochemical Properties of Starch

a) **Gelatinization:** Upon thermal treatment in aqueous environments, starch granules undergo water absorption, swelling, and eventual rupture. The liberation of amylose and amylopectin from granular structures results in viscous paste formation. The gelatinization temperature of starch varies according to source material [19].
b) **Retrogradation:** During cooling processes, gelatinized starch undergoes retrogradation, wherein amylose and amylopectin molecules reassociate, resulting in gel-like structure formation. Retrogradation phenomena are more pronounced in high-amylose starches and less evident in starches with elevated amylopectin content [21].
c) **Swelling Power and Solubility:** The swelling power of starch refers to the ability of starch granules to absorb water and expand during gelatinization. This property is particularly high in waxy starches, which have low amylose content. Swelling power influences the viscosity and texture of starch pastes and gels. Solubility varies between starch sources, with some starches (such as potato starch) being more soluble in water than others, such as corn starch [22].

I.2.6 Corn Starch

Corn starch (alternatively termed maize starch) is obtained from corn kernel endosperm (Zea mays). It represents one of the most commercially significant and extensively utilized starches due to elevated global corn production and extraction feasibility. Corn starch granules typically exhibit size ranges from 2 to 30 mm and can demonstrate polygonal, round, or irregular morphologies, depending on extraction methodology.

The versatility of corn starch is predominantly attributed to its molecular composition, particularly its amylose-to-amylopectin proportion, which influences its gelling and thickening characteristics [23].

I.2.7 Applications of Starch

Starch demonstrates widespread utilization across diverse industries based on its versatile characteristics [24].

- In the cosmetic industry, starch is valued for its natural origin and multifunctional characteristics. It is commonly employed as an absorbent, mattifying, and texturizing agent in formulations such as powders, dry shampoos, and creams. Its gentle, biodegradable nature renders it suitable for sensitive skin applications and environmentally conscious formulations.
- In food industry applications, starch functions as a thickening agent, stabilizer, and is preferred in clean-label product formulations.
- Starch also contributes to environmentally friendly detergents and bioplastic materials.
- Starch finds utilization in pharmaceutical applications for drug delivery systems, tablet formulations, and as a component in adhesives for bookbinding applications.

I.3 Alginate

I.3.1 Definition of alginates

Alginates are natural anionic polymers extracted mainly from brown seaweed, where they account for up to 40% of dry weight. Identified in the 19^{e} century by Edward C. C . Stanford using a sodium bicarbonate extraction method, their structure was proposed in 1930 [25]. They form gels in the presence of divalent ions, which has encouraged their industrial and scientific use. Alginates can be found as sodium, calcium or magnesium salts, the sodium salt being the most widely used due to its solubility in water. Some bacteria, such as Azotobacter vinelandii, also produce similar alginates [26].

I.3.2 Structure and Chemical Composition of Alginate:

Alginate is a linear, anionic polysaccharide composed of β-(1→4)-linked D-mannuronic acid (M) and α-(1→4)-linked L-guluronic acid (G) residues. These monomeric units are arranged in Homopolymeric (M-blocks or G-blocks) and Heteropolymeric (MG-blocks) sequences, whose distribution and ratio vary depending on the biological source. This block arrangement governs the molecular conformation and stiffness of the polymer chain. The G-blocks, in particular, exhibit a higher affinity for divalent cations such as Ca^{2+}, due to their rigid structure, which plays a crucial role in the ionic crosslinking mechanism. Additionally, alginate's behavior in aqueous media is influenced by environmental factors such as pH, which can modulate its ionization state and conformation in solution [27].

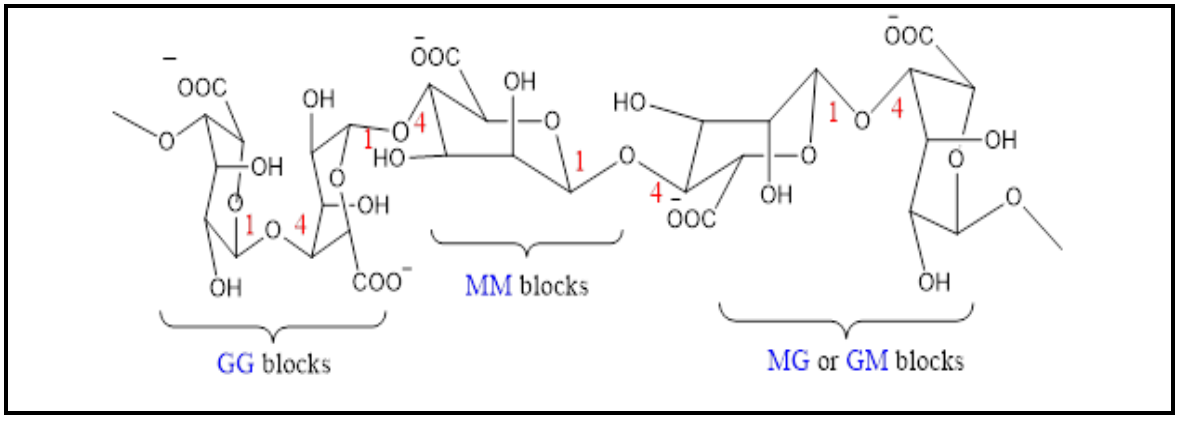

Figure I.3.2.1: Chemical structure of Alginate

I.3.3 Physical and chemical properties of alginate

Alginate is an essential component for many industrial and medical applications since it is a naturally occurring polymer with unique physical-chemical characteristics. Solubility, viscosity, stability, and gelation capability are its main attributes. which are detailed in the table below

Table 1.3.3: Physical and chemical properties of alginate.

Property	Description	References
Molecular Weight	Molecular weight (32,000–400,000 g/mol) influences application range and solution viscosity .	[28]
Viscosity	Viscosity increases as pH decreases, peaking between pH 3 and 3.5 due to hydrogen bonding with carboxyl groups. It remains stable between pH 6 and 8.	[28]
Stability	Sodium alginate is more stable as powder than solution, forms pH-dependent gels, and tolerates brief heat sterilization but degrades under prolonged thermal exposure or high pH.	[28]
Solubility	ideal for watery applications; insoluble in more than 30% alcohol, forms a viscous solution in cold water.	[28]
Gelation	Ionic cross-linking with divalent cations (Ca^{2+}, Ba^{2+}) via carboxyl groups in guluronic acid blocks ("egg-box" model) forms hydrogels; essential for wound dressings and drug delivery.	[27]

I.3.4 Sodium alginate

Brown seaweed, such as Laminaria and Ascophyllum, are the primary source of sodium alginate (E401), a naturally occurring polysaccharide. Alginic acid, a big molecule made up of mannuronate and guluronate blocks, is the source of it. Alginate is typically found as a white or cream-colored powder that is odorless and soluble in water when it is in its sodium salt form. Because of its ability to form gels in the presence of calcium ions, its gelling, thickening, and stabilizing qualities are used in a variety of industrial sectors, particularly in the food business. Moreover, sodium alginate is a safe and environmentally beneficial substance because it is non-toxic and biodegradable [29].

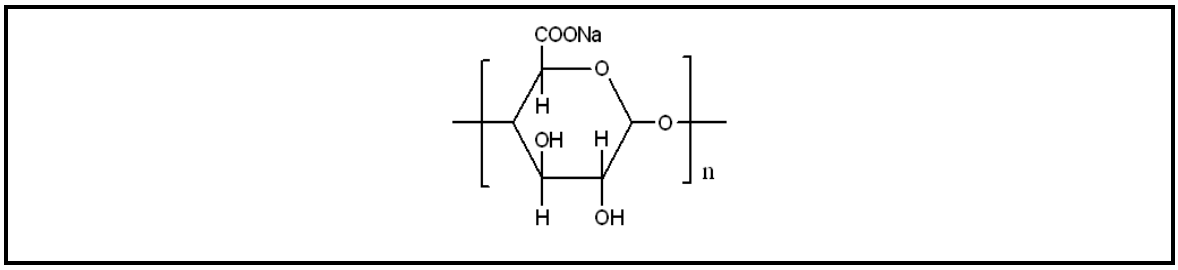

Figure I.3.4.1: Chemical structure of Sodium Alginate

I.3.5 Applications of Sodium Alginate

Alginate is a naturally occurring polymer that was first used in the food industry for a variety of applications, including covering fruits and vegetables, protecting against bacteria and viruses, and acting as a gelling, thickening, stabilizing, or emulsifying agent. Since then, its uses have grown considerably. Its nontoxicity, biodegradability, and biocompatibility have prompted investigation in the biomedical and pharmaceutical sectors. Nowadays, alginate is used in a variety of forms, including films, hydrogels, tablets, capsules, and nanoparticles, for purposes ranging from tissue regeneration and wound healing to medication administration in the treatment of diseases including diabetes and obesity. This adaptability highlights the value of alginate in both sophisticated medical procedures and food-related applications [25].

I.4 Polyvinyl Alcohol PVA

I.4.1 Definition of PVA

A common hydrophilic synthetic polymer in the industrial, biomedical, and environmental domains is polyvinyl alcohol (PVA). The hydrophilic characteristics of PVA are derived from the partial or complete hydrolysis of poly(vinyl acetate) (PVAc), which substitutes hydroxyl groups (-OH) for acetate groups (-$OCOCH_3$). It is a material of choice for medical applications due to its water solubility, biocompatibility, non-toxicity, and biodegradability, particularly in the production of films, hydrogels, and controlled-release medication systems [30]. PVA was discovered in 1924 by German scientists Hermann and Haehnel, and because of its special set of qualities, it has been used in a wide range of industrial and biological fields [31].

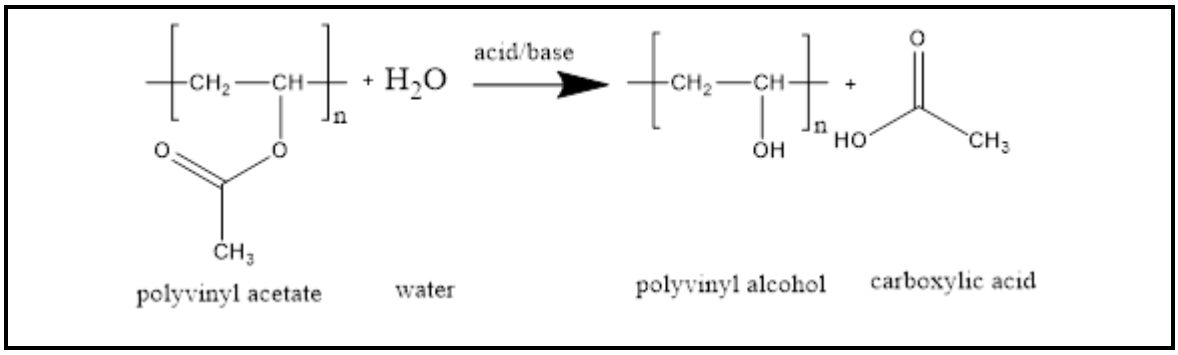

Figure I.4.1.1: Making polyvinyl alcohol by hydrolysis

I.4.2 Chemical structure of PVA

A linear arrangement of carbon atoms linked to many hydroxyl groups (-OH)arranged laterally characterizes the chemical makeup of poly (vinyl alcohol) (PVA). $[-CH_2\text{-}CHOH-]_n$ is the repeating unit of the polymer, and 'n' indicates the number of monomer units in the polymer. The controlled hydrolysis of polyvinyl acetate (PVAc), which substitutes hydroxyl groups for acetate groups ($-OCOCH_3$), is how PVA is made. The structural properties of PVA are strongly influenced by the degree of hydrolysis, which is defined as the ratio of hydroxylated to acetylated units. PVA can be totally or partially hydrolyzed, depending on the degree of hydrolysis, which affects its solubility and crystallinity [32].

Moreover, PVA's semi-crystalline structure is influenced by the strong network of intramolecular and intermolecular hydrogen interactions, which is strengthened by the presence of hydroxyl groups. Its diverse qualities and effectiveness in both organic and aqueous settings depend heavily on its particular structural arrangement [33].

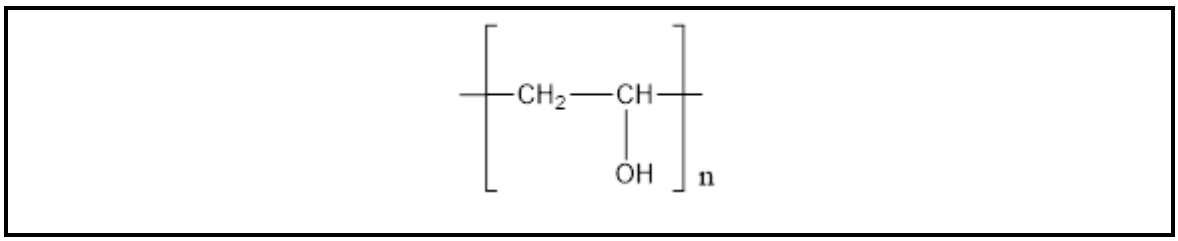

Figure I.4.2.1: Chemical structure of PVA

I.4.3 Chemical and physical properties of PVA

PVA is a hydrophilic polymer whose key properties such as solubility, thermal behavior and mechanical strength depend on its degree of hydrolysis and molecular weight, as shown in the table below.

Table 1.4.3: Chemical and physical properties of PVA.

Property	Description	References
Molecular weight	Molecular weight range 20,000–400,000	[31]
Polymer Type	Hydrophilic polymer whose properties are influenced by the degree of hydrolysis and molecular weight.	[30]
Hydrolysis Degree	Completely hydrolyzed (>98%): more water-resistant and stable. 87–89% partially hydrolyzed: more soluble but less resistant.	[34]
Crystallinity	semi-crystalline; stiffness and tensile strength are impacted by crystallinity, which varies from 20% to 50%.	[35]
Thermal Properties	Temperature of glass transition: 58°C to 85°C. Temperature range for melting: 180°C to 230°C.	[36]
Solubility	Excellent solubility in water and a few polar solvents, including N,N-dimethylformamide (DMF) and dimethyl sulfoxide (DMSO).	[34]
Biocompatibility & uses	Biocompatible, non-toxic, and thermally stable; frequently utilized in biomedical applications, particularly hydrogels.	[33,37]

I.4.4 Applications of Polyvinyl Alcohol

A very adaptable polymer used in many industrial and biological fields is poly (vinyl alcohol) (PVA). It is an essential material for many applications due to its unique qualities, which include water solubility, biocompatibility, and non-toxicity.

Because of its mechanical properties and chemical resilience, PVA is used in industry to produce films, adhesives, biodegradable packaging, and emulsion stabilizers.

PVA is essential in the biomedical industry, especially in drug delivery systems. It is frequently utilized as a drug encapsulation medium because of its capacity to create stable, bioactive hydrogels. PVA hydrogels enable regulated release of active substances, resulting in a more efficient and focused medication delivery method with fewer adverse effects. This substance is also used in tissue engineering and wound healing dressings, where it promotes tissue regeneration by serving as a scaffold for cell proliferation [32].

PVA is used in sophisticated technologies and environmental domains in addition to medicine. Water-soluble sheets for environmentally friendly packaging, filtration membranes, and composite materials enhanced with nanoparticles are among its applications. It is a popular material for many industrial and environmental applications because of its ability to interact with a wide range of substances [36].

I.5 Ascorbic acid (Vitamin C)

I.5.1 Definition and Fundamental Properties of Ascorbic Acid

Often referred to as vitamin C, ascorbic acid is a water-soluble chemical molecule with a molar mass of 176.13 g/mol and the molecular formula $C_6H_8O_6$. Under the designation E300, this lactone with an enediolated structure is categorized as an antioxidant. This substance often manifests as a crystalline powder that ranges from white to slightly yellowish. It is crucial in neutralizing reactive oxygen species (ROS) and reactive nitrogen species (RNS) because of its strong reducing power, which helps shield biological macromolecules from oxidative stress. Additionally, it plays a role in basic physiological functions like collagen manufacturing. Albert Szent-Györgyi discovered ascorbic acid in 1928. It is well known for being unstable in oxidizing and acidic settings,

necessitating the use of suitable techniques to maintain its integrity all the way to the intestinal absorption site [38].

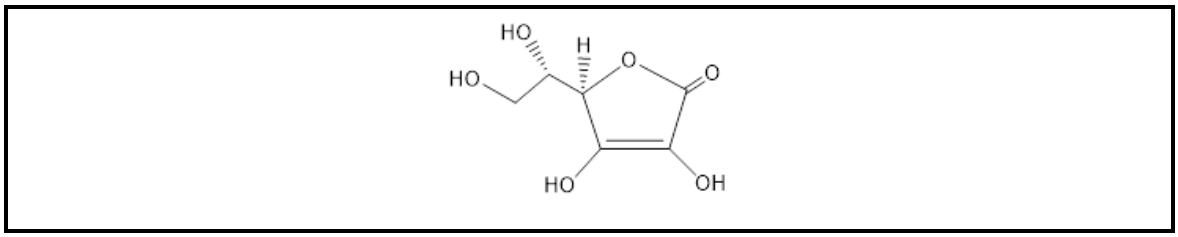

Figure I.5.1.1: Chemical structure of Ascorbic acid (Vitamin C)

I.5.2 Applications of Ascorbic Acid

Ascorbic acid, also known as vitamin C, has numerous applications due to its biological and antioxidant qualities. In pharmacy and biomedicine, it helps make collagen, heals wounds, strengthens the immune system, corrects deficiencies, and acts as an adjuvant in antiviral and anticancer treatments. It is added to hydrogels and nanoparticles, two controlled-release methods, to increase its stability and effectiveness. Its brightening and anti-aging properties are used in cosmetics to increase firmness, brightness, and skin elasticity. Additionally, the food industry uses it as an antioxidant preservative (E300) [38].

I.6 Drug delivery system

I.6.1 Controlled Oral drug delivery of VC

Vitamin C (ascorbic acid), a water-soluble antioxidant, holds a significant promise in drug delivery applications. However, its incorporation into oral hydrogel-based delivery systems is challenged by its chemical stability under acidic conditions. Hydrogels provide a protective and adjustable matrix that can enable controlled release, potentially enhancing Vitamin C bioavailability. In vivo release assessments in the gastric pH 1.4-3 and intestinal pH 6.8-7.4 are essential to characterize release and stability throughout gastrointestinal transit. Release in the acidic gastric environment is unfavorable due to VC's susceptibility to oxidative degradation and acid-catalyzed hydrolysis, which reduce its therapeutic efficacy before absorption [39]. Moreover, the stomach lacks sodium-dependent vitamin C transporters (SVCT1 and SVCT2), which are critical for efficient

intestinal uptake. In contrast, the small intestine provides a more favorable milieu for VC stability and absorption, making targeted release in the small intestinal desirable. Consequently, designing hydrogels that restrict premature release in the stomach while promoting sustained release in the small intestinal is crucial to improving VC's systemic bioavailability, and therapeutic effectiveness in oral drug delivery systems [38].

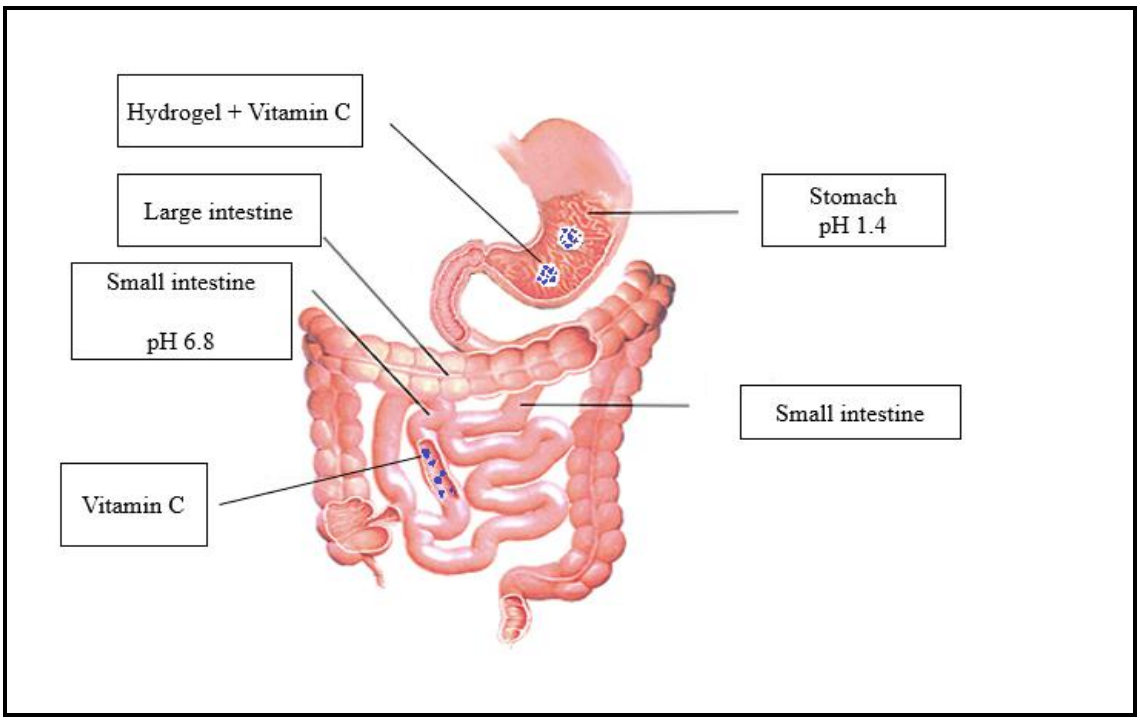

Figure I.6.1.1: Controlled Release of Vitamin C in the Digestive system via biohydrogel carrier

I.6.2 The quantity of drug released

The amount of drug released indicates how much of the active pharmaceutical ingredient (API) within a medication formulation becomes accessible for the body to absorb. This measurement serves as a critical factor in studies examining drug release and dissolution, which evaluate the rate at which a medication is released from its dosage form across different time periods [40].

References

[1] Lh. Yahia, « History and Applications of Hydrogels », *J. Biomed. Sci.*, vol. 04, nº 02, 2015, doi: 10.4172/2254-609X.100013.

[2] Y. Zhang et Y. Huang, « Rational Design of Smart Hydrogels for Biomedical Applications », *Front. Chem.*, vol. 8, p. 615665, 2021, doi: 10.3389/fchem.2020.615665.

[3] M. Bustamante-Torres, D. Romero-Fierro, B. Arcentales-Vera, K. Palomino, H. Magaña, et E. Bucio, « Hydrogels Classification According to the Physical or Chemical Interactions and as Stimuli-Sensitive Materials », *Gels*, vol. 7, nº 4, p. 182, 2021, doi: 10.3390/gels7040182.

[4] J. M. Dodda, K. Deshmukh, D. Bezuidenhout, et Y.-C. Yeh, « Hydrogels: Definition, History, Classifications, Formation, Constitutive Characteristics, and Applications », in *Multicomponent Hydrogels*, 1re éd., J. M. Dodda, K. Deshmukh, et D. Bezuidenhout, Éd., The Royal Society of Chemistry, 2023, p. 1-25. doi: 10.1039/BK9781837670055-00001.

[5] N. H. Thang, T. B. Chien, et D. X. Cuong, « Polymer-Based Hydrogels Applied in Drug Delivery: An Overview », *Gels*, vol. 9, nº 7, p. 523, 2023, doi: 10.3390/gels9070523.

[6] A. Revete *et al.*, « Advancements in the Use of Hydrogels for Regenerative Medicine: Properties and Biomedical Applications », *Int. J. Biomater.*, vol. 2022, p. 1-16, 2022, doi: 10.1155/2022/3606765.

[7] K. T. Nguyen et J. L. West, « Photopolymerizable hydrogels for tissue engineering applications », *Biomaterials*, vol. 23, nº 22, p. 4307-4314, 2002, doi: 10.1016/S0142-9612(02)00175-8.

[8] Z. Zhang *et al.*, « A fast and versatile cross-linking strategy via *o* -phthalaldehyde condensation for mechanically strengthened and functional hydrogels », *Natl. Sci. Rev.*, vol. 8, nº 4, p. nwaa128, 2021, doi: 10.1093/nsr/nwaa128.

[9] Z. Ahmad *et al.*, « Versatility of Hydrogels: From Synthetic Strategies, Classification, and Properties to Biomedical Applications », *Gels*, vol. 8, nº 3, p. 167, 2022, doi: 10.3390/gels8030167.

[10] M. Song, J. Wang, J. He, D. Kan, K. Chen, et J. Lu, « Synthesis of Hydrogels and Their Progress in Environmental Remediation and Antimicrobial Application », *Gels*, vol. 9, nº 1, p. 16, 2022, doi: 10.3390/gels9010016.

[11] G. Stojkov, Z. Niyazov, F. Picchioni, et R. K. Bose, « Relationship between Structure and Rheology of Hydrogels for Various Applications », *Gels*, vol. 7, nº 4, p. 255, 2021, doi: 10.3390/gels7040255.

[12] J. Compart, A. Singh, J. Fettke, et A. Apriyanto, « Customizing Starch Properties: A Review of Starch Modifications and Their Applications », *Polymers*, vol. 15, nº 16, p. 3491, 2023, doi: 10.3390/polym15163491.

[13] K. Seetharaman et E. Bertoft, « Perspectives on the history of research on starch: Part I: On the linkages in starch », *Starch - Stärke*, vol. 64, nº 9, p. 677-682, 2012, doi: 10.1002/star.201200088.

[14] S. Park et Y.-R. Kim, « Clean label starch: production, physicochemical characteristics, and industrial applications », *Food Sci. Biotechnol.*, vol. 30, nº 1, p. 1-17, 2021, doi: 10.1007/s10068-020-00834-3.

[15] C. P. Palanisamy, B. Cui, H. Zhang, S. Jayaraman, et G. Kodiveri Muthukaliannan, « A Comprehensive Review on Corn Starch-Based Nanomaterials: Properties, Simulations, and Applications », *Polymers*, vol. 12, nº 9, p. 2161, 2020, doi: 10.3390/polym12092161.

[16] K. Koshenaj et G. Ferrari, « A Comprehensive Review on Starch-Based Hydrogels: From Tradition to Innovation, Opportunities, and Drawbacks », *Polymers*, vol. 16, nº 14, p. 1991, 2024, doi: 10.3390/polym16141991.

[17] L. Dai, J. Zhang, et F. Cheng, « Effects of starches from different botanical sources and modification methods on physicochemical properties of starch-based edible films », *Int. J. Biol. Macromol.*, vol. 132, p. 897-905, 2019, doi: 10.1016/j.ijbiomac.2019.03.197.

[18] Q. Su, L. Chen, L. Sun, K. Liu, et K. Gong, « Differences and Mechanism of Waxy Corn Starch and Normal Corn Starch in the Preparation of Recrystallized Resistant Starch (RS3) », *Foods*, vol. 13, nº 13, p. 2039, 2024, doi: 10.3390/foods13132039.

[19] K. Bashir et M. Aggarwal, « Physicochemical, structural and functional properties of native and irradiated starch: a review », *J. Food Sci. Technol.*, vol. 56, nº 2, p. 513-523, 2019, doi: 10.1007/s13197-018-3530-2.

[20] M. K. Marichelvam, M. Jawaid, et M. Asim, « Corn and Rice Starch-Based Bio-Plastics as Alternative Packaging Materials », *Fibers*, vol. 7, nº 4, p. 32, 2019, doi: 10.3390/fib7040032.

[21] Q. Chang, B. Zheng, Y. Zhang, et H. Zeng, « A comprehensive review of the factors influencing the formation of retrograded starch », *Int. J. Biol. Macromol.*, vol. 186, p. 163-173, 2021, doi: 10.1016/j.ijbiomac.2021.07.050.

[22] C.-L. Lin, J.-H. Lin, J.-J. Lin, et Y.-H. Chang, « Properties of High-Swelling Native Starch Treated by Heat-Moisture Treatment with Different Holding Times and Iterations », *Mol. Basel Switz.*, vol. 25, nº 23, p. 5528, 2020, doi: 10.3390/molecules25235528.

[23] J.-K. Yu et Y.-S. Moon, « Corn Starch: Quality and Quantity Improvement for Industrial Uses », *Plants Basel Switz.*, vol. 11, nº 1, p. 92, 2021, doi: 10.3390/plants11010092.

[24] S. C. Alcázar-Alay et M. A. A. Meireles, « Physicochemical properties, modifications and applications of starches from different botanical sources », *Food Sci. Technol. Camp.*, vol. 35, nº 2, p. 215-236, 2015, doi: 10.1590/1678-457X.6749.

[25] S. Thomas, P. M. Visakh, et Aji. P. Mathew, Éd., *Advances in Natural Polymers: Composites and Nanocomposites*, vol. 18. in Advanced Structured Materials, vol. 18. Berlin, Heidelberg: Springer Berlin Heidelberg, 2013. doi: 10.1007/978-3-642-20940-6.

[26] R. Ahmad Raus, W. M. F. Wan Nawawi, et R. R. Nasaruddin, « Alginate and alginate composites for biomedical applications », *Asian J. Pharm. Sci.*, vol. 16, nº 3, p. 280-306, 2021, doi: 10.1016/j.ajps.2020.10.001.

[27] R. Abka-khajouei, L. Tounsi, N. Shahabi, A. K. Patel, S. Abdelkafi, et P. Michaud, « Structures, Properties and Applications of Alginates », *Mar. Drugs*, vol. 20, nº 6, p. 364, 2022, doi: 10.3390/md20060364.

[28] O. Frent *et al.*, « Sodium Alginate—Natural Microencapsulation Material of Polymeric Microparticles », *Int. J. Mol. Sci.*, vol. 23, nº 20, p. 12108, 2022, doi: 10.3390/ijms232012108.

[29] P. Rosiak, I. Latanska, P. Paul, W. Sujka, et B. Kolesinska, « Modification of Alginates to Modulate Their Physic-Chemical Properties and Obtain Biomaterials with Different Functional Properties », *Molecules*, vol. 26, nº 23, p. 7264, 2021, doi: 10.3390/molecules26237264.

[30] D. Feldman, « Poly(Vinyl Alcohol) Recent Contributions to Engineering and Medicine », *J. Compos. Sci.*, vol. 4, nº 4, p. 175, 2020, doi: 10.3390/jcs4040175.

[31] S. Aruldass, V. Mathivanan, A. R. Mohamed, et C. T. Tye, « Factors affecting hydrolysis of polyvinyl acetate to polyvinyl alcohol », *J. Environ. Chem. Eng.*, vol. 7, nº 5, p. 103238, 2019, doi: 10.1016/j.jece.2019.103238.

[32] Sota Asano, « Polyvinyl Alcohol: A Comprehensive Overview », *Adv. Mater. Sci. Res.*, vol. 7, nº 5, p. 199-200, 2024, doi: 10.37532/aaasmr.2024.7(5).199-200.

[33] J. Zhou *et al.*, « Dynamic intermolecular interactions through hydrogen bonding of water promote heat conduction in hydrogels », *Mater. Horiz.*, vol. 7, nº 11, p. 2936-2943, 2020, doi: 10.1039/D0MH00735H.

[34] M. Bercea, « Recent Advances in Poly(vinyl alcohol)-Based Hydrogels », *Polymers*, vol. 16, nº 14, p. 2021, 2024, doi: 10.3390/polym16142021.

[35] B. M. Baraker et B. Lobo, « Spectroscopic analysis of $CdCl_2$ doped PVA–PVP blend films », *Can. J. Phys.*, vol. 95, nº 8, p. 738-747, 2017, doi: 10.1139/cjp-2016-0848.

[36] M. Bercea, « Recent Advances in Poly(vinyl alcohol)-Based Hydrogels », *Polymers*, vol. 16, nº 14, p. 2021, 2024, doi: 10.3390/polym16142021.

[37] V. M. Sardinha, L. L. Lima, W. D. Belangero, C. A. Zavaglia, V. P. Bavaresco, et J. R. Gomes, « Tribological characterization of polyvinyl alcohol hydrogel as substitute of articular cartilage », *Wear*, vol. 301, nº 1-2, p. 218-225, 2013, doi: 10.1016/j.wear.2012.11.054.

[38] A. Alberts, E.-T. Moldoveanu, A.-G. Niculescu, et A. M. Grumezescu, « Vitamin C: A Comprehensive Review of Its Role in Health, Disease Prevention, and Therapeutic Potential », *Molecules*, vol. 30, nº 3, p. 748, 2025, doi: 10.3390/molecules30030748.

[39] X. Yin *et al.*, « Chemical Stability of Ascorbic Acid Integrated into Commercial Products: A Review on Bioactivity and Delivery Technology », *Antioxidants*, vol. 11, nº 1, p. 153, 2022, doi: 10.3390/antiox11010153.

[40] K. Nakayama *et al.*, « Quantification of API content in pharmaceutical tablets within milliseconds by time-stretch near-infrared transmission spectroscopy », *J. Pharm. Biomed. Anal.*, vol. 249, p. 116372, 2024, doi: 10.1016/j.jpba.2024.116372.

MATERIALS AND METHODS

This chapter outlines the materials and products used to accomplish the research objectives and operating methods along with their characterization methods.

Part 1. The equipment

II.1.1 Materials

Table II.2: The chemical products used in the research

Chemical products	Chemical structure	Suppliers	Molar mass
Starch	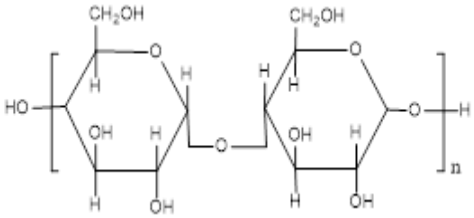	Commercial product from the local store	Variable ~162 (Per glucose unit)
PVA 87%-90% (Polyvinyl alcohol)	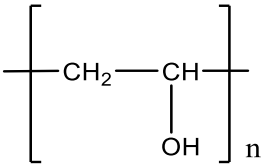	SIGMA-ALDRICH	~ 44 (Per unit)
Sodium Alginate	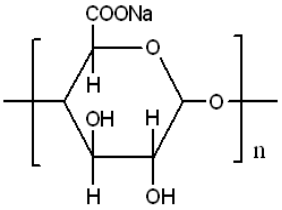	SIGMA-ALDRICH	Variable ~216 (Per unit)
$CaCl_2$	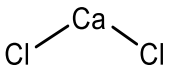	SIGMA-ALDRICH	110.98
Ascorbic acid	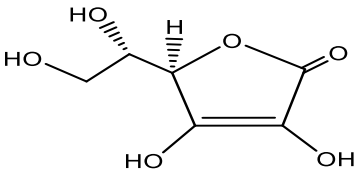	SIGMA-ALDRICH	176.13

DPPH	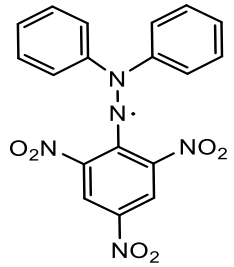	Alfa Aesar	394.32
Methanol	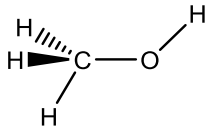	Honeywell	32.04
NH_4OH	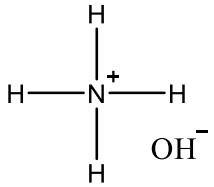	BIOCHEM Chemopharma	35.05
NH_4Cl	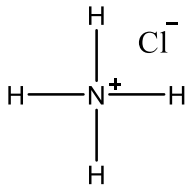	Fluka Chemika	53.49
$C_6H_8O_7$	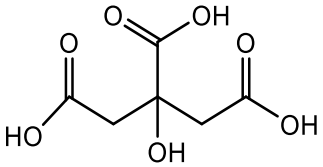	NENTECH LTD	210.14
Na_2HPO_4	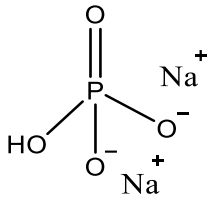	Merck Millipore Supelco	177.99
NaCl	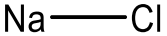	BIOCHEM Chemopharma	58.44
HCl 37%	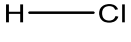	BIOCHEM RECTAPUR	36.46

NaOH	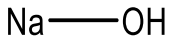	BIOCHEM Chemopharma	40
KH_2PO_4	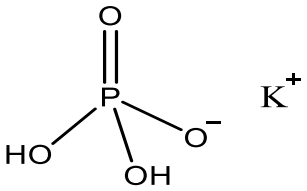	Eisen-Golden Laboratories	136.09

II.1.2 Instruments

Table II.3: The Materials used in the research

Material	Brand
Magnetic stirrer	VELP SCIENTIFICA
Analytical balance	Sartorius BP 211 D
pH meter	Starter 2100 OHAUS
Ultraviolet-Visible Spectrophotometry (UV-Vis)	Optizen 2120UV
X-ray Fluorescence (XRF)	Thermo SCIENTIFIC Niton XL3t
X-ray Diffraction (XRD)	RIGAKU Ultima IV
Fourier Transform Infrared Spectroscopy (FTIR)	Perkin Elmer Spectrum Two

Part 2. Experimental Methods

II.2.1 Preparation of biohydrogels

In this research, biohydrogels were prepared using biomaterials and $CaCl_2$ as a cross-linking agent through two distinct synthesis methods. The first approach employed conventional cross-linking synthesis, while the second utilized a freeze-thaw cycle methodology.

II.2.1.1 Preparation of polyvinyl alcohol/alginate and starch/alginate biohydrogels with $CaCl_2$

Biohydrogels were synthesized using two polymer systems: PVA/Sodium Alginate and starch/Sodium Alginate. Each system was prepared by dissolving 7% of either PVA or corn Starch with 3% Sodium Alginate in distilled water under stirring. Calcium chloride ($CaCl_2$) was added at 3% and 1% to induce gelation through calcium-mediated crosslinking. The mixtures were heated under reflux to ensure polymer dissolution and network formation. The resulting hydrogels were then left to dry at room temperature paraphrase [1].

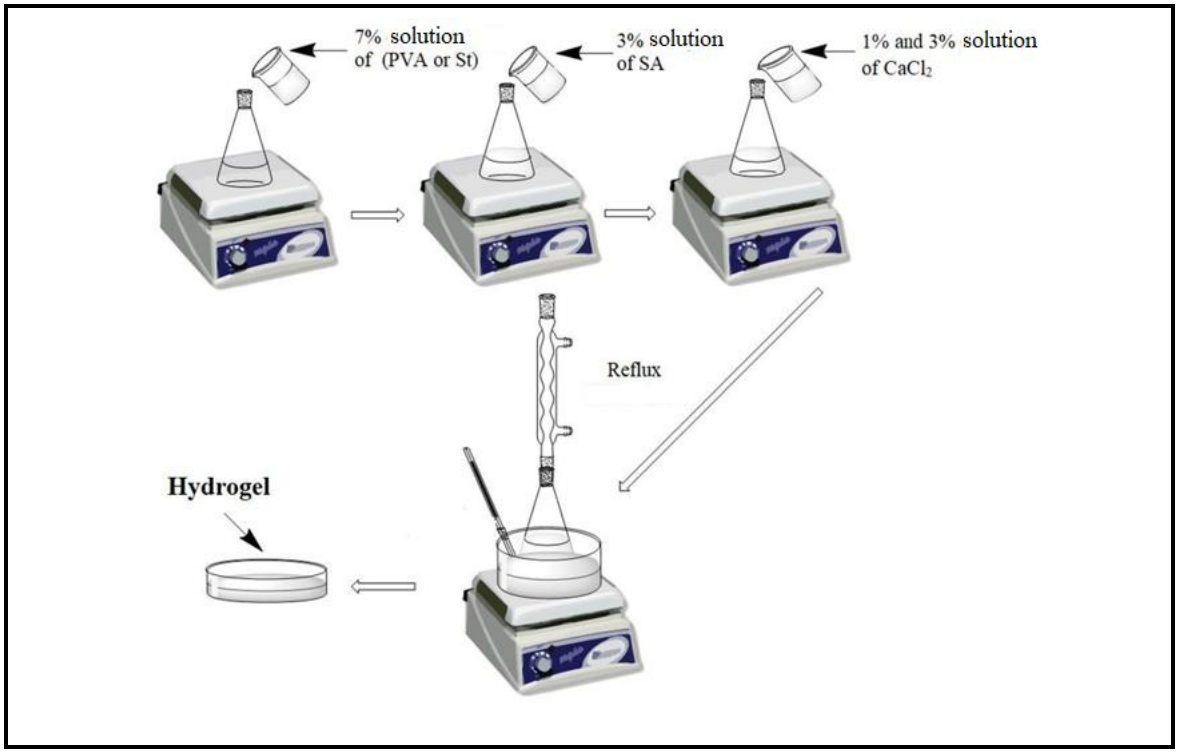

Figure II.2.1.1: Preparation method of PVA/SA St/SA biohydrogels with $CaCl_2$.

II.2.1.2 Preparation of PVA/alginate and starch/alginate hydrogels with $CaCl_2$ by freeze–thaw cycles

Biohydrogel networks were synthesized via combined physical and chemical crosslinking methodologies using PVA/alginate and starch/alginate. The PVA-based hydrogel was fabricated through freeze-thaw cycles, wherein PVA and Sodium Alginate aqueous solutions were individually prepared and subsequently blended in a 70:30 under continuous mechanical stirring. The resultant mixture was subjected to three successive freeze–thaw cycles to induce physical crosslinking. Subsequent ionic crosslinking was

achieved by immersion in a 3% calcium chloride solution for 24h. The hydrogels were then purified through sequential washing with distilled and bidistilled water under agitation and air-dried at an ambient temperature.

For starch-based hydrogel, the same methodology was employed, replacing PVA with corn starch [2].

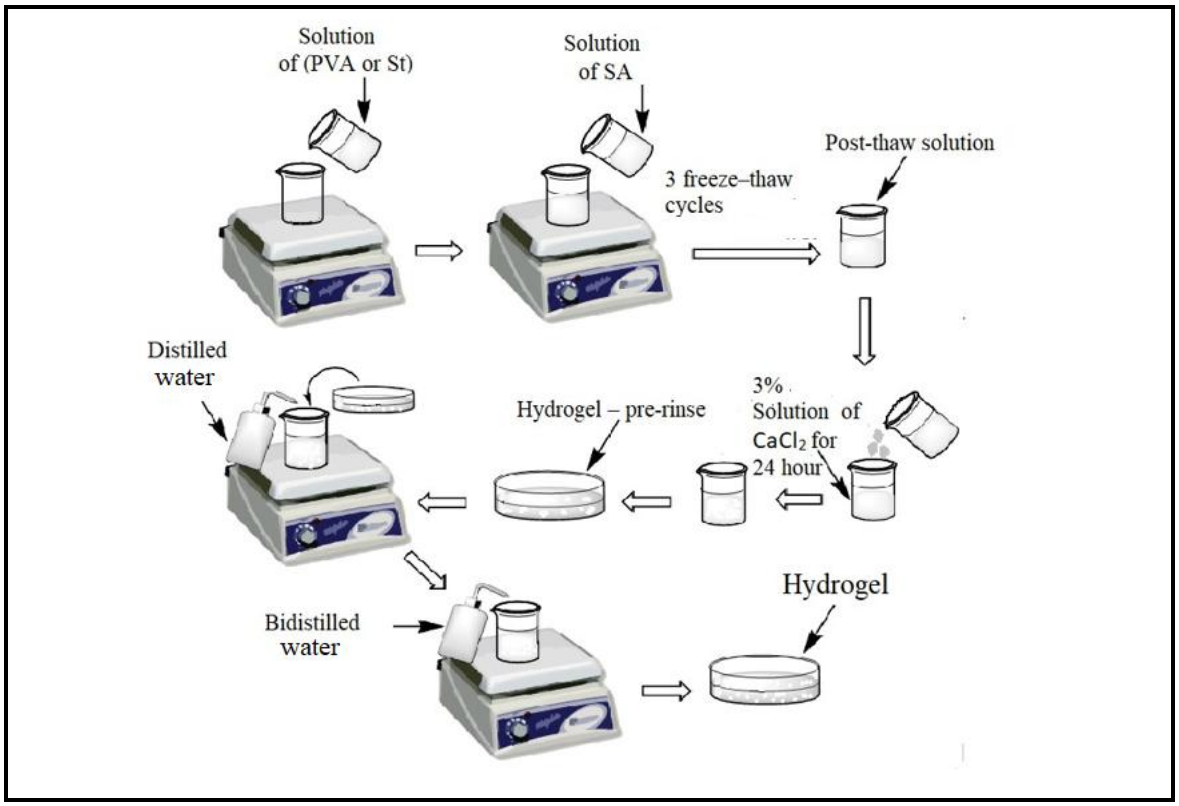

Figure II.2.1.2: Preparation method of PVA/SA and St/SA biohydrogels with $CaCl_2$ by freeze thaw cycles.

II.2.2 Preparation of media for evaluating hydrogel behavior

The media for swelling tests of hydrogels were prepared to achieve acidic, neutral, and basic conditions. An acidic pH 3 was achieved by mixing disodium phosphate (0.2 M) with citric acid (0.1 M). The basic pH 9 was obtained by combining ammonium chloride (0.2 M) and ammonium hydroxide (0.2 M). Finally, a neutral solution was prepared using distilled water.

II.2.3 Swelling test

The swelling rate (Sr) quantifies the solvent uptake capacity of hydrogel relative to its anhydrous mass. In this work, swelling behavior was studied for all previously prepared

hydrogel samples in distilled water for pH ≈ 7 as well as in buffer solutions of pH 3 and 9. The experiment was conducted at a constant temperature of 25°C. Each sample was immersed in the respective solution, and the swelling ratio was first measured after every 30 minutes up to 3 hours on the first day, then every 24 hours up to 72 hours. Before each measurement, the excess surface solvent was gently removed using a paper towel to ensure accurate weight recording [2]. The swelling ratio was subsequently calculated using a defined experimental relationship (Equation 1):

$$\text{Sr}\ (\%) = \frac{((W_t - W_0)\ )}{W_t} \times 100 \qquad (1)$$

Where:

- **Wt** is the weight of the swollen hydrogel at a given time t
- **W0** is the initial dry weight of the hydrogel

This test helps determine how pH and time influence the swelling behavior of the hydrogels under controlled conditions.

II.2.4 Analytical techniques

II.2.4.1 Fourier Transform Infrared Spectroscopy (FTIR)

Fourier Transform Infrared Spectroscopy (FTIR) is an analytical technique used to identify the chemical bonds, and functional groups present in a material. In this study, FTIR analysis was performed on four hydrogel samples to investigate their chemical structure and confirm the presence of specific functional groups related to the components of the hydrogels.

II.2.4.2 X-ray Fluorescence (XRF)

X-ray Fluorescence (XRF) is a technique used to identify and measure the elements present in a material. By analyzing the unique X-ray signatures emitted by a sample when excited, both the elemental composition and their concentrations can be determined. In this study, four powdered hydrogel samples were analyzed by XRF to identify and compare the presence of elements introduced during the preparation process.

II.2.4.3 X-ray Diffraction (XRD)

X-ray Diffraction (XRD) was employed to investigate the crystalline structure of the hydrogel samples. Four hydrogel formulations were subjected to XRD analysis to assess their degree of crystallinity and to detect any crystalline phases present. The resulting diffraction patterns provided insights into the structural characteristics of the materials. The measurements were carried out using a RIGAKU ULTIMA-IV diffractometer operating at 20 °C, with an applied voltage of 40 kV and a current of 30 mA. Bragg's Law is the fundamental principle that governs the diffraction of X-rays by a crystal lattice. This constructive interference results in the intense peaks observed in X-ray diffraction patterns. (Equation 2):

$$n\lambda=2d\sin\theta \quad (2)$$

Where:

- **n** is an integer known as the order of reflection
- **λ** is the wavelength of the incident X-rays
- **d** is the interplanar spacing, which is the distance between adjacent parallel planes of atoms in the crystal lattice.
- **θ** is the angle of incidence (and reflection) of the X-ray beam with respect to the crystal planes.

II.2.4.4 Ultraviolet-Visible Spectrophotometry (UV)

UV-Vis spectrophotometry is a quantitative analytical technique that measures the absorption of ultraviolet and visible radiation by a sample. The degree of light absorption is directly proportional to the concentration of the absorbing analyte and the optical path length through the sample, a principle formalized by the Beer-Lambert Law (Equation 3)

$$A=\epsilon_{(\lambda)}\cdot l\cdot C \quad (3)$$

Where:

- **A** is the absorbance at a specific wavelength (λ).
- **ϵ(λ)** is the molar absorptivity (or molar extinction coefficient) at that wavelength. Its units are typically $L\cdot mol^{-1}\cdot cm^{-1}$.

- **l** is the optical path length through the sample, usually expressed in centimeters (cm).
- **C** is the molar concentration of the analyte in the solution ($mol \cdot L^{-1}$).

II.2.4.5 Calibration Curve and Concentration

for enhanced accuracy and to address potential non-ideal behavior, a calibration curve is frequently employed. This involves measuring the absorbance of a series of standard solutions with known concentrations under identical instrumental settings. A plot of absorbance versus concentration yields a linear relationship with a slope equivalent to $\epsilon \cdot l$. The concentration of an unknown sample is then determined by interpolating its measured absorbance on this calibration curve. To ensure accurate measurements, a suitable blank solution, lacking the analyte, is used to nullify any background absorbance from the solvent or other non-absorbing matrix components.

- Molar extinction coefficient of ascorbic acid at pH 7 $\epsilon_{265} = 14500\ L \cdot mol{-}1 \cdot cm{-}1$

[3].

If the molar absorptivity at a chosen analytical wavelength (often the wavelength of maximum absorbance, λmax) is known, the unknown concentration of a known sample can be directly calculated using the rearranged Beer-Lambert Law (Equation 4)

$$C = \frac{A}{\epsilon(\lambda max) \cdot l} \qquad (4)$$

II.2.4.5.1 Characterization of ascorbic acid by UV-vis spectrophotometry and calibration curve

A stock solution of ascorbic acid was prepared by dissolving 25 mg of ascorbic acid in 25 mL of distilled water under constant stirring until complete dissolution. All preparations and handling were performed under dark conditions to prevent degradation of ascorbic acid. For the calibration curve, aliquots of 0.05, 0.1, 0.15, 0.2, 0.25 mL of the stock solution were pipetted and diluted appropriately to get 5, 10, 15, 20, 25 µg/mL and construct the calibration points at pH 7. The same procedure was repeated using buffer solutions at 3 and 9 instead of distilled water, to assess the stability of ascorbic acid under different pH conditions [4].

II.2.5 Evaluation of the antioxidant activity

Following the preparation and characterization of biohydrogels, two representative samples ((PVA/SA)Ca3 and (St/SA)Ca1) were selected for antioxidant activity evaluation using the DPPH (2,2-diphenyl-1-picrylhydrazyl) radical scavenging assay. Ascorbic acid was used as a positive control standard to validate the assay and provide a reference for comparative evaluation of the antioxidant capacity of the biohydrogel samples [5].

II.2.5.1 Principle

The DPPH (2,2-diphenyl-1-picrylhydrazyl) assay is a widely employed method for evaluating antioxidant activity. This compound is notable for its ability to generate stable free radicals, a property attributed to the delocalization of unpaired electrons within its molecular structure. The presence of these radicals imparts a deep violet color to the solution. When an antioxidant is introduced, it reduces the DPPH radicals, leading to a visible fading of the color. This color change can be quantitatively monitored using spectrophotometry at a wavelength of 517 nm [5].

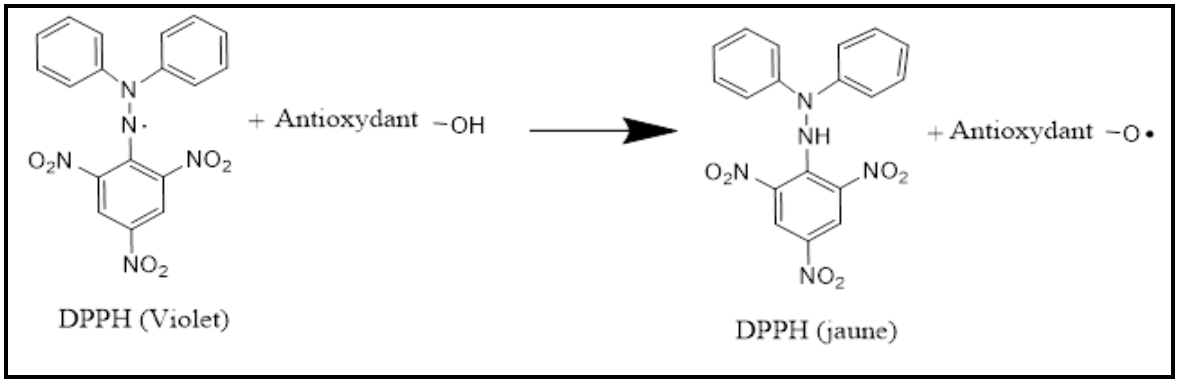

Figure II.2.5.1: DPPH Radical reduction reaction.

II.2.5.2 DPPH Antioxidant Activity Assay Protocol

For the DPPH solution, 5 mg of DPPH powder was dissolved in 100 mL of methanol. A stock solution of ascorbic acid was prepared at a concentration of 2% and then diluted 100-fold to obtain a working solution.

To evaluate the antioxidant activity, different volumes of the diluted ascorbic acid solution were mixed with the DPPH solution. Specifically, 2 mL of DPPH solution was combined with 10 µL, 30 µL, 50 µL, 70 µL, and 100 µL of the ascorbic acid solution, respectively. After mixing, the samples were kept in the dark at room temperature.

The same protocol was applied to evaluate the antioxidant activity of two hydrogel samples: (St/SA)Ca1 and (PVA/SA)Ca3. For these, the same volumes and measurement conditions were used to ensure a consistent comparison with the ascorbic acid standard.

The absorbance of each mixture was measured using a UV-Vis spectrophotometer at 517 nm, at time intervals of 10 minutes, up to 30 minutes [6]. The decrease in absorbance indicated the scavenging activity of ascorbic acid against DPPH free radicals and it was calculated by Equation 5:

$$\text{Radical-scavenging activity (I\%)} = \frac{A_0 - A}{A_0} \times 100 \quad (5)$$

Where:

A_0 the absorbance of DPPH in the absence of antioxidants

A are the absorbance of DPPH in the presence of antioxidants

II.2.6 Drug delivery system

Following the antioxidant activity assessment, the biohydrogels were further evaluated for drug delivery applications. To enhance the investigation, alternative methods of incorporating vitamin C (L-ascorbic acid) were explored in the same hydrogel formulations used for DPPH testing. Vitamin C was chosen as the active pharmaceutical ingredient due to its water solubility and potent antioxidant properties, which complement the intrinsic antioxidant capacity of the hydrogels and align with the therapeutic goals.

II.2.6.1 Preparation of hydrogels with VC

II.2.6.1.1 Preparation of VC-loaded hydrogels

VC was loaded into two different hydrogels using an equilibrium partitioning method. The dried hydrogels (St/SA)Ca1, (PVA/SA)Ca3 were completely immersed in a 1% VC

solution and gently agitated at room temperature in the dark. After 24 hours, the VC-loaded hydrogels were removed and rinsed with bidistilled water to eliminate any unbound VC from the surface. The remaining VC solution and the washing water were collected for analysis. The concentration of unloaded VC in these solutions was quantified using a UV-Visible spectrophotometer, based on a standard calibration curve [7]. The loading efficiency (LE) was calculated using the following equation 6:

$$LE\ (\%) = \frac{M_0 - M_e}{M_0} \times 100 \qquad (6)$$

Where:

M_0 is the initial amount of VC in solution

M_e is the amount of VC remaining after loading

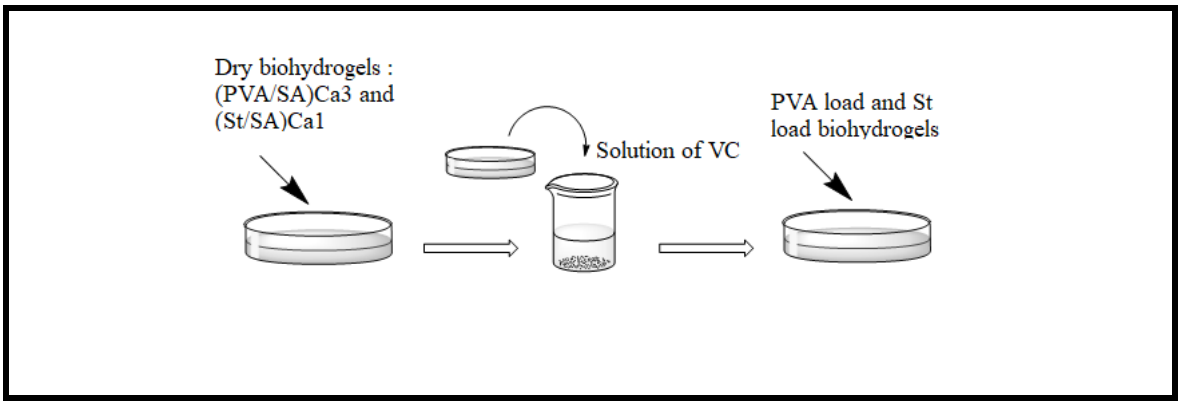

Figure II.2.6.1.1: VC Loaded biohydrogels

II.2.6.1.2 Preparation of VC-Encapsulated Hydrogels with $CaCl_2$ Comparative Study with and without Reflux

a) Preparation of PVA/Alginate Hydrogels Containing $CaCl_2$ and VC

Polyvinyl alcohol PVA/alginate hydrogels were prepared by dissolving 7% PVA and 3% Sodium Alginate in 25 mL of distilled water under continuous magnetic stirring until a homogeneous solution was obtained. In both preparations 1% ascorbic acid was then added. From this point onward, all steps were carried out in the dark to prevent photodegradation. In the first preparation, calcium chloride was added at a concentration of 3%, and the mixture was heated under reflux. After cooling, the resulting hydrogels were dried at room temperature in the dark. In the second preparation, the same procedure was followed, but without the reflux step; calcium chloride was added, and the solution

was stirred at room temperature. The hydrogels were then left to form and dried at ambient temperature, with light protection maintained throughout.

a) Preparation of Starch/Alginate Hydrogels Containing $CaCl_2$ and VC

Starch-based hydrogels were prepared by dissolving 7% corn starch and 3% Sodium Alginate in 25 mL of distilled water under continuous magnetic stirring. Mild heating was applied as necessary to ensure complete dissolution. Once a homogeneous solution was obtained, the mixture was cooled to room temperature, and 1% ascorbic acid was added. From this point onward, all procedures were conducted under light-protected conditions to prevent photodegradation. In the first preparation, calcium chloride ($CaCl_2$) was added at a concentration of 1%, and the mixture was subjected to reflux heating under continuous stirring. After cooling to room temperature, the resulting hydrogel was left to dry at an ambient temperature in the dark. In the second preparation, the same procedure was followed, except that no reflux heating was applied after the addition of $CaCl_2$; instead, the mixture was stirred at room temperature. In both cases, light protection was maintained throughout the entire process, and no additional thermal treatment was applied during drying.

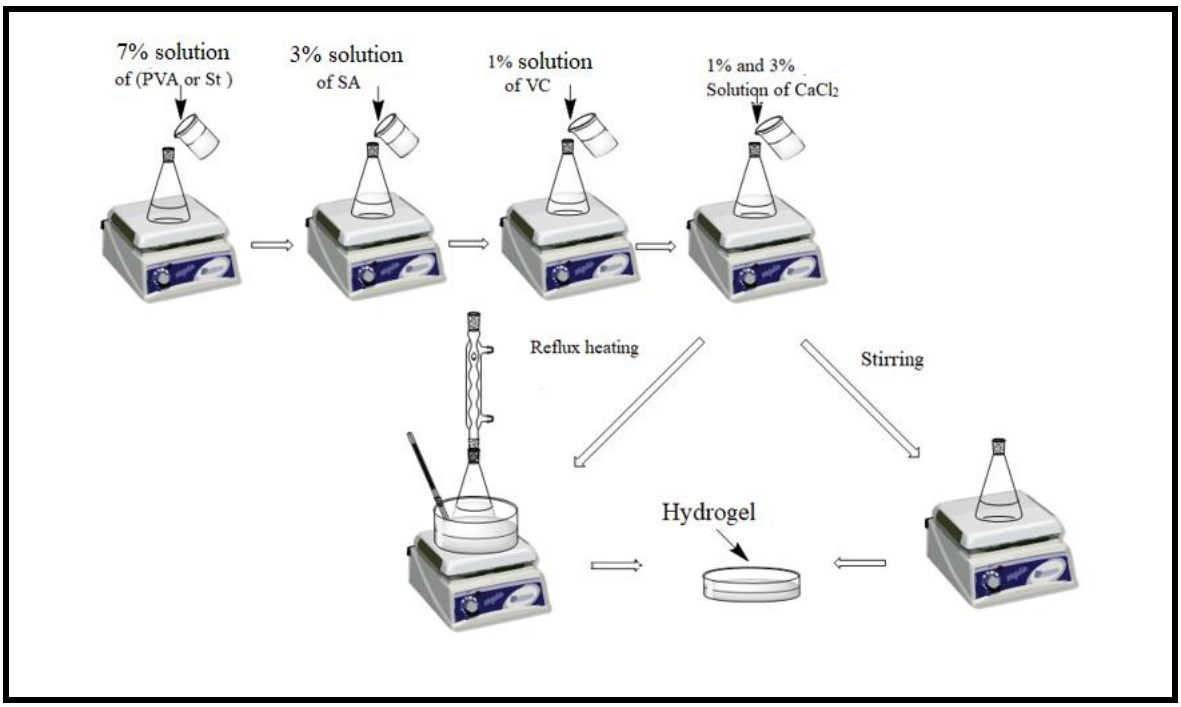

Figure II.2.1.6.2: VC Encapsulated biohydrogels

II.2.6.2 In vitro VC release experiments

The in vitro drug release study was carried out on all vitamin C-loaded and encapsulated biohydrogels under simulated gastrointestinal conditions.

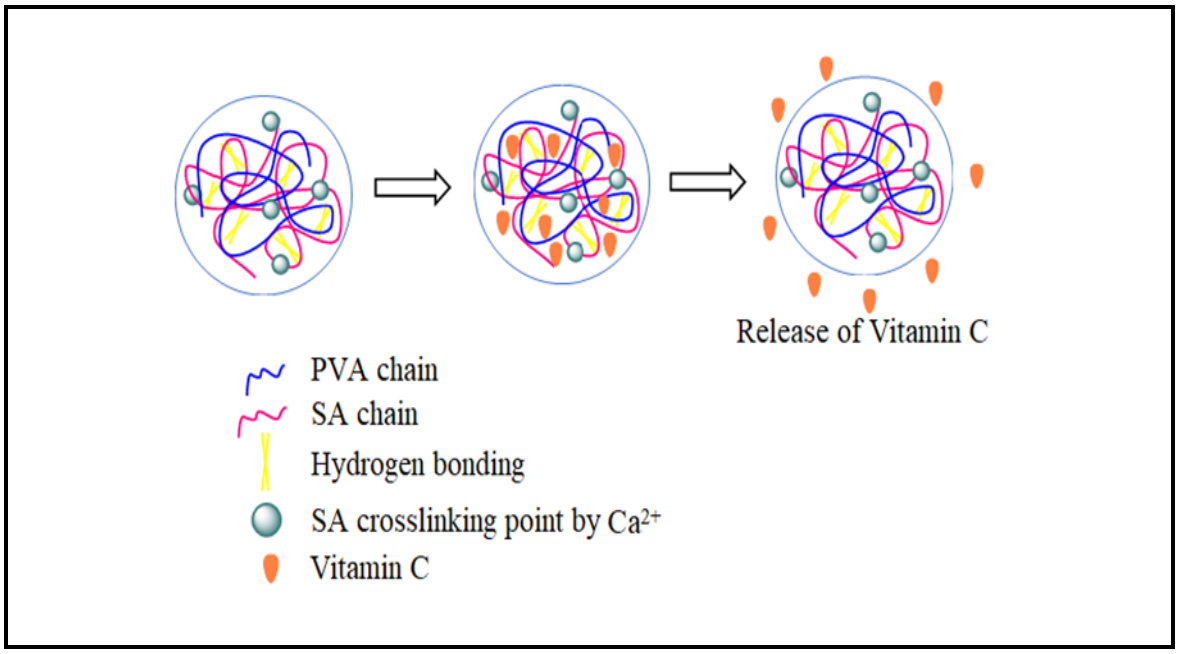

Figure II.2.6.2: VC Release from PVA/SA biohydrogel.

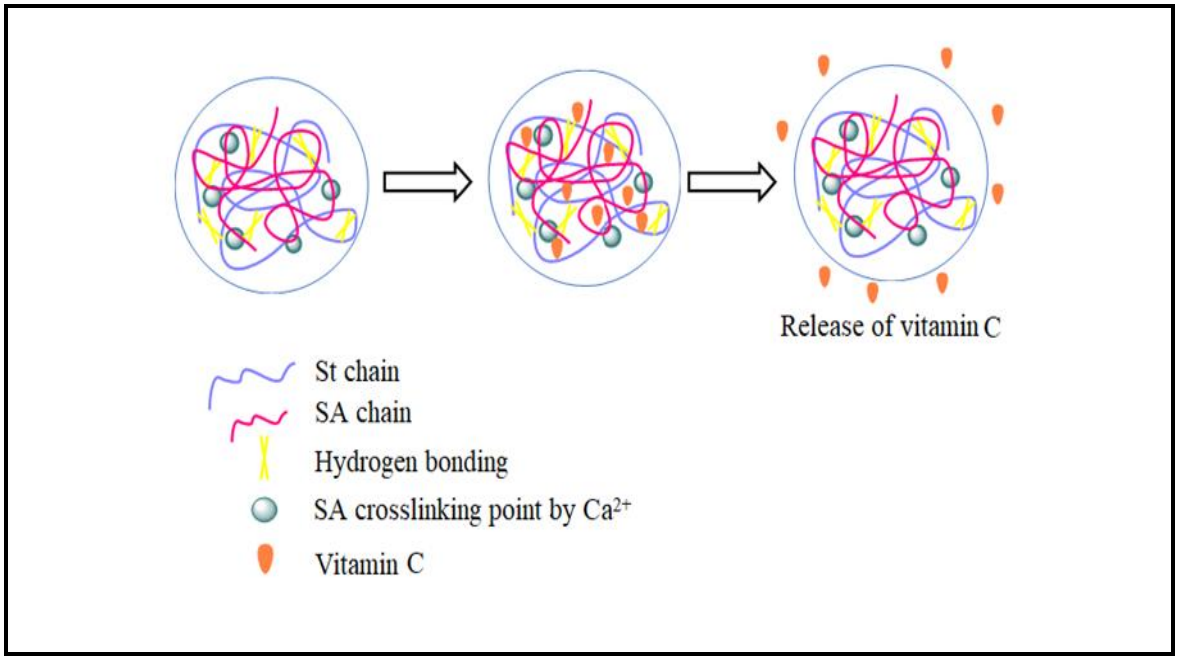

Figure II.2.6.3: VC Release from St/SA biohydrogel.

II.2.6.2.1 Preparation of Simulated Physiological Media

Two simulated physiological media were prepared to investigate the release behavior of the hydrogels: simulated gastric fluid (GFS) and simulated intestinal fluid (IFS).

The simulated gastric fluid (GFS, pH 1.4) was formulated by dissolving sodium chloride (NaCl) in distilled water, followed by the gradual addition of concentrated hydrochloric acid (HCl, 37%) until the target pH was reached. This medium replicates the acidic conditions of the gastric environment and is suitable for evaluating the stability and release performance of materials intended for oral administration under gastric conditions.

The simulated intestinal fluid (IFS, pH 6.8) was prepared by dissolving monobasic potassium phosphate (KH_2PO_4) in distilled water, with pH adjustment carried out using a 0.2 M sodium hydroxide (NaOH) solution. This buffer system reproduces the mildly basic conditions of the small intestine and is widely utilized to simulate the post-gastric environment in studies of enteric drug delivery [8].

II.2.6.2.2 Quantity of drug released of encapsulated hydrogels

The in vitro drug release study for encapsulated hydrogels was conducted using 50 mL of simulated gastric fluid (GFS, pH 1.4) for the initial 2 hours, followed by 50 mL of simulated intestinal fluid (IFS, pH 6.8) for the subsequent 48 hours. At predetermined time intervals, 200 µL of the release medium was sampled and immediately replenished with an equal volume of fresh medium to maintain a constant volume. The amount of drug released was determined based on the measured concentrations in the collected samples, with appropriate corrections applied for dilution and medium replacement, according to the standard calculation by equation 7

$$\text{Quantity of drug released (mg)} = \frac{\text{DF.C.Vt}}{1000} \qquad (7)$$

Where:

- **C:** Concentration is often determined by UV-Vis spectroscopy using a calibration curve (absorbance vs. concentration).
- **DF:** Dilution factor accounts for any dilution done before measurement.
- **Vt:** Volume of dissolution medium is the total volume in which the drug is dissolved.
- **Division by 1000** converts micrograms to milligrams if concentration is in µg/mL

The percentage of drug release is then calculated by equation 8:

$$\frac{q_t}{q_0}\% = \frac{\text{Quantity of drug released (mg)}}{\text{Dose (mg)}} \times 100 \qquad (8)$$

Where:

- **Dose (mg):** is the total amount of drug initially present in the dosage form 50 mg.

II.2.6.2.3 Cumulative release of loaded hydrogels

For the in vitro release evaluation, hydrogel samples loaded with vitamin C (VC) were initially incubated in 50 mL of simulated gastric fluid (GFS, pH 1.4) for 2 hours. Subsequently, the samples were transferred to 50 mL of simulated intestinal fluid (IFS, pH 6.8) and maintained therein until the release profile reached a plateau. All experiments were carried out at a constant temperature of 37 °C with continuous agitation at 50 rpm. At predetermined intervals, 200 µL of the release medium was collected and immediately replaced with an equal volume of fresh medium to ensure a constant total volume throughout the duration of the study. The concentration of VC released at each time point was determined by UV-Visible spectroscopy, using a standard calibration curve [7]. The cumulative release percentage of VC was then calculated using the following equation 9:

$$\text{Cumulative release (\%)} = \frac{V_e \sum_1^{n-1} C_i + V_0 C_n}{m_{vc}} \qquad (9)$$

Where

- $\mathbf{m_{vc}}$ the amounts of VC in the hydrogel
- $\mathbf{V_0}$ is the volume of the release medium 50 mL
- $\mathbf{C_n}$ concentration of VC in the n^{th} sample

References

[1] M. Afshar, G. Dini, S. Vaezifar, M. Mehdikhani, et B. Movahedi, « Preparation and characterization of sodium alginate/polyvinyl alcohol hydrogel containing drug-loaded chitosan nanoparticles as a drug delivery system », *J. Drug Deliv. Sci. Technol.*, vol. 56, p. 101530, 2020, doi: 10.1016/j.jddst.2020.101530.

[2] M. Huang, Y. Hou, Y. Li, D. Wang, et L. Zhang, « High performances of dual network PVA hydrogel modified by PVP using borax as the structure-forming accelerator », *Des. Monomers Polym.*, vol. 20, n° 1, p. 505-513, 2017, doi: 10.1080/15685551.2017.1382433.

[3] J. R. Witmer, B. J. Wetherell, B. A. Wagner, J. Du, J. J. Cullen, et G. R. Buettner, « Direct spectrophotometric measurement of supra-physiological levels of ascorbate in plasma », *Redox Biol.*, vol. 8, p. 298-304, 2016, doi: 10.1016/j.redox.2016.02.004.

[4] A. P. Desai, « UV Spectroscopic Method for Determination of Vitamin C (Ascorbic Acid) Content in Different Fruits in South Gujarat Region », *Int. J. Environ. Sci. Nat. Resour.*, vol. 22, n° 2, 2019, doi: 10.19080/IJESNR.2019.21.556056.

[5] X. Li, D. Chen, G. Wang, et Y. Lu, « Probing the interaction of human serum albumin with DPPH in the absence and presence of the eight antioxidants », *Spectrochim. Acta. A. Mol. Biomol. Spectrosc.*, vol. 137, p. 1144-1152, 2015, doi: 10.1016/j.saa.2014.08.140.

[6] J. K. Cherif, I. M'Rabet, M. El Habiri, R. Abidi, et A.-M. Albrecht-Gary, « Mesure de l'activité antiradicalaire du jus et des peaux d'oranges tunisiennes par le radical DPPH », *Fruits*, vol. 61, n° 2, p. 99-107, 2006, doi: 10.1051/fruits:2006008.

[7] X. Hu, Y. Wang, L. Zhang, et M. Xu, « Formation of self-assembled polyelectrolyte complex hydrogel derived from salecan and chitosan for sustained release of Vitamin C », *Carbohydr. Polym.*, vol. 234, p. 115920, 2020, doi: 10.1016/j.carbpol.2020.115920.

[8] A. M. Kaimal et R. S. Singhal, « Bigels for controlled gastric release of ascorbic acid: Impact on rheology, texture, thermal stability and antioxidant activity », *Food Hydrocoll. Health*, vol. 4, p. 100171, 2023, doi: 10.1016/j.fhfh.2023.100171.

RESULTS AND DISCUSSION

Part 1: Biohydrogels preparation

We studied the formulation and production yield of biohydrogels made from starch and PVA, crosslinked with $CaCl_2$. Diagrams were developed to show the structural formation of Starch/SA and PVA/SA hydrogel networks.

III.1.1 Formulation Parameters and Yield of Starch and PVA-based Biohydrogels Crosslinked with $CaCl_2$

Table III.1: Formulation parameters of Starch and PVA based biohydrogels crosslinked with $CaCl_2$

Hydrogel	Starch/SA%	PVA/SA%	$CaCl_2$ %	Hydrogel weight after gelation (g)	Weight of dry hydrogel (g)
(PVA/SA)Ca1	X	7/3	1	47.13	5.01
(PVA/SA)Ca3	X	7/3	3	48.74	5.36
(St/SA)Ca1	7/3	X	1	49.03	5.82
(St/SA)Ca3	7/3	X	3	48.48	5.14

Table III.2: Formulation parameters of freeze-thaw Starch and PVA based biohydrogels Crosslinked with CaCl2

Hydrogel	Starch/SA %	PVA/SA %	$CaCl_2$ %	Hydrogel weight after gelation (g)	Weight of dry hydrogel (g)
F/T(PVA/SA)Ca3	X	70/30	3	21.02	1.26
F/T(St/SA)Ca3	70/30	X	3	9.91	0.78

The tables III.1 and III.2 correspond to the hydrogel masses recorded immediately after gelation and after drying, allowing for an evaluation of the efficiency and consistency of

the synthesis process. All formulations, whether based on PVA/SA or St/SA and using 1% or 3% $CaCl_2$ as the crosslinking agent, resulted in comparable gelation weights, suggesting uniform water absorption and successful network formation.

Differences in dry weight reflect the impact of polymer type and crosslinker concentration on the solid content retained after drying. Starch-based hydrogels generally showed slightly higher dry weights compared to their PVA counterparts in the first table, which may indicate higher polymer incorporation or stronger network density in starch formulations.

In the Table III.2, here the formulations were standardized by volume percentage, the PVA/SA hydrogel F/T(PVA/SA)Ca3 yielded significantly higher values for both gelation and dry mass than the starch/SA formulation F/T(St/SA)Ca3. This suggests that under the same preparation conditions, the PVA-based system forms a more robust gel matrix, retaining more solid material after drying.

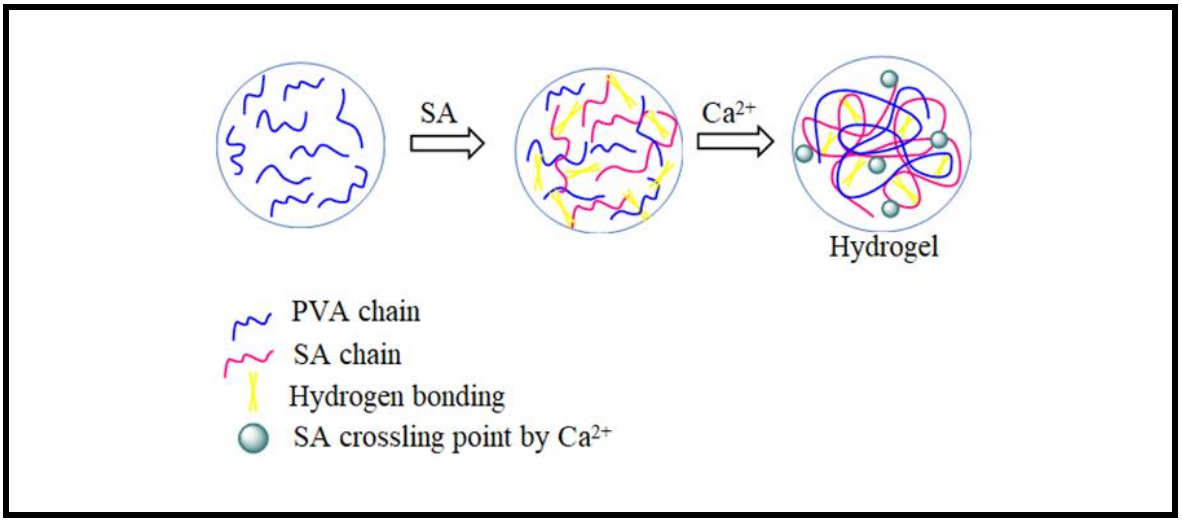

Figure III.1.1.1: Formation of PVA/SA biohydrogel crosslinked by Ca^{2+}.

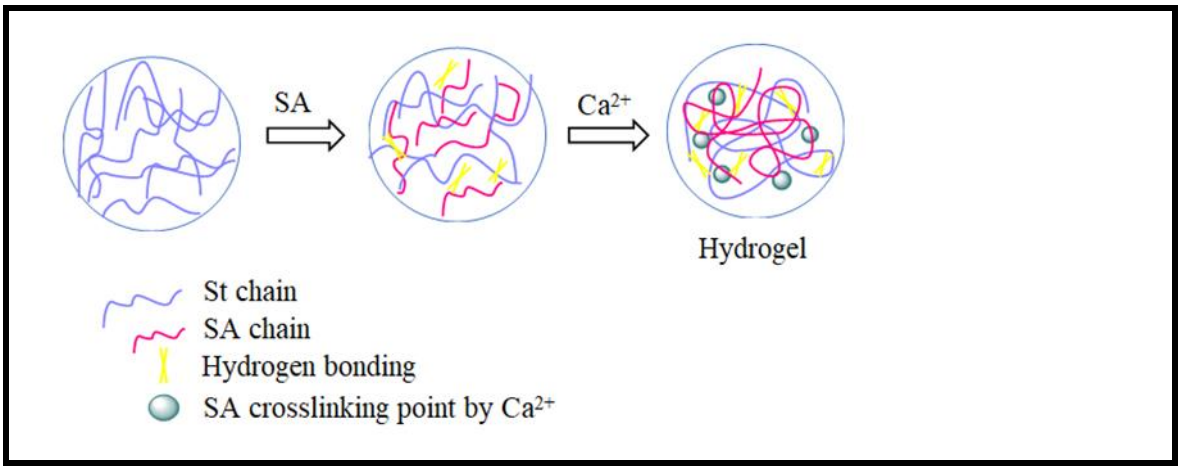

Figure III.1.1.2: Formation of St/SA biohydrogel crosslinked by Ca^{2+}.

Part 2: Study of bio hydrogels

III.2.1 Swelling test

A swelling study was carried out on various hydrogels crosslinked with different concentrations of $CaCl_2$ to evaluate their behavior in different pH environments. The results obtained in acidic (pH 3), neutral (pH 7), and alkaline (pH 9) media are presented from Figure III.2.1.1 to Figure III.2.1.12

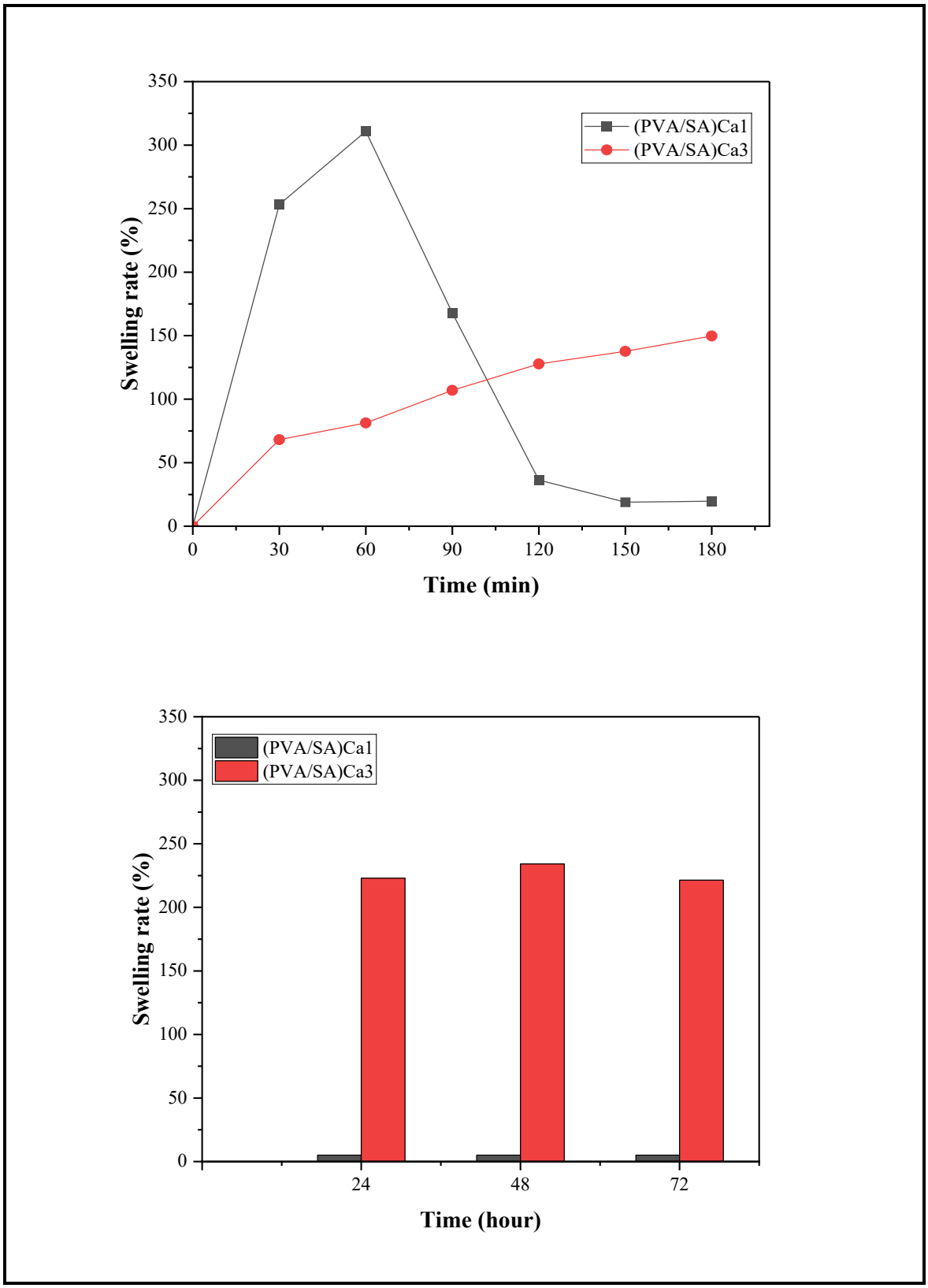

Figure III.2.1.1: Swelling behavior of the PVA biohydrogels as a function of time at pH 3, under constant temperature 25°C.

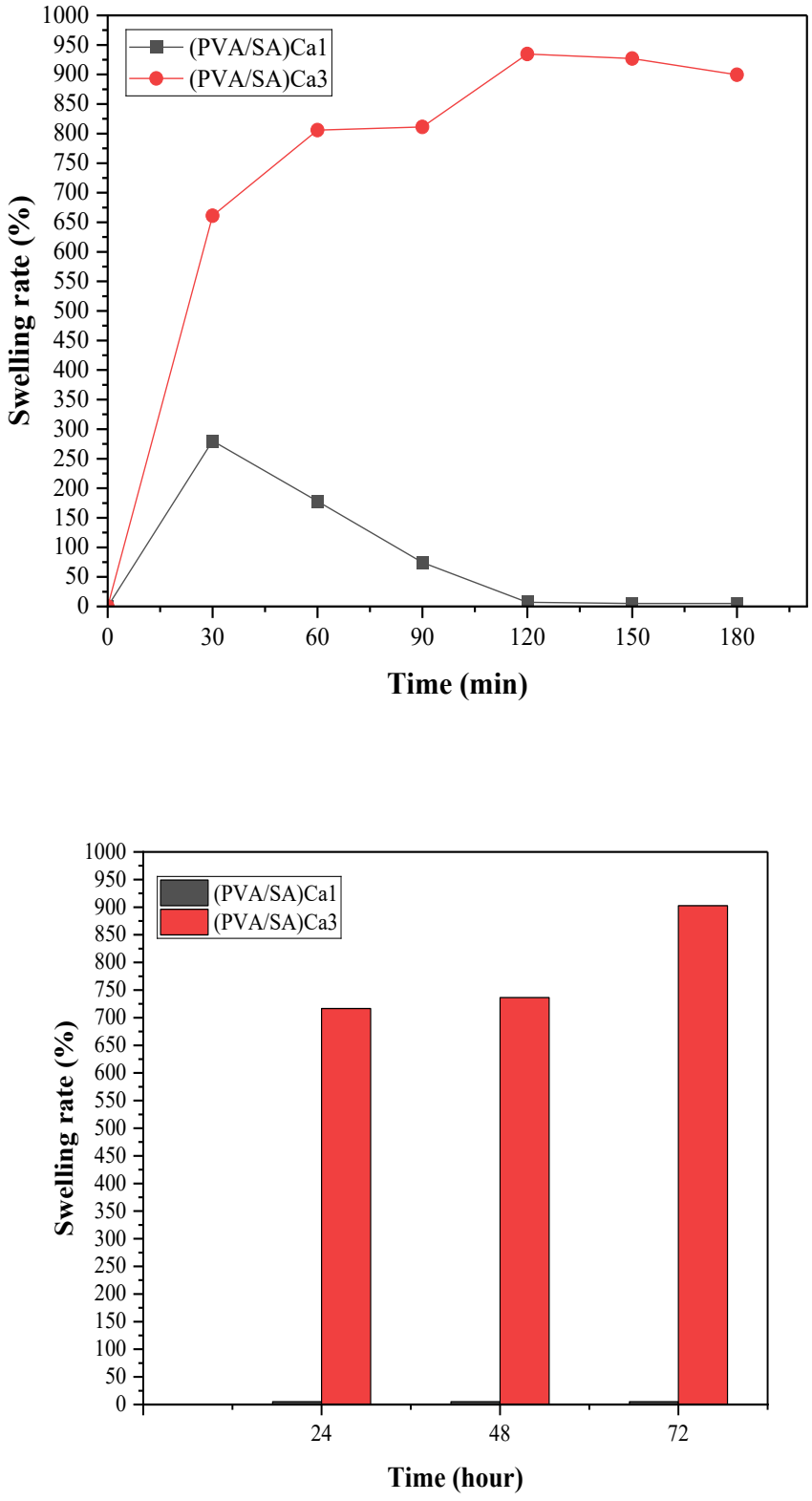

Figure III.2.1.2: Swelling behavior of the PVA biohydrogels as a function of time at pH 7, under constant temperature 25°C.

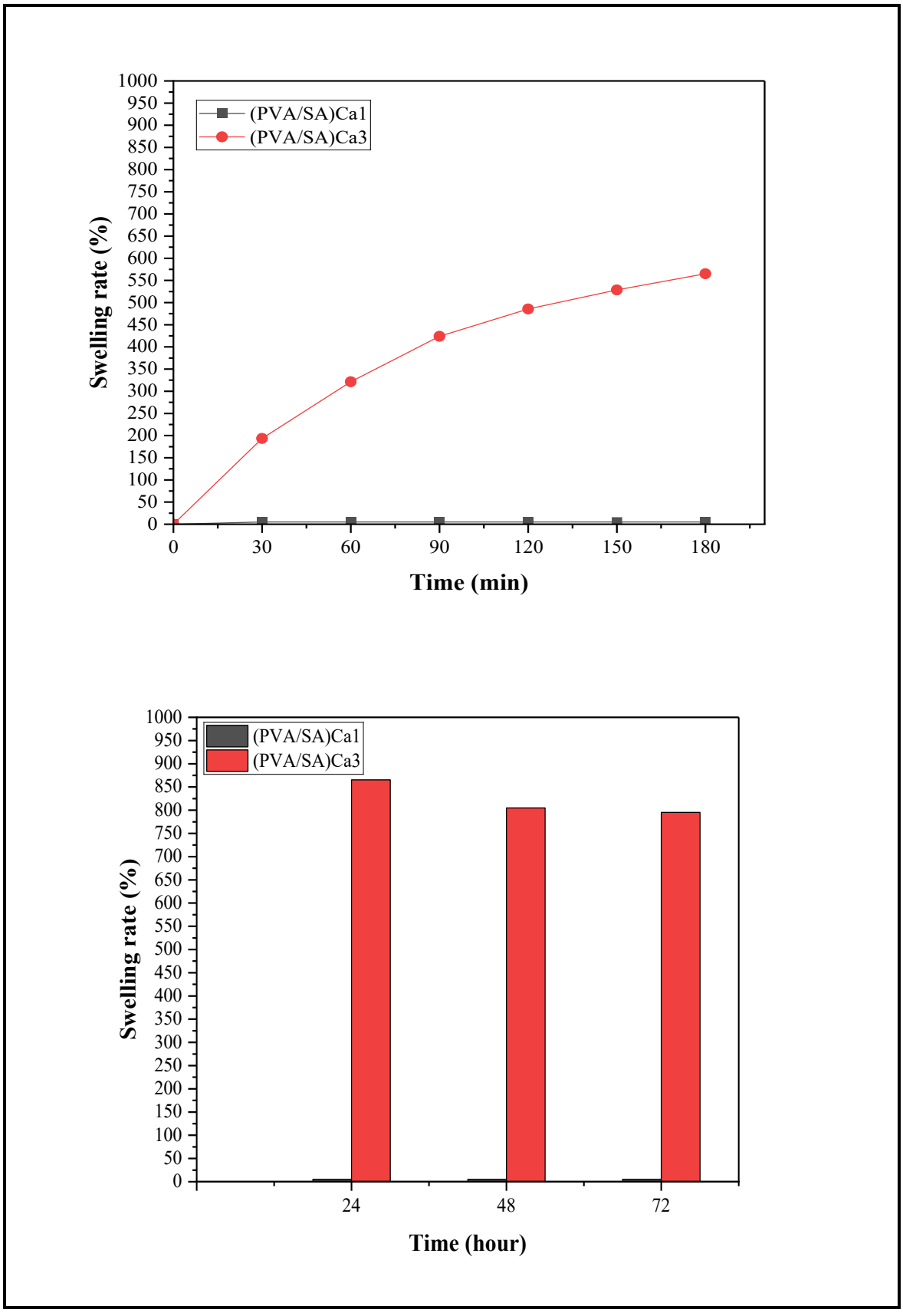

Figure III.2.1.3: Swelling behavior of the PVA biohydrogels as a function of time at pH 9, under constant temperature 25°C.

The study of the swelling of 1% and 3% PVA hydrogels at pH 3, 7 and 9 reveals a strong pH dependency: at pH 3, PVA 1% swells rapidly (310.85% at 60 min) but decays, while PVA 3% is more stable with maximum swelling at 48h (234.16%). At pH 7, PVA 1% disintegrates after initial swelling (280.26% at 30 min), while PVA 3% reaches high maximum swelling at 120 min (934.52%) with a peak at 72 h (902.78%). At pH 9, PVA 1% degrades rapidly, and PVA 3% shows maximum swelling at 24 h (865.4%) after swelling at 180 min (565.06%). These results underline the significant impact of pH and concentration on the stability and swelling capacity of PVA hydrogels.

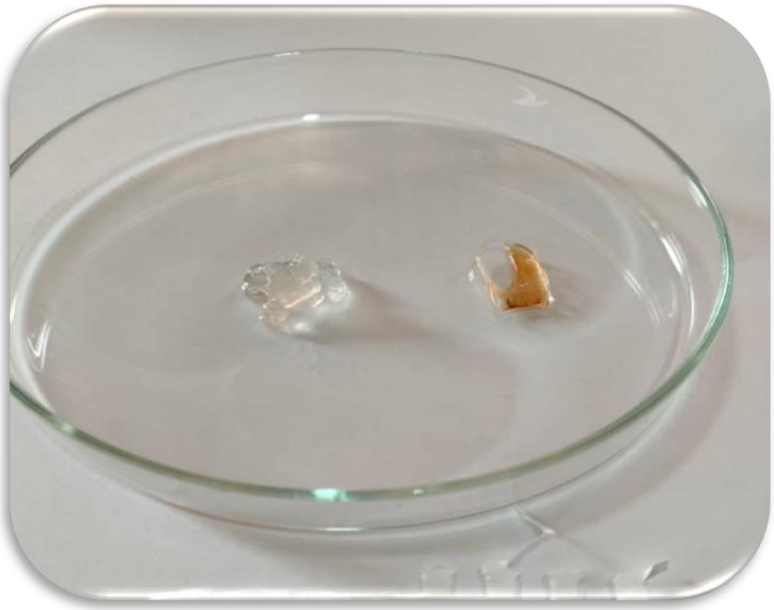

Figure III.2.1.4: Dry and Swollen States pf (PVA/SA)Ca3 biohydrogel after 48 h at pH 7 at 25°C.

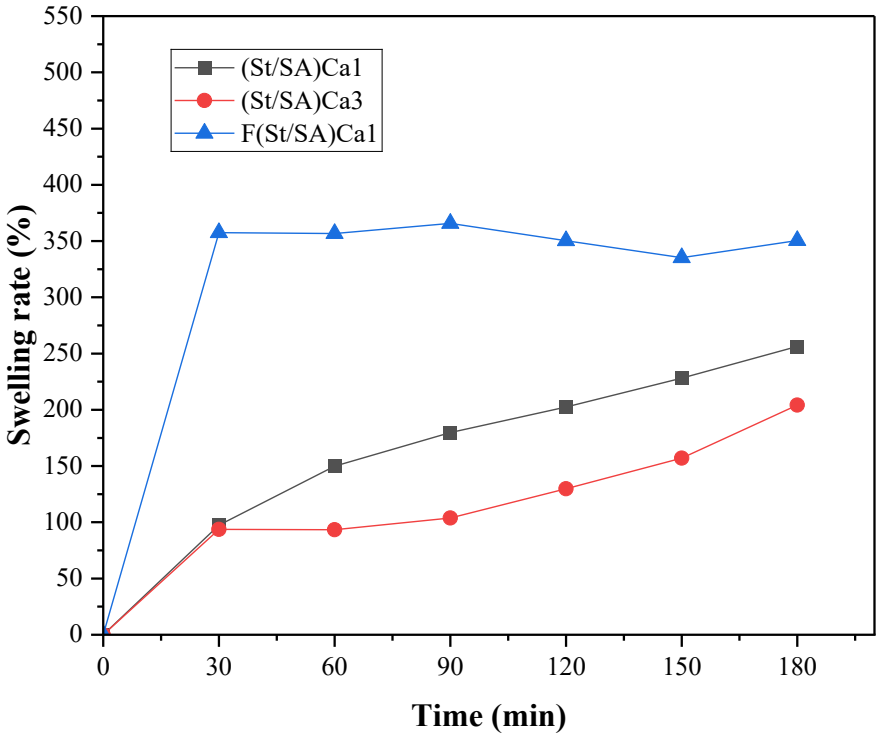

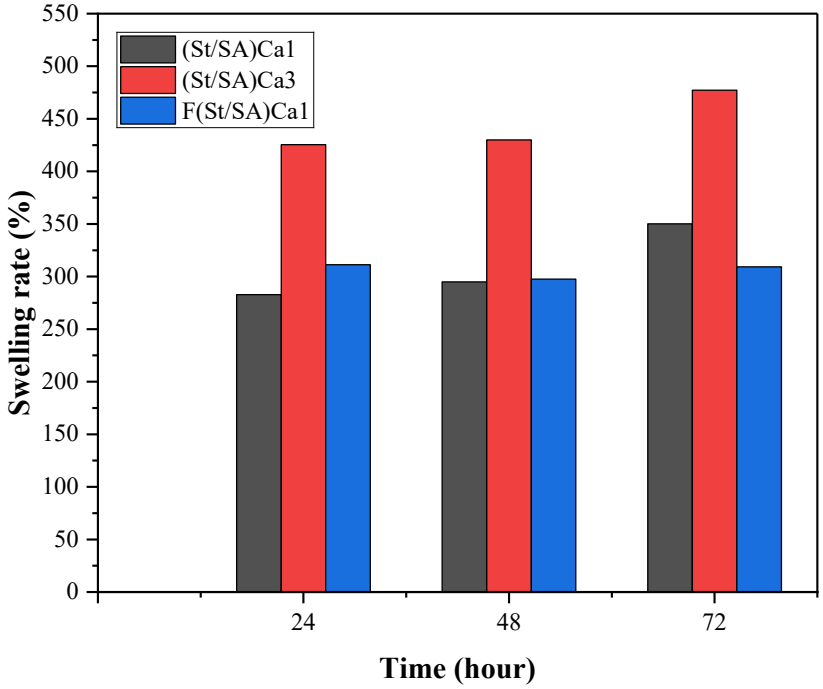

Figure III.2.1.5: Swelling behavior of the Starch biohydrogels as a function of time at pH 3, under constant temperature conditions 25°C.

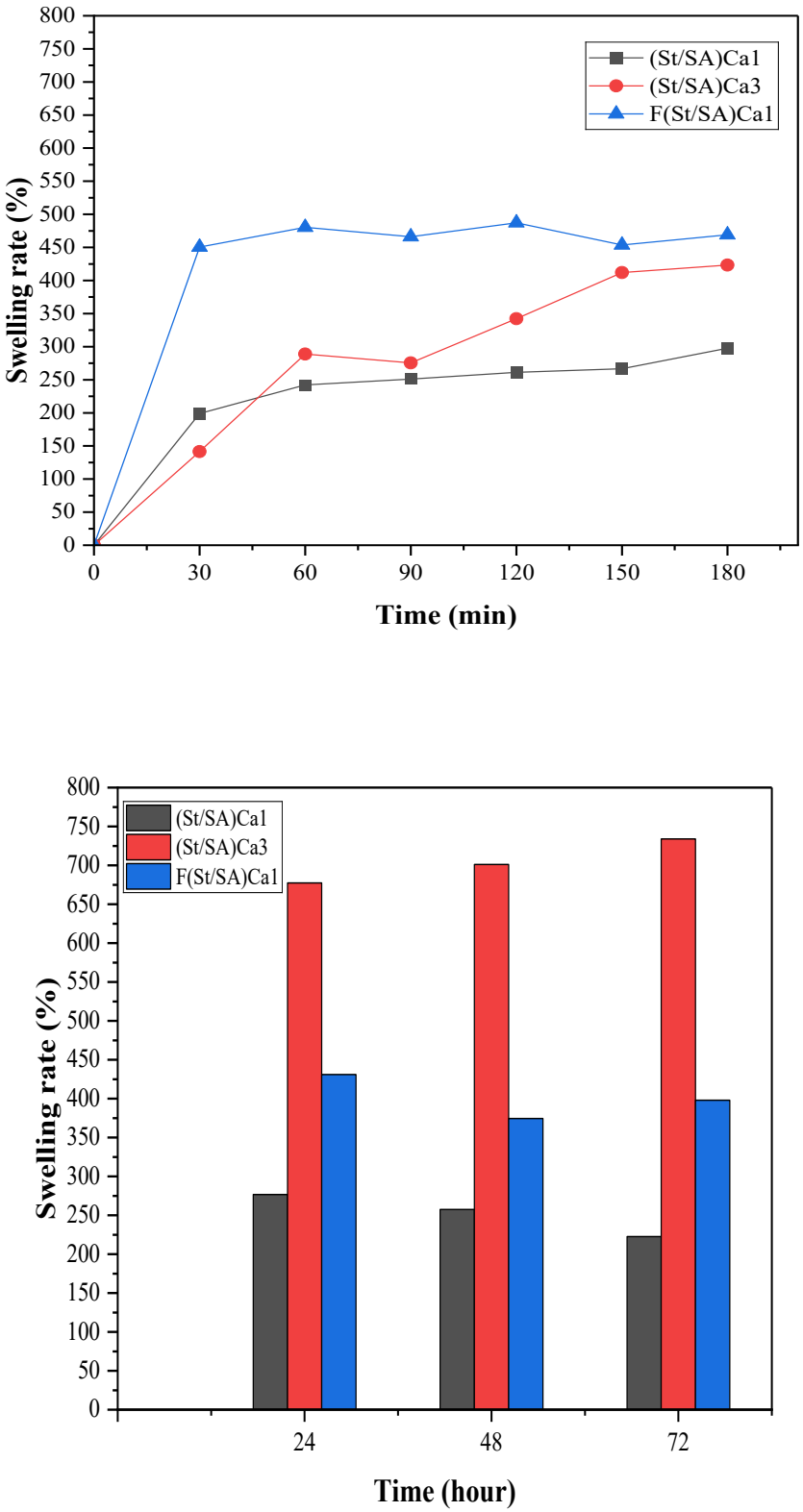

Figure III.2.1.6: Swelling behavior of the Starch Biohydrogels as a function of time at pH 7, under constant temperature conditions 25°C.

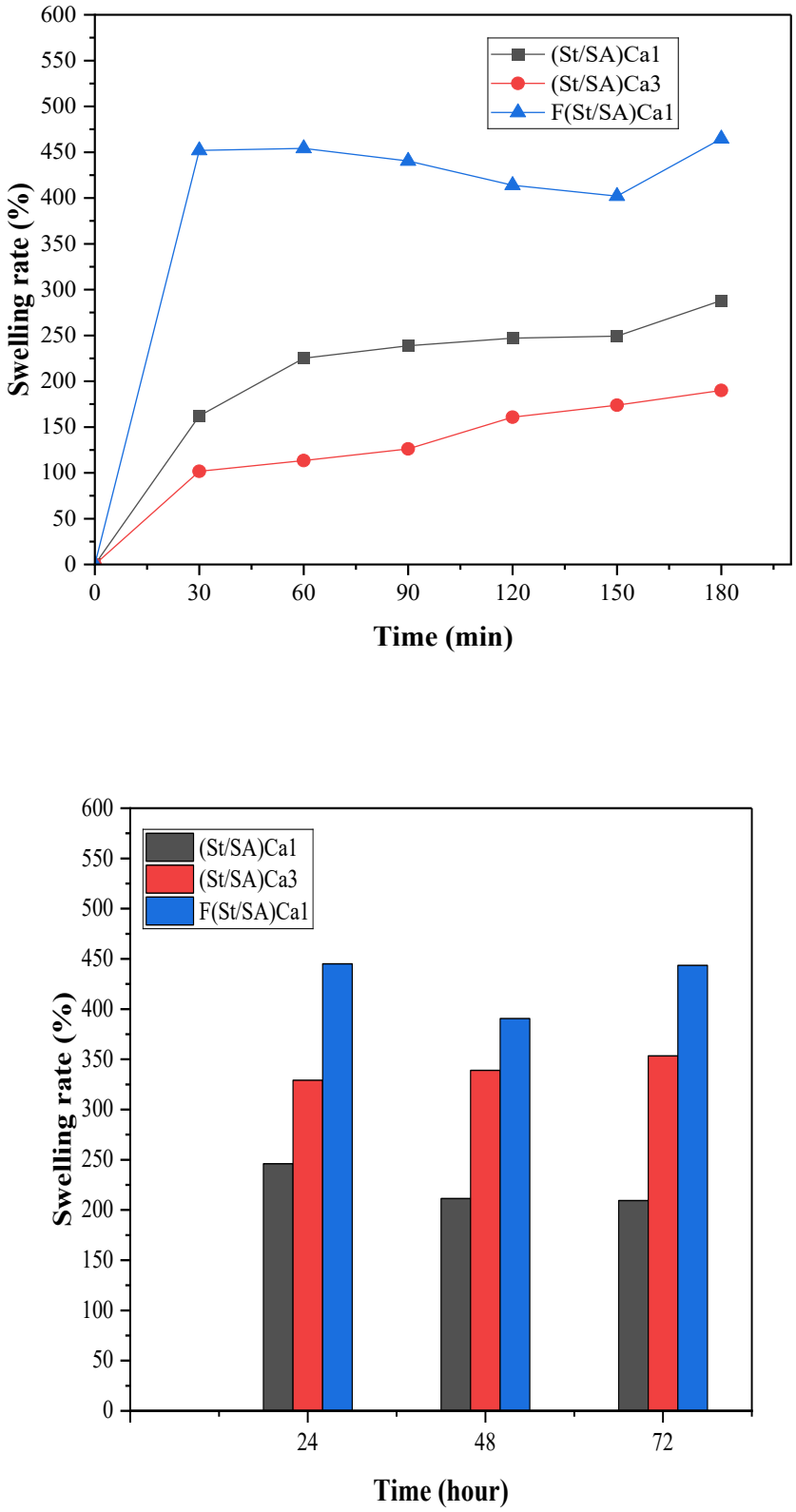

Figure III.2.1.7: Swelling behavior of the Starch biohydrogels as a function of time at pH 9, under constant temperature conditions 25°C.

The study of the swelling of 1% and 3% starch (St) and film St hydrogels at pH 3, 7 and 9 reveals a strong pH dependency: at pH 3, Film St 1% swells rapidly (365.59% at 30 min), while St 3% reaches a maximum at 72 h (477.17%). At pH 7, Film St 1% swells significantly (487.06% at 120 min), while St 3% reaches higher swelling at 72 h (733.92%). At pH 9, Film St 1% reaches 464.72% at 180 min, while St 3% continues to swell, achieving a maximum at 72 h (353.37%). These results underline the significant impact of pH, polymer type, and concentration on the swelling behavior of starch-based hydrogels.

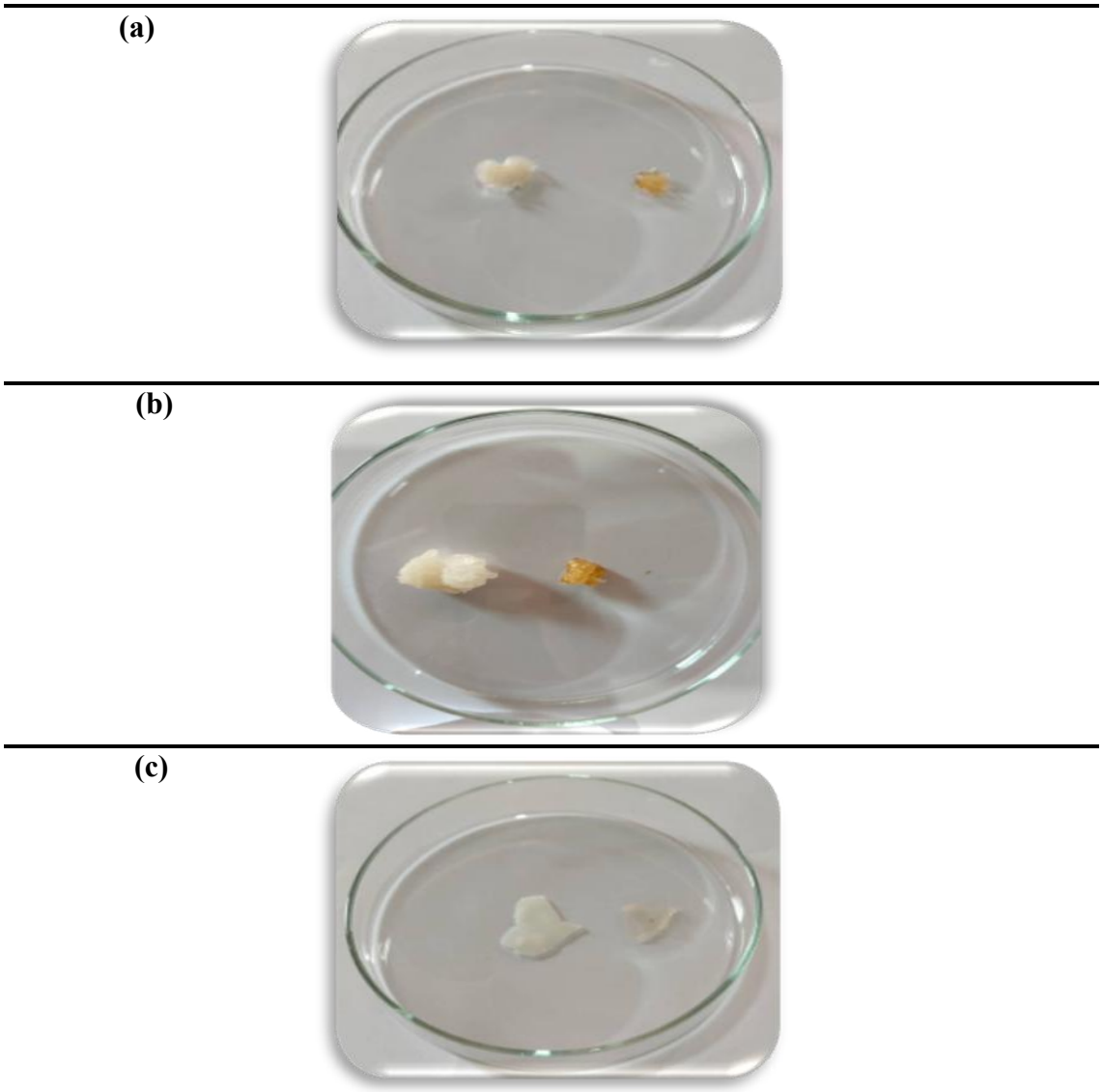

Figure III.2.1.8: Dry and Swollen states of **(a)** (St/SA)Ca1 and **(b)** (St/SA)Ca3 and **(c)** F(St/SA)Ca1 biohydrogels after 48 h at pH 7 at 25°C.

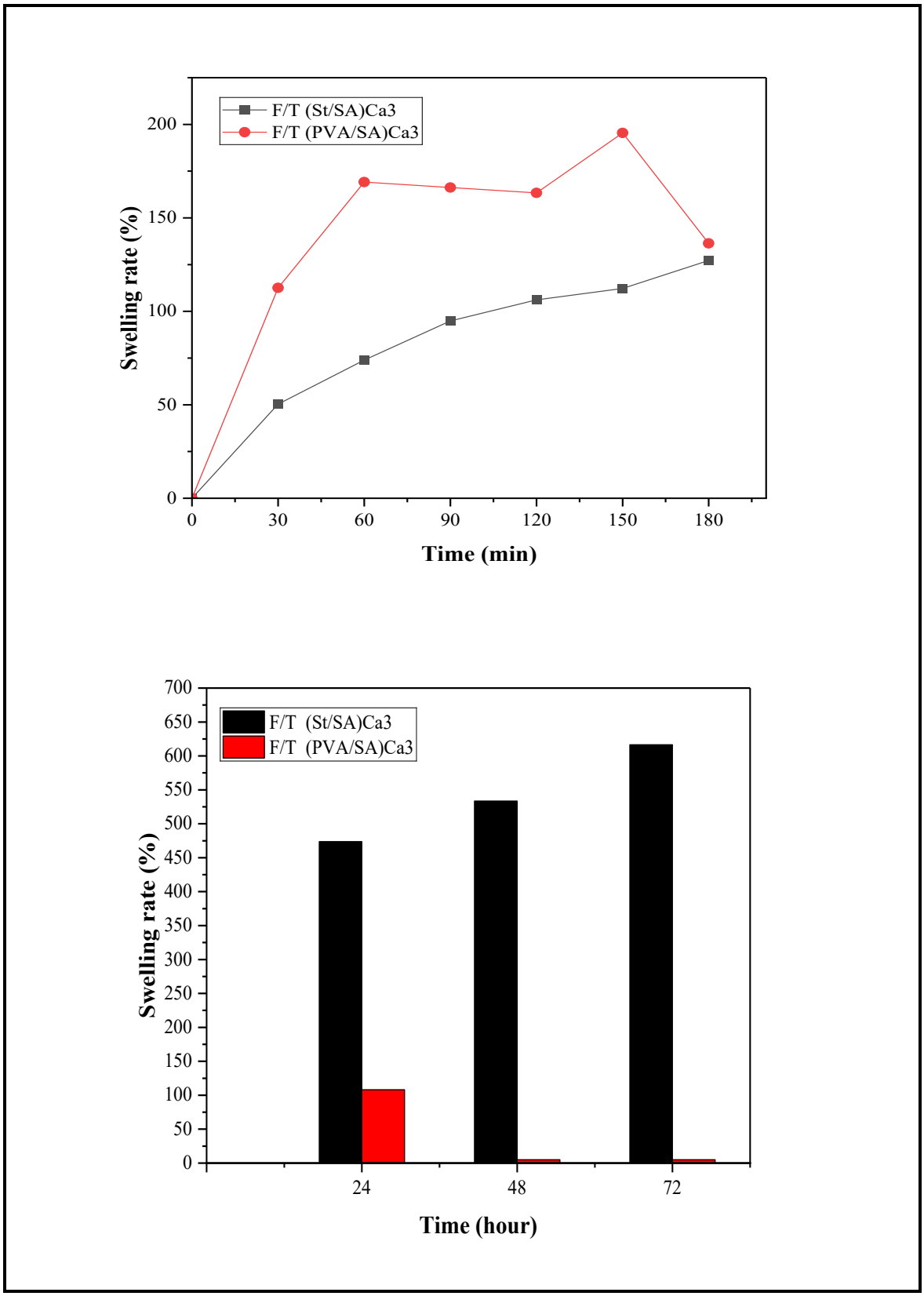

Figure III.2.1.9: Swelling behavior of the PVA, Starch biohydrogels prepared via the freezing-thawing method as a function of time at pH 3, under constant temperature conditions 25°C.

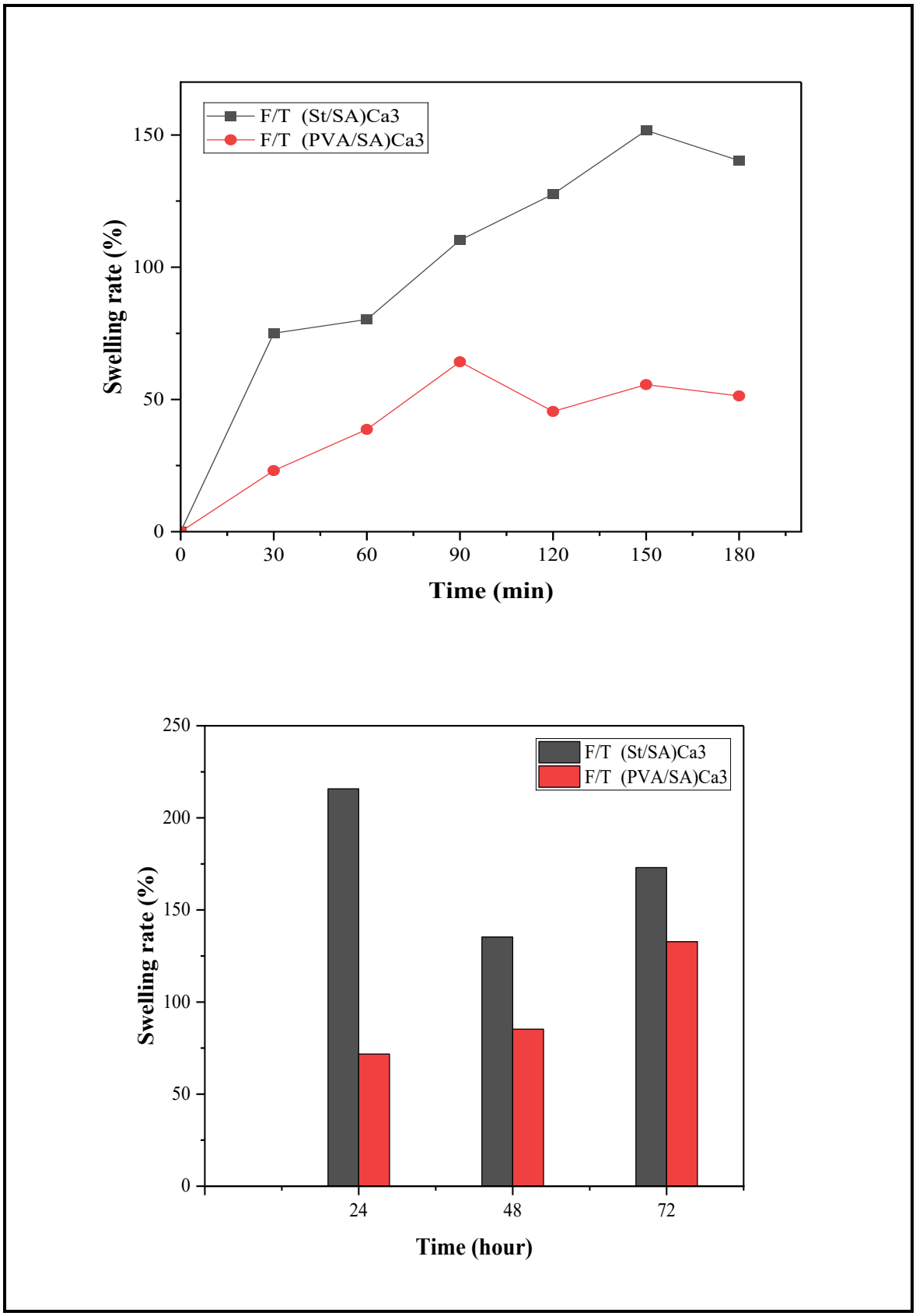

Figure III.2.1.10: Swelling behavior of the PVA, Starch biohydrogels via the freezing-thawing method as a function of time at pH 7, under constant temperature Conditions 25°C.

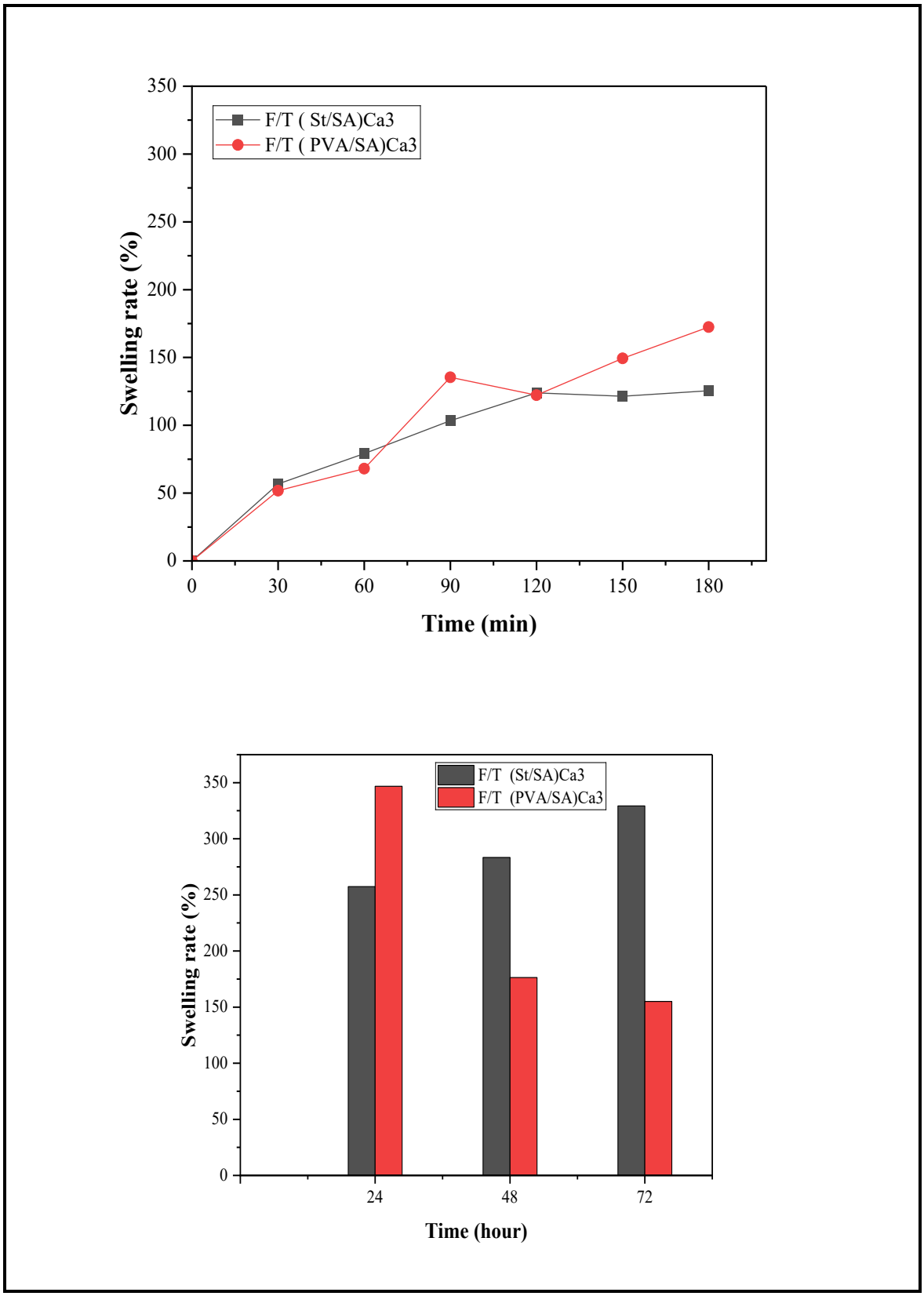

Figure III.2.1.11: Swelling behavior of the PVA, Starch biohydrogels prepared via the freezing-thawing method as a function of time at pH 9, under constant temperature conditions 25°C.

The swelling analysis of 3% F/T PVA and F/T St hydrogels at pH 3, 7 and 9 reveal distinct behaviors: at pH 3, F/T PVA swells to 195.44% at 150 min before degradation, while F/T St reaches 127.23% at 180 min and peaks at 616.48% at 72 h. At pH 7, F/T PVA shows a low initial maximum swelling (64.2% at 90 min) increasing to 132.81% at 72h, while F/T St peaks at 151.73% at 150 min and 215.75% at 24 h. At pH 9, F/T PVA swells to 172.44% at 180 min with a maximum of 346.80% at 24 h, and F/T St reaches 125.48% at 180 min with a peak of 329.32% at 72 h. These Figures underline the significant influence of polymer composition and pH on the swelling and stability of hydrogels prepared by freeze-thawing.

(a)

(b)

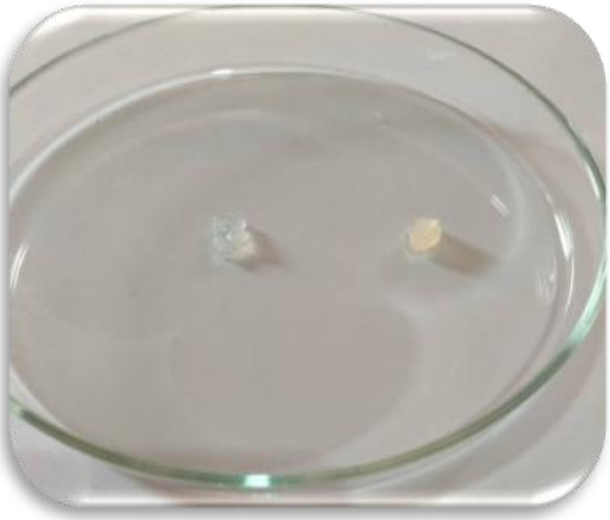

Figure III.2.1.12: Dry and Swollen states of **(a)** F/T(St/SA)Ca3 and **(b)** F/T (PVA/SA)Ca1 biohydrogels after 48 h at pH 7 at 25°C.

Table III.3: Maximum swelling rate of biohydrogels at diffrent pH values

Hydrogel	pH		
	3	**7**	**9**
(St/SA)Ca1	350.05 %	297.73 %	288.14 %
(St/SA)Ca3	477.17 %	733.92 %	353.37 %
F(St/SA)Ca1	364.69 %	487.06 %	464.72 %
(PVA/SA)Ca1	310.85 %	280.26 %	X
(PVA/SA)Ca3	234.16 %	934.52 %	856.4 %
F/T (St/SA)Ca3	616.48 %	215.75 %	329.32 %
F/T (PVA/SA)Ca3	195.44 %	132%	346.8 %

X: Our hydrogel dissolved within the first few minutes

As the Table III.3 is showing the swelling behavior of biohydrogels is profoundly influenced by both crosslinking agent concentration and preparation method. For (St/SA) biohydrogels, increasing $CaCl_2$ concentration from 1% to 3% led to higher maximum swelling rate, with (St/SA)Ca3 showing 733.92% swelling at pH 7 versus 297.73% for (St/SA)Ca1. A higher concentration of $CaCl_2$ leads to a more extensive and robust three-dimensional network. This denser, more interconnected structure can effectively entrap a larger volume of water molecules within its matrix resulting in higher swelling ratios.

Similarly, PVA/SA hydrogels showed notable swelling increases with higher $CaCl_2$ concentrations, particularly at pH 7 and 9, where (PVA/SA)Ca3 swelled to 934.52% and 856.40% respectively, while (PVA/SA)Ca1 completely dissolved at pH 9. The primary crosslinking mechanism remains ionic interaction between Ca^{2+} and alginate. While PVA itself does not ionically crosslink with Ca^{2+}, its hydroxyl groups can form hydrogen bonds with alginate, contributing to the overall network stability and further enhancing water retention. A more stable and highly crosslinked alginate network, reinforced by PVA's presence, leads to a greater capacity for water.

Preparation method significantly affected swelling behavior. For St/SA biohydrogels, the normal method produced higher swelling at pH 7, 733.92% and pH 9, 353.37% compared to freezing-thaw method 215.75% and 329.32%. However, at pH 3, freezing thaw yielded higher swelling 616.48% vs 477.17%. The differences observed with the freezing-thaw method are attributed to its impact on the internal morphology of the hydrogel. Freezing-

thawing cycles can induce phase separation and lead to the formation of a more heterogeneous, often macroporous, structure. At pH 7 and 9, the normal method likely produces a more uniform and hydrophilic network for St/SA, optimizing the interaction with water. The reduction in swelling for F/T (St/SA)Ca3 at these pH values might suggest that the freezing-thaw process leads to denser, less accessible regions for water, or that the specific crosslinking points formed by Ca^{2+} are less effective in a phase-separated network. Conversely, the superior swelling at pH 3 for F/T (St/SA)Ca3 suggests that the acidic environment, coupled with the macroporous structure induced by freezing thawing, may enhance chain relaxation and water absorption. In acidic conditions, some carboxyl groups on the alginate may become protonated, reducing electrostatic repulsion and potentially allowing the more porous structure to imbibe a larger volume of water.

For PVA/SA, the freezing-thaw method generally resulted in lower swelling rates across most pH values when comparing (PVA/SA)Ca3 to F/T(PVA/SA)Ca3. For instance, at pH 7, (PVA/SA)Ca3 swelled to 934.52%, whereas F/T(PVA/SA)Ca3 only reached 132%. However, at pH 9, F/T (PVA/SA)Ca3 exhibited a substantial 346.80% swelling. The generally lower swelling of F/T(PVA/SA)Ca3 compared to (PVA/SA)Ca3 is likely due to the dominant effect of physical crosslinking within the PVA component during freezing-thawing. PVA is well-known for forming strong hydrogen bonds and developing microcrystalline regions upon repeated freezing and thawing cycles. This physical crosslinking creates a denser, more rigid network that significantly restricts polymer chain mobility and hinders the uptake of water, thereby leading to lower swelling ratios. Despite the presence of ionically crosslinked alginate, the strong physical crosslinking of PVA appears to be the dominant factor in limiting swelling. The exception at pH 9 for F/T(PVA/SA)Ca3 suggests a unique interaction at this alkaline pH. It is possible that the increased deprotonation of carboxyl groups in the sodium alginate at high pH leads to significant electrostatic repulsion within the network. This internal repulsive force, even in the physically crosslinked PVA/SA network, might be sufficient to overcome some of the constricting effects of physical crosslinking, allowing for a greater degree of chain expansion and subsequent water absorption at this specific pH.

III.2.2 Fourier Transform Infrared Spectroscopy FTIR

The purpose of the FTIR analysis performed on our hydrogels is to identify their characteristic absorption bands and compare them with those reported in the literature. The corresponding results are presented in Figures III.2.2.1 and III.2.2.2.

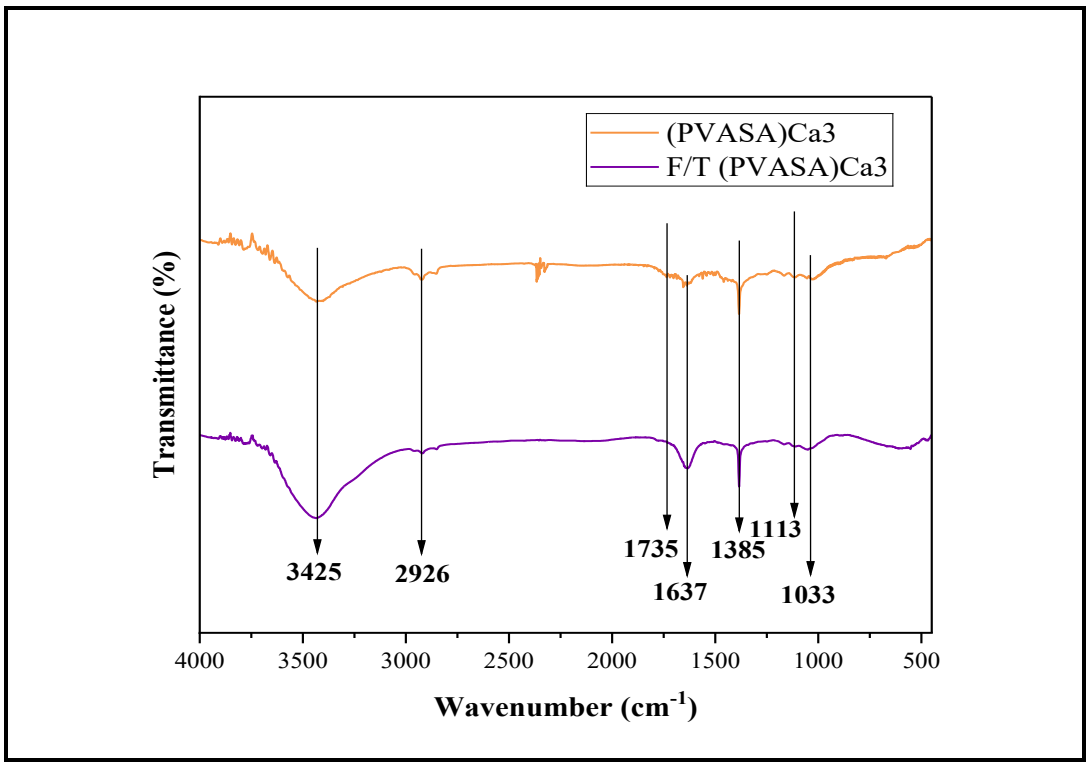

Figure III.2.2.3: FTIR spectroscopic analysis of PVA/SA biohydrogels.

Table III.4: FTIR spectroscopic analyses of PVA/SA biohydrogels

Wavenumber (cm^{-1})		Functional Group
Research	Literature [1,2]	
3425	3424 - 3444	-OH (stretch)
2926	2924 - 2960	CH2 (stretch) symmetrically and asymmetrically
1736	1733	C = O (stretch)
1637	1617	COO^- asymmetrically
1385	1417	COO^- symmetrically
1033 - 1113	1030	C-O-C (stretching)

PVA/alginate hydrogels crosslinked with 3% $CaCl_2$, prepared either by the conventional method (PVA/SA)Ca3 or by freeze-thaw cycles F/T(PVA/SA)Ca3, exhibit characteristic FTIR spectra (Figure III.1.2.1). A broad peak centered at 3425 cm^{-1} corresponds to O–H stretching vibrations, indicating a significant presence of hydrogen bonds. The peak at 2926 cm^{-1} is assigned to C–H vibrations of methylene (CH_2) groups in PVA. A distinct peak appears at 1736 cm^{-1}, attributed to C=O stretching vibrations. The bands observed at 1637 cm^{-1} and 1385 cm^{-1} correspond to asymmetric and symmetric vibrations of carboxylate (COO^-) groups, confirming the ionic crosslinking with Ca^{2+} ions. Finally, the spectral region between 1033 and 1113 cm^{-1} is characteristic of C–O–C linkages in the polysaccharide structure.

Although the spectra from both preparation methods are largely similar, the hydrogels obtained via freeze-thaw cycles display more intense bands, especially in the O–H and COO^- regions. This suggests enhanced molecular organization and a higher degree of crosslinking. These findings are consistent with literature reports (Table III.4) and confirm the efficiency of both synthesis routes.

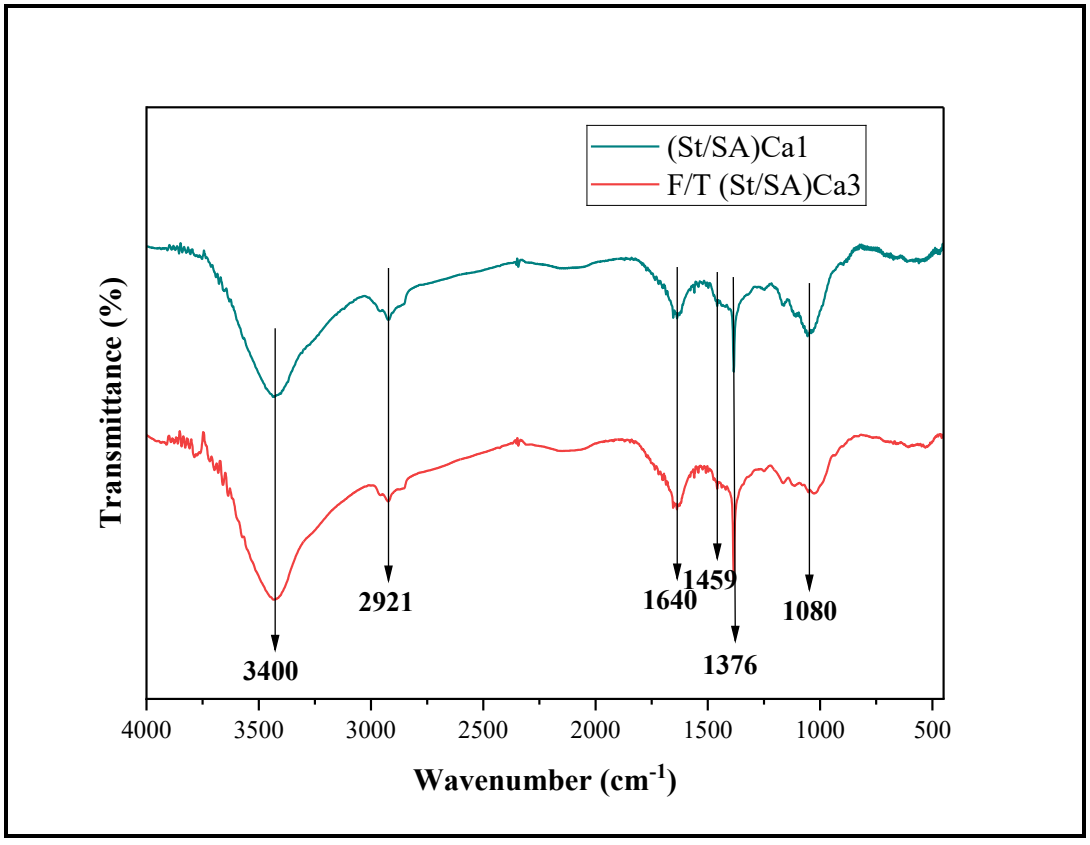

Figure III.4.2.2: FTIR spectroscopic analysis of St/SA biohydrogels.

Table III.5: FTIR spectroscopic analyses of St/SA biohydrogels

Wavenumber (cm^{-1})		Functional Group
Research	Literature [2,3]	
3400	3291	-OH (stretch)
2921	2926	C-H (stretch)
1640	1617	COO^- asymmetrically
1459	1417	COO^- symmetrically
1376	1372	CH_2 , CH
1080	1151	C-O-C (stretching)

Both spectra show a broad peak centered around 3400 cm-¹, characteristic of O-H bond elongation vibrations, reflecting the abundant presence of hydroxyl groups and the formation of a network of hydrogen bonds between the starch and alginate chains.

The peak at 2921 cm-¹ corresponds to the C-H vibrations of the methylene groups. Two notable bands appear at 1640 cm-¹ (asymmetric vibration) and 1459 cm-¹ (symmetric vibration), associated with carboxylate groups (COO^-), confirming the ionic interaction between sodium alginate and Ca^{2+} ions. The peak at 1376 cm-¹ is attributed to deformation vibrations of CH_2/CH_3 groups, while that at 1080 cm-¹ corresponds to C-O-C vibrations typical of starch glycosidic bonds.

Although the spectra are broadly similar, differences in intensity are observed. The F/T(St/SA)Ca3 hydrogel shows more intense bands, particularly in the regions corresponding to hydrogen bonds (O-H) and carboxylates (COO-), suggesting a higher degree of cross-linking induced by the freeze-thaw method. These observations are consistent with literature data (Table III.5) and confirm the combined structuring effect of ionic cross-linking and heat treatment on hydrogel network architecture.

III.2.3 X-ray Fluorescence XRF

XRF analysis was carried out to determine the elemental composition of the raw materials and the synthesized hydrogels. The chemical elements identified in PVA, Starch, and Sodium Alginate are presented in Table III.6, while those detected in the different hydrogel formulations are shown in Table III.7.

Table III.6: The chemical elements present in PVA, Starch and Sodium Alginate

	PVA	Starch	S Alginate
Bal	96.772	97.839	94.988
Ca	0.155	0.112	1.035
Si	2.235	1.443	2.667
Cl	0.139	0.113	0.356

Table III.7: The chemical elements present in the biohydrogels

	(St/SA)Ca1 (%)	(PVA/SA)Ca3 (%)	F/T(St/SA)Ca3 (%)	F/T(PVA/SA)Ca3 (%)
Bal	94.744	90.481	89.579	87.568
Ca	2.226	5.860	7.866	10.091
Si	1.459	1.256	0.923	1.010
Cl	1.030	2.145	1.470	1.192

The elemental composition of both the raw materials and the synthesized hydrogels was evaluated using X-ray fluorescence (XRF), with the results summarized in Tables III.6 and III.7. The raw materials polyvinyl alcohol (PVA), Starch, and Sodium Alginate show a predominance of light elements such as carbon and oxygen, which are not directly quantified due to the limitations of XRF in detecting low atomic number elements. Their presence is instead reflected in the high balance (Bal) values. Notably, sodium alginate exhibited a higher native calcium content (1.035%) compared to starch (0.112%) and PVA (0.155%), consistent with its natural origin and its known association with calcium ions.

Following crosslinking with calcium chloride ($CaCl_2$), all hydrogel formulations (St/SA)Ca1, (PVA/SA)Ca3, F/T(St/SA)Ca3, and F/T(PVA/SA)Ca3 demonstrated a clear increase in calcium concentration, confirming the effective incorporation of Ca^{2+} ions into

the polymer networks. The variation in calcium levels among the different hydrogel types suggests differences in crosslinking density and affinity for calcium, potentially influenced by the polymer composition and synthesis conditions, such as freeze–thaw cycles

Overall, the XRF analysis validates the successful crosslinking of the hydrogel matrices with $CaCl_2$ and highlights the impact of polymer type and processing method on elemental incorporation. These findings provide essential insight into the structural and chemical integrity of the developed hydrogel systems and support the subsequent physico-chemical characterizations.

III.2.4 X-Ray Diffraction XRD

X-ray diffraction (XRD) is an essential analytical technique for characterizing the crystal structure and molecular organization of polymers and hydrogels. It reveals structural variations linked to material composition and preparation methods, such as freeze-thaw. In this section, DRX profiles of base polymers (PVA, Starch, Sodium Alginate) and synthesized hydrogels, prepared with or without the freeze-thaw method, are presented and analyzed (Figures III.2.4.1 to III.2.4.3). These results provide key information on the crystallinity and internal organization of hydrogel networks, crucial parameters influencing their functional properties.

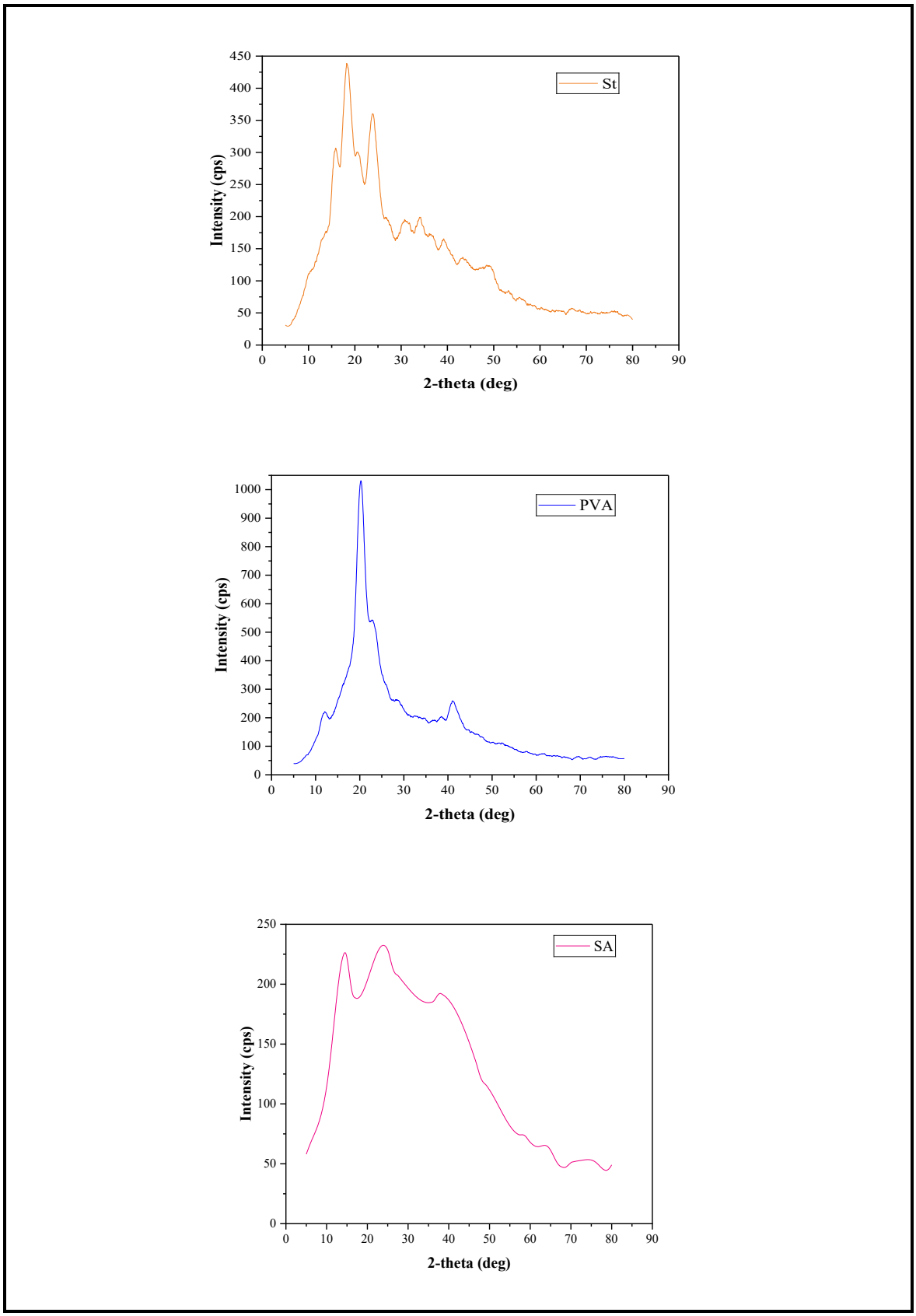

Figure III.2.4.1: X-ray Diffraction (XRD) patterns for the structural characterization of PVA, Starch and Sodium Alginate.

Figure III.2.4.1 presents X-ray diffraction (XRD) patterns of the base polymers: PVA, Starch, and Sodium Alginate. Starch shows sharp and distinct peaks in the 2θ range of 15–25°, revealing a well-defined semi-crystalline structure. PVA exhibits a relatively intense but broader peak near 2θ ≈ 19°, which is characteristic of moderate crystallinity. In contrast, Sodium Alginate displays a diffuse pattern with broad and low-intensity peaks, indicative of an amorphous structure. These variations reflect the intrinsic structural organization of each polymer, which can significantly affect the performance of hydrogels in terms of crosslinking efficiency, swelling capacity, and mechanical integrity.

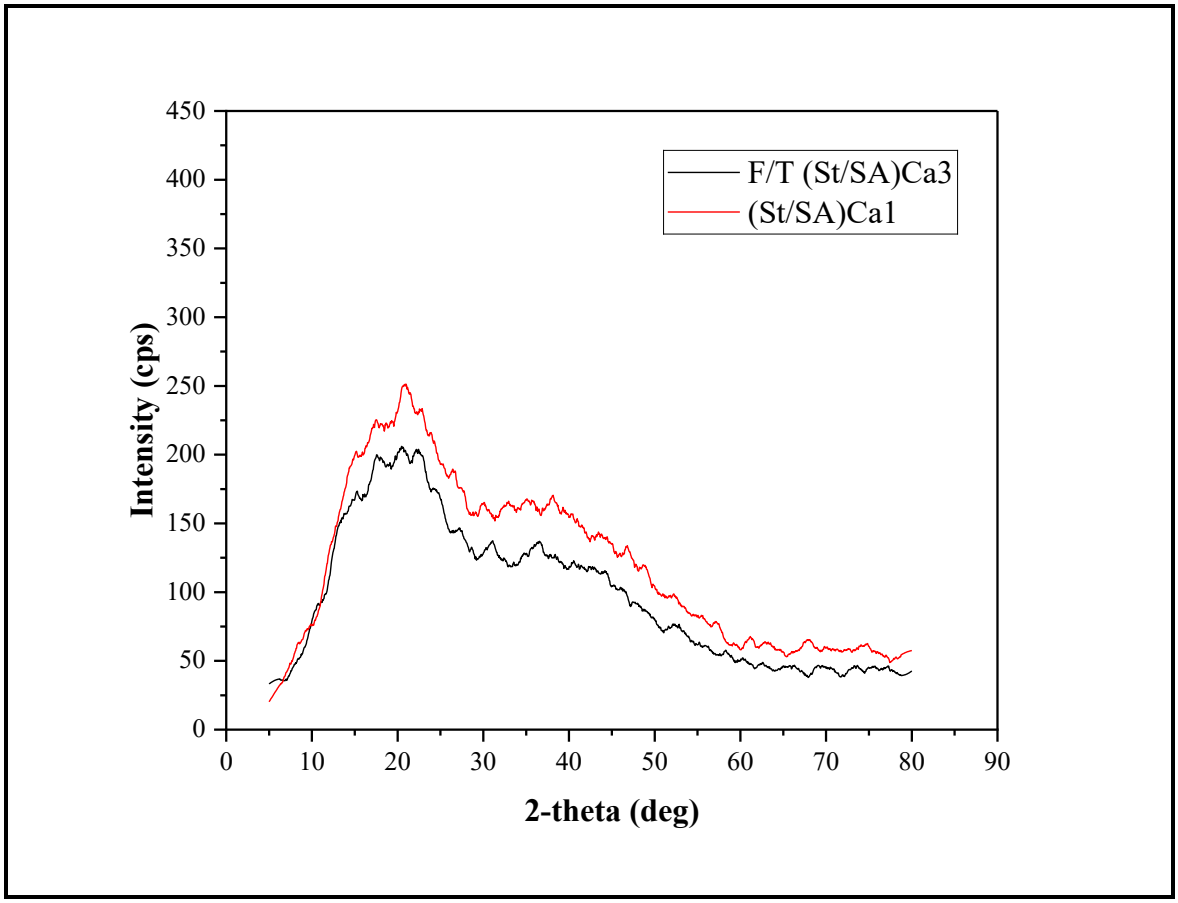

Figure III.2.4.2: Structural characterization of freeze-thawed Starch/Sodium Alginate biohydrogel and Starch/Sodium Alginate biohydrogel by X-Ray Diffraction (XRD).

Analysis of XRD diffractograms (Figure III.2.4.2) compares $CaCl_2$ crosslinked Starch/Sodium Alginate hydrogels prepared with and without the freeze-thaw (F/T) method. Both show a main peak around 2θ ≈ 20°, characteristic of a predominantly amorphous structure. However, the hydrogel subjected to the freeze-thaw method shows

a slight decrease in the intensity of the main peak, as well as better definition of the secondary peaks. These differences indicate a modification of the internal structure.

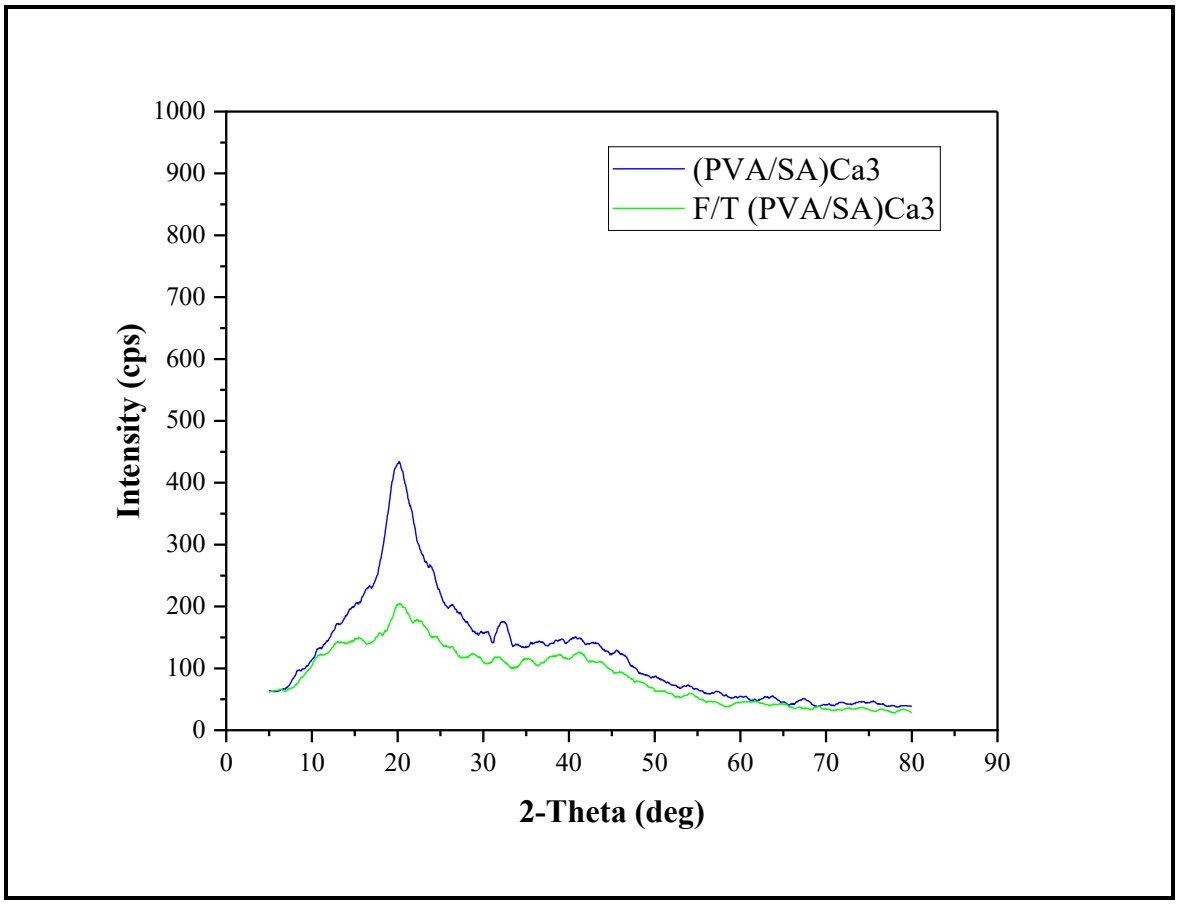

Figure III.2.4.3: Structural characterization of freeze-thawed PVA/Alginate biohydrogel and PVA/Sodium Alginate biohydrogel by X-Ray Diffraction (XRD).

Figure III.2.4.3 shows the XRD diffractograms of $CaCl_2$ crosslinked PVA/Sodium Alginate hydrogels, with and without application of the freeze-thaw method. The (PVA/SA)Ca3 hydrogel shows a broad peak centered around $2\theta \approx 19°$, typical of a predominantly amorphous structure with some ordered areas. After application of the freeze-thaw method, the profile of F/T (PVA/SA)Ca3 reveals a notable decrease in the intensity of the main peak, suggesting a possible reduction in crystallinity. This change indicates that freeze-thaw cycles modify the internal organization of the network, which could influence the final properties of the hydrogel.

III.2.5 Calibration curve of ascorbic acid at different pH

Figures III.2.5.1 to III.2.5.3 illustrate the UV-Vis analysis of ascorbic acid carried out at three different pH levels (3, 7 and 9) respectively, with the aim of establishing the

corresponding calibration curves and observing the impact of pH on its absorption behavior.

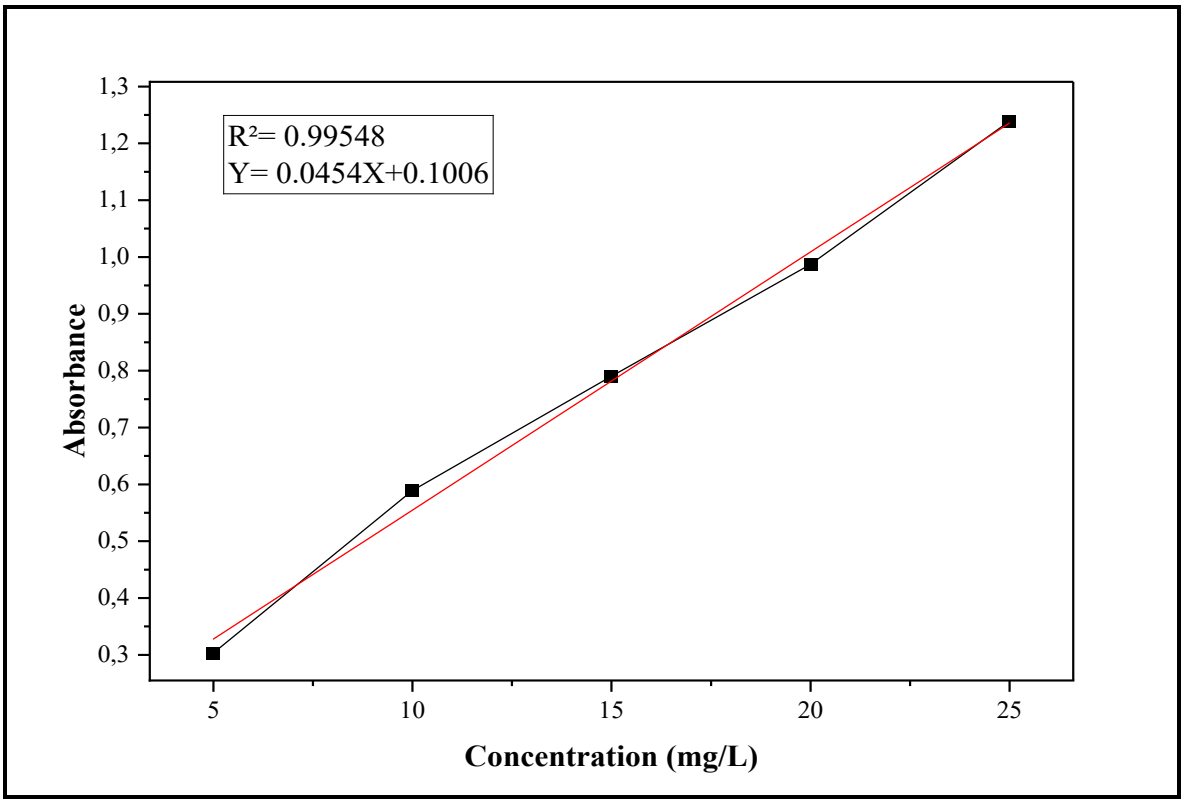

Figure III.2.5.1: Calibration curve of Ascorbic acid at pH 3 at 25°C.

Figure III.2.5.1 shows the calibration curve for ascorbic acid obtained by UV-Vis spectrophotometry at pH 3 and 25°C. Absorbance increases linearly with concentration, according to the equation $Y = 0.0454\,X + 0.1006$, with a coefficient of determination $R^2 = 0.99548$. This strong correlation confirms the reliability of the method in this concentration range. The slope of the line (0.0454) reflects the sensitivity of the measurement under these conditions.

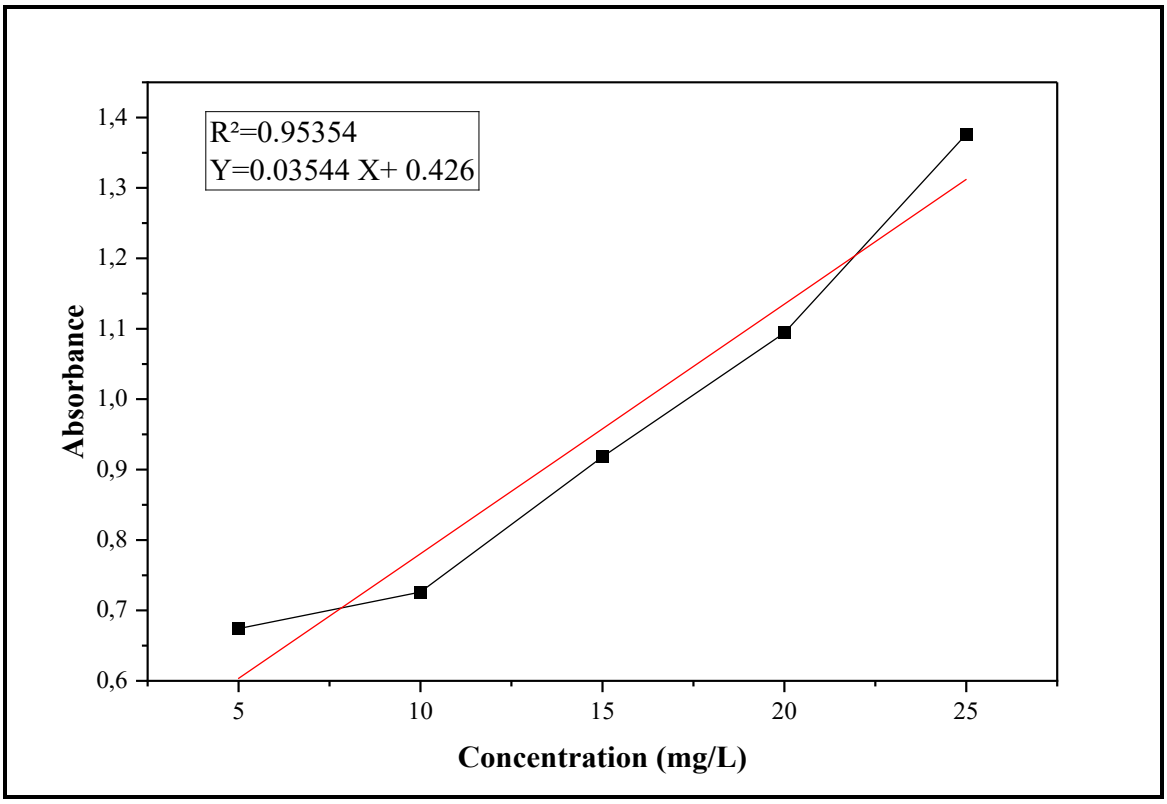

Figure III.2.5.2: Calibration curve of Ascorbic acid at pH 7 at 25°C.

Figure III.2.5.2 shows the calibration curve for ascorbic acid by UV-Vis spectrophotometry at pH 7 and 25°C. Absorbance varies linearly with concentration, according to the equation $Y = 0.03544\,X + 0.426$, with a coefficient of determination $R^2 = 0.95354$. This good correlation confirms the reliability of the method at this pH. The slope of the line (0.03544) reflects a sensitivity slightly lower than that observed at pH 3.

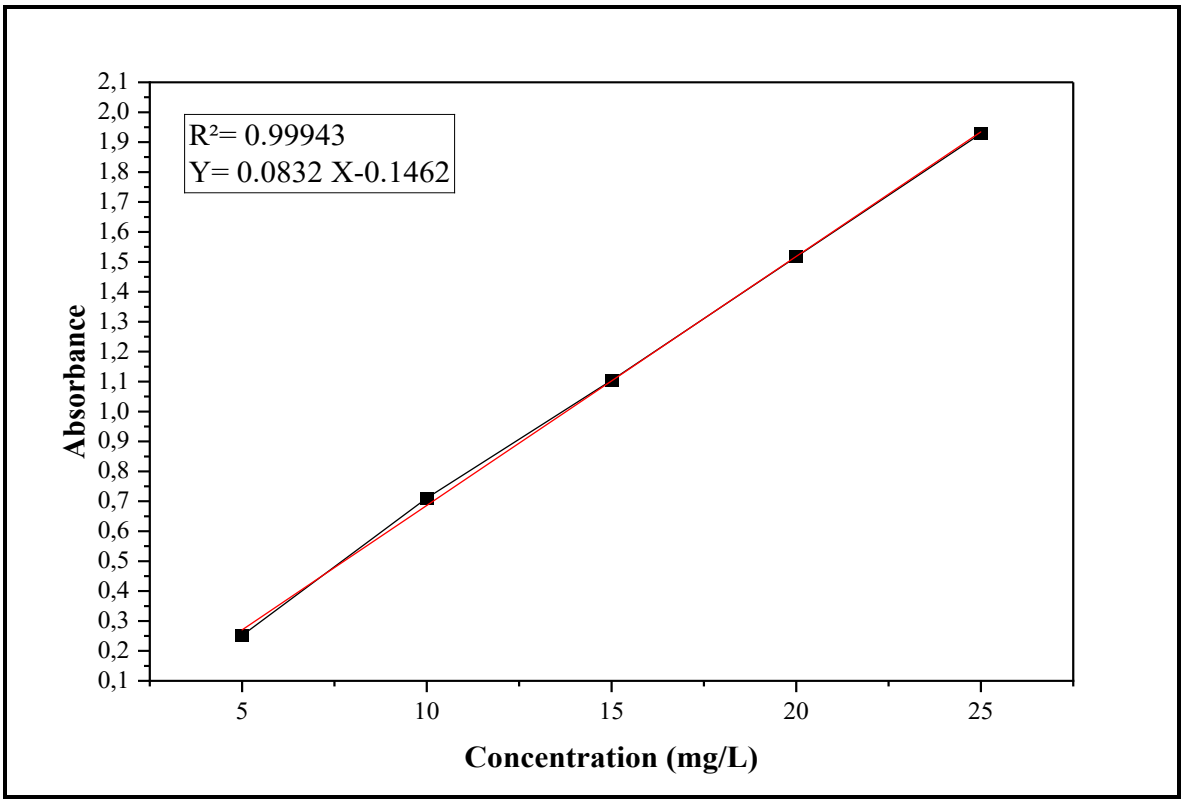

Figure III.2.5.3: Calibration curve of Ascorbic acid at pH 9 at 25°C.

Figure III.2.5.3 shows the calibration curve for ascorbic acid obtained by UV-Vis spectrophotometry at pH 9 and 25°C. The relationship between absorbance and concentration is modeled by the equation $Y = 0.0832\,X - 0.1462$, the coefficient of determination ($R^2 = 0.99943$) reveals a less marked linear correlation than that observed at pH 3 and 7, reflecting a greater dispersion of experimental points. The slope of the line (0.0832) indicates a slightly higher sensitivity, although the precision of the method is reduced at this pH.

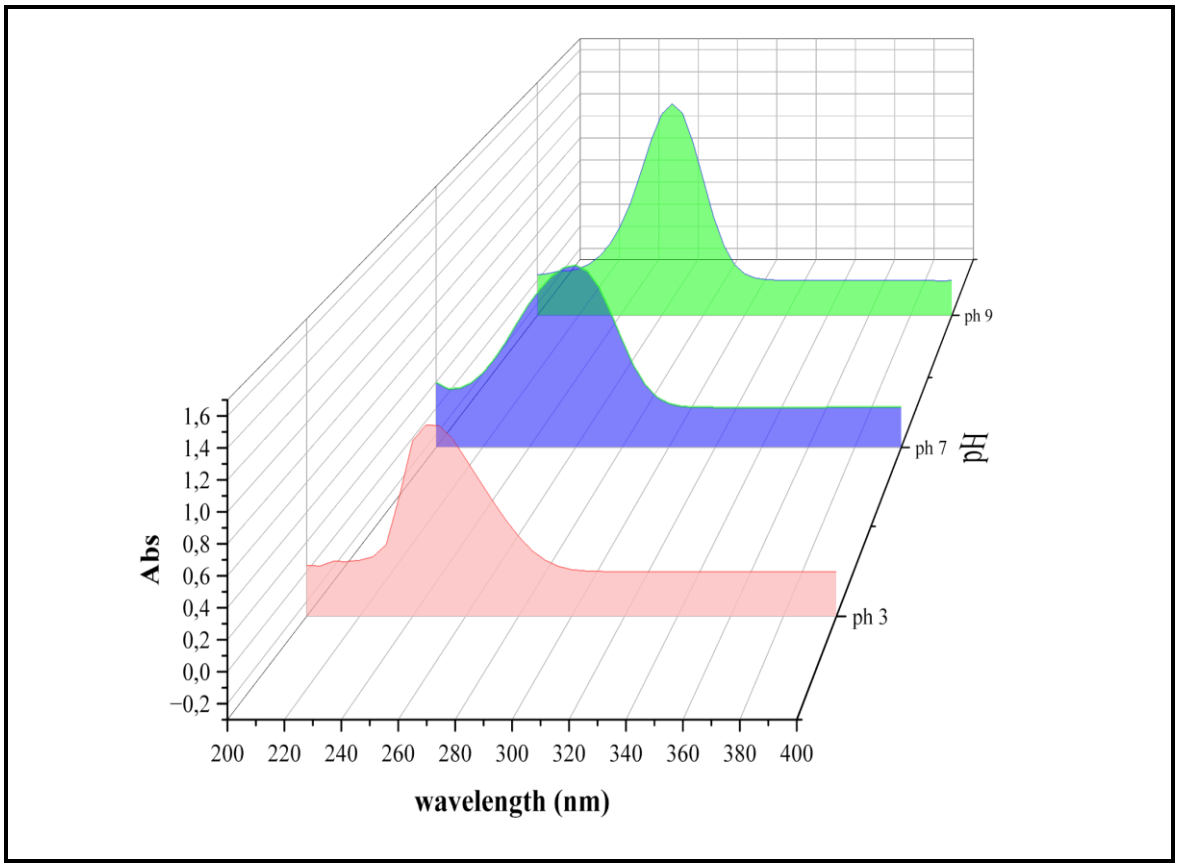

Figure III.2.5.4: UV-Vis Calibration curve of ascorbic acid (15mg/L) at pH 3, 7 and 9 at 25°C.

Figure III.2.5.4 shows the influence of pH on the UV-Vis spectrum of ascorbic acid (15 mg/L, 25°C). At pH 3, the spectrum shows an absorbance maximum (λmax) at 245 nm with moderate intensity (absorbance = 0.987), reflecting the predominance of the protonated form. At pH 7, a slight increase in λmax at 260 nm is observed, accompanied by a higher absorbance (1.094), indicating the onset of deprotonation. Finally, at pH 9, λmax reaches 265 nm with a maximum absorbance of 1.516, indicating more marked deprotonation and a change in the electronic structure of the molecule. This progressive bathochromic shift in λmax, together with the intensification of absorbance, reflects greater conjugation resulting from the ionization of functional groups. These results confirm that ascorbic acid is a highly pH-sensitive molecule, a major asset for drug delivery applications, particularly in targeted delivery systems where the stimulus is pH.

Part 3: Application of bio hydrogels

Following the swelling tests and physicochemical characterizations, two biohydrogels (PVA/SA)Ca3 and (St/SA)Ca1 were selected for further evaluation of the antioxidant activity

III.3.1 Evaluation of the antioxidant activity

III.3.1.1 Antioxidant Activity of Ascorbic Acid evaluated by the DPPH Radical Scavenging Assay

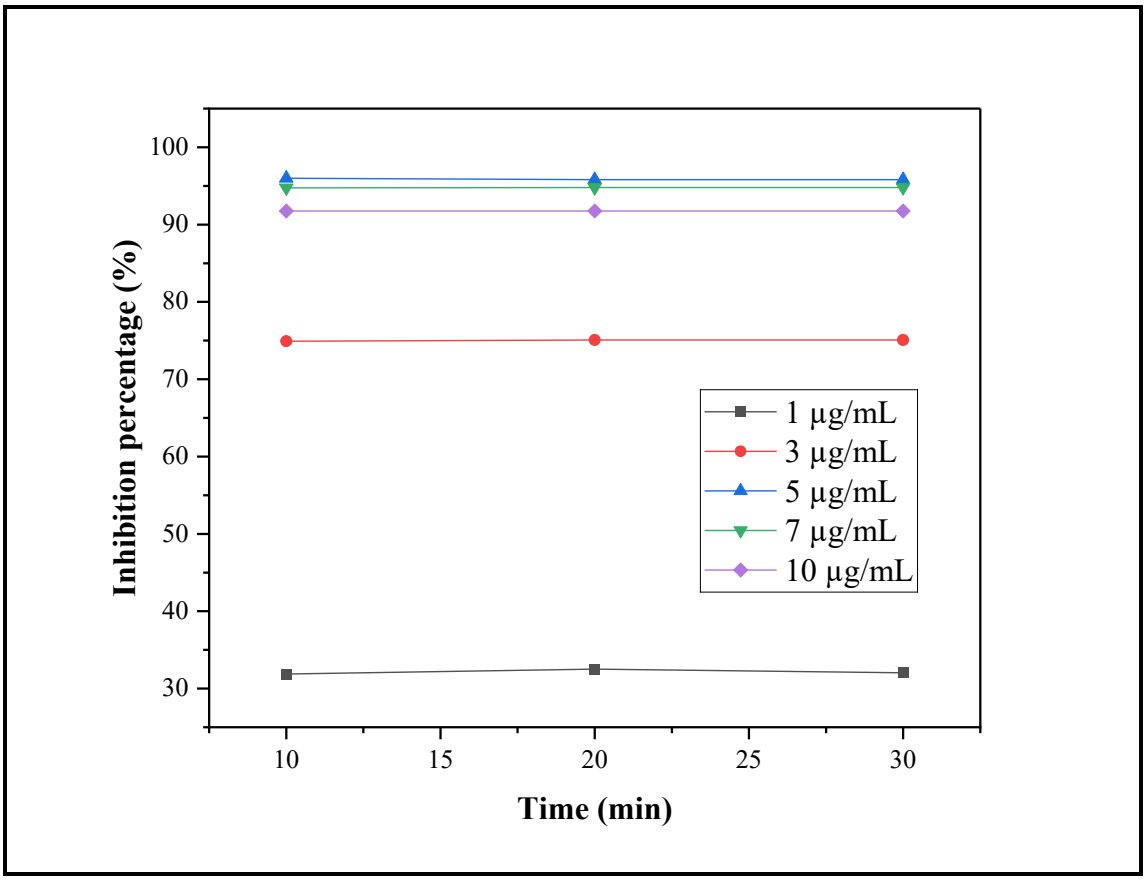

Figure III.3.1.1: Antioxidant Activity of Ascorbic acid evaluated by the DPPH Radical Scavenging Assay.

Figure III.3.1.1 shows the antioxidant activity of ascorbic acid as a function of concentration and time, as assessed by the DPPH radical scavenging assay. Measurements taken at 10, 20, and 30 minutes show a clear positive correlation between ascorbic acid concentration and the percentage of radical inhibition. At low concentrations (1 µg/mL), moderate inhibition of around 32% is observed as early as 10 minutes, while at 3 µg/mL,

inhibition reaches approximately 75%. At higher concentrations (5, 7, and 10 µg/mL), the inhibition exceeds 90%, with rapid stabilization occurring within the first few minutes, indicating fast reaction kinetics and a strong antioxidant response. From the Figure III.3.1.1 the IC_{50} was determined as the concentration of ascorbic acid required to inhibit 50% of the DPPH radicals. This parameter is commonly used to evaluate antioxidant effectiveness: the lower the IC_{50}, the higher the antioxidant activity. In this study, the IC_{50} was found to be 1.8 µg/mL, confirming the high radical scavenging capacity of ascorbic acid. In addition to its potency, ascorbic acid demonstrated rapid antioxidant kinetics. Most of the radical scavenging activity occurred within the first 10 minutes, especially at higher concentrations, after which the inhibition percentage reached a plateau. This fast reaction suggests that ascorbic acid interacts promptly with DPPH radicals, a characteristic that is particularly desirable in biomedical applications where immediate antioxidant action is needed.

III.3.1.2 Antioxidant Activity of (PVA/SA)Ca3 hydrogel evaluated by the DPPH Radical Scavenging Assay

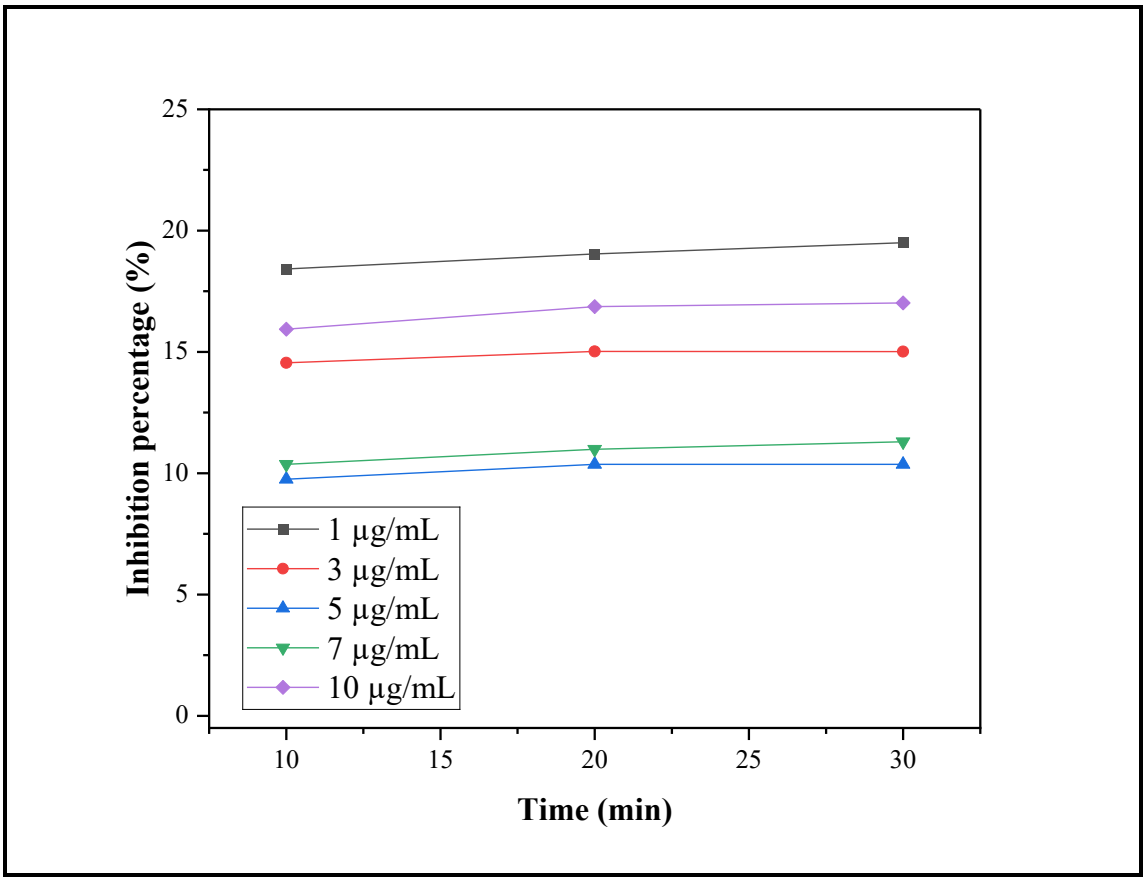

Figure III.3.1.2: Antioxidant Activity of (PVA/SA)Ca3 biohydrogel evaluated by the DPPH Radical Scavenging Assay.

Figure III.3.1.2 illustrates the antioxidant activity of the (PVA/SA)Ca3 hydrogel, as assessed by the DPPH radical scavenging assay at concentrations ranging from 1 to 10 µg/mL over a 30-minute period. The Figure reveals a modest capacity of the hydrogel to scavenge DPPH radicals, with the percentage of inhibition ranging from approximately 10% to 20% across the tested conditions. Notably, the lowest concentration (1 µg/mL) exhibits an inhibition increasing from around 18.4% to 19.5%, while the highest concentration (10 µg/mL) shows an increase from about 15.9% to 17.0%. Interestingly, the intermediate concentrations do not consistently follow a direct dose-response relationship across all time points. The relatively minor increase in inhibition over the 30-minute duration for each concentration suggests a gradual interaction between the (PVA/SA)Ca3 hydrogel and the DPPH radical. Overall, the (PVA/SA)Ca3 hydrogel demonstrates a weak to moderate antioxidant activity under these experimental conditions, with a limited dependence on concentration within the tested range. Due to its very low radical scavenging capacity, it was not possible to determine the IC_{50} value for the (PVA/SA)Ca3 hydrogel, as it failed to reach 50% inhibition at any of the tested concentrations

III.3.1.3 Antioxidant Activity of (St/SA)Ca1 hydrogel evaluated by the DPPH Radical Scavenging Assay

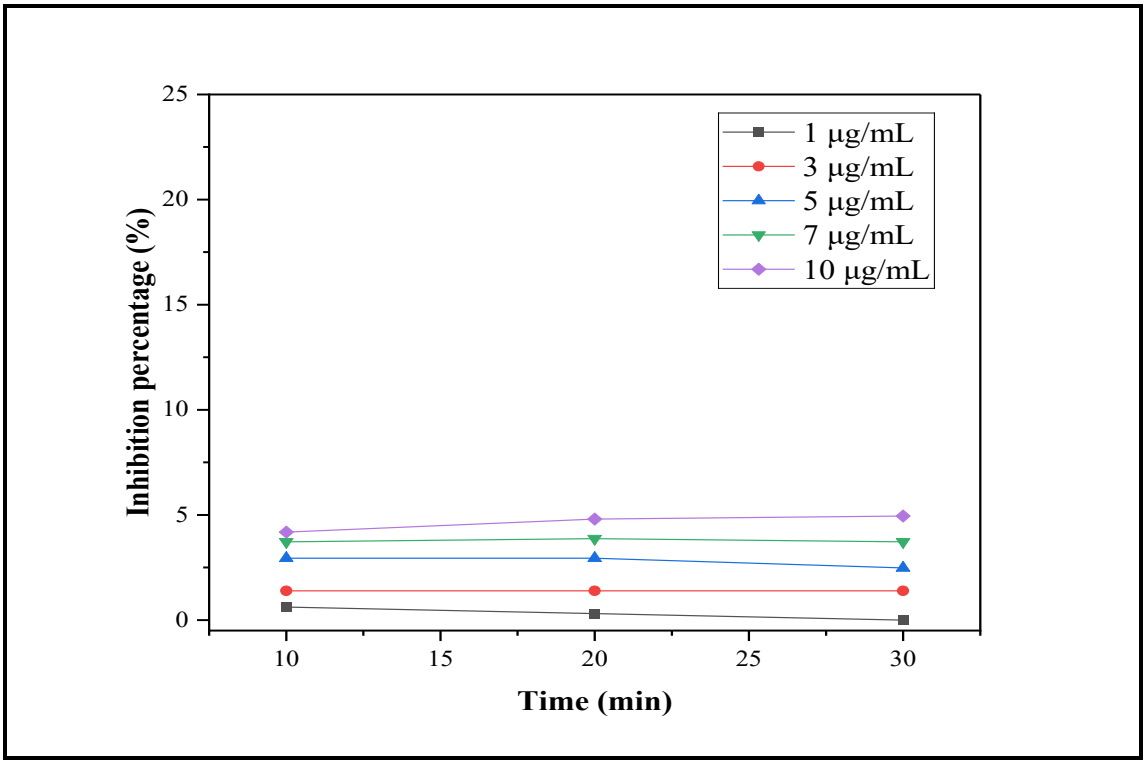

Figure III.3.1.3: Antioxidant Activity of (St/SA)Ca1 biohydrogel evaluated by the DPPH Radical Scavenging Assay.

Figure III.3.1.3 presents the antioxidant activity of the (St/SA)Ca1 hydrogel, evaluated by the DPPH radical scavenging assay at concentrations ranging from 1 to 10 µg/mL over 30 minutes. The Figure reveals a very limited capacity of the hydrogel to scavenge DPPH radicals, with the percentage of inhibition remaining below 5% across all tested conditions. Specifically, at 1 µg/mL, the inhibition is near zero, and even at the highest concentration of 10 µg/mL, the inhibition only reaches approximately 5% at 30 minutes. Furthermore, the inhibition percentages show minimal variation over the 30-minute period for each concentration, suggesting a slow interaction between the hydrogel and the DPPH radical. This profile indicates that the (St/SA)Ca1 hydrogel, within the tested concentration range, exhibits a negligible antioxidant activity as assessed by the DPPH assay, contrasting sharply with the activity observed for known antioxidants like ascorbic acid. Due to this very low radical scavenging capacity, it was not possible to determine the IC_{50} value for the (St/SA)Ca1 hydrogel, as it failed to reach 50% inhibition at any of the tested concentrations.

III.3.2.1 In vitro release

III.3.2.1.1 Loaded hydrogels release

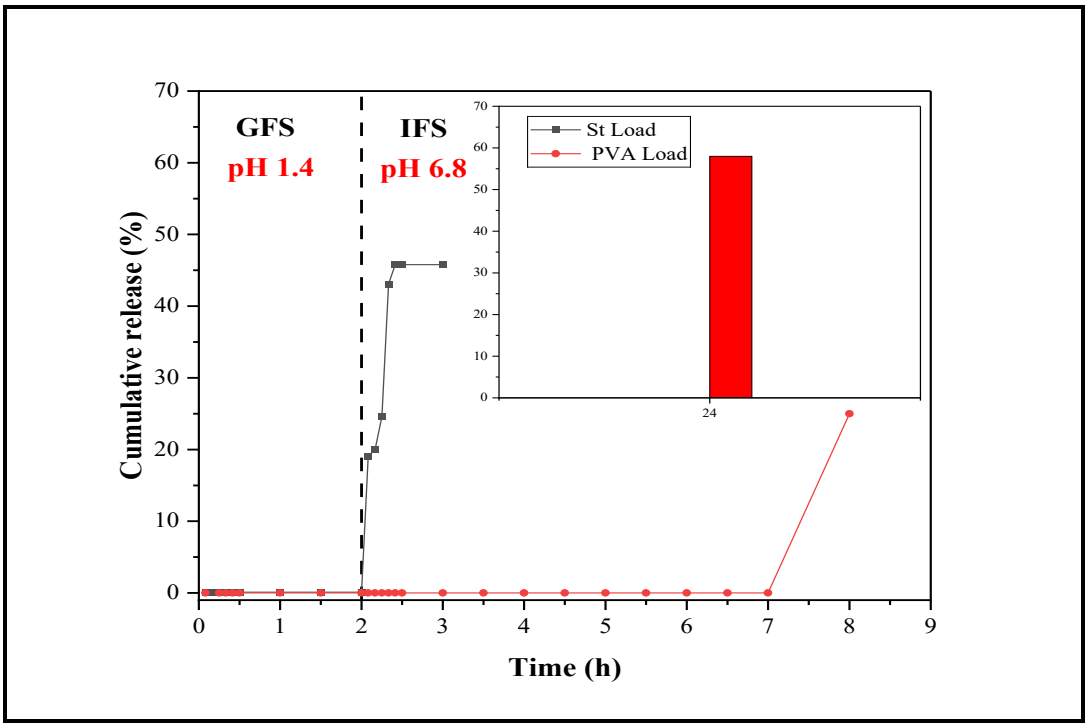

Figure III.3.2.1.1: Cumulative VC Release from the Loaded biohydrogels in GFS and IFS as a function of time at a temperature of 37°C.

The loading efficiency of vitamin C (VC) within hydrogels was investigated, revealing distinct loading capacities. The PVA Load hydrogel achieved a loading efficiency (LE) of 87.23%, significantly surpassing the 55.92% LE observed for the starch St Load hydrogel. This enhanced loading capacity is primarily attributed to the highly interconnected three-dimensional polymeric network inherent to these hydrogels, which facilitates efficient VC loading. Furthermore, the formation of intramolecular hydrogen bonds between the functional groups of the hydrogel and VC molecules plays a crucial role in VC retention, thereby augmenting the overall loading efficiency.

In vitro release was assessed by sequentially immersing the VC-loaded hydrogels in simulated gastric fluid (GFS pH 1.4) for the initial 2 hours, followed by transfer to simulated intestinal fluid (IFS pH 6.8) for an additional 22 hours, with the results presented in Figure III.3.2.1. The resultant release profiles demonstrated sustained and pH-responsive behavior. Notably, no significant release of VC was detected during the GFS exposure, indicating the stability of the hydrogels under acidic conditions.

Conversely, a pronounced increase in VC release was observed upon transition to the IFS environment. Specifically, the St Load hydrogel exhibited a rapid release of 45.79% of its encapsulated VC within the first hour in IFS. In contrast, the PVA Load hydrogel demonstrated a more gradual release, culminating in a maximum cumulative release of 57.98% after 22 hours in IFS.

These findings underscore the promise of VC-loaded hydrogels as viable oral drug delivery systems. Their capacity for controlled and site-specific release mechanisms holds potential for minimizing gastrointestinal adverse effects and optimizing therapeutic outcomes.

III.3.2.1.2 Encapsulated VC release

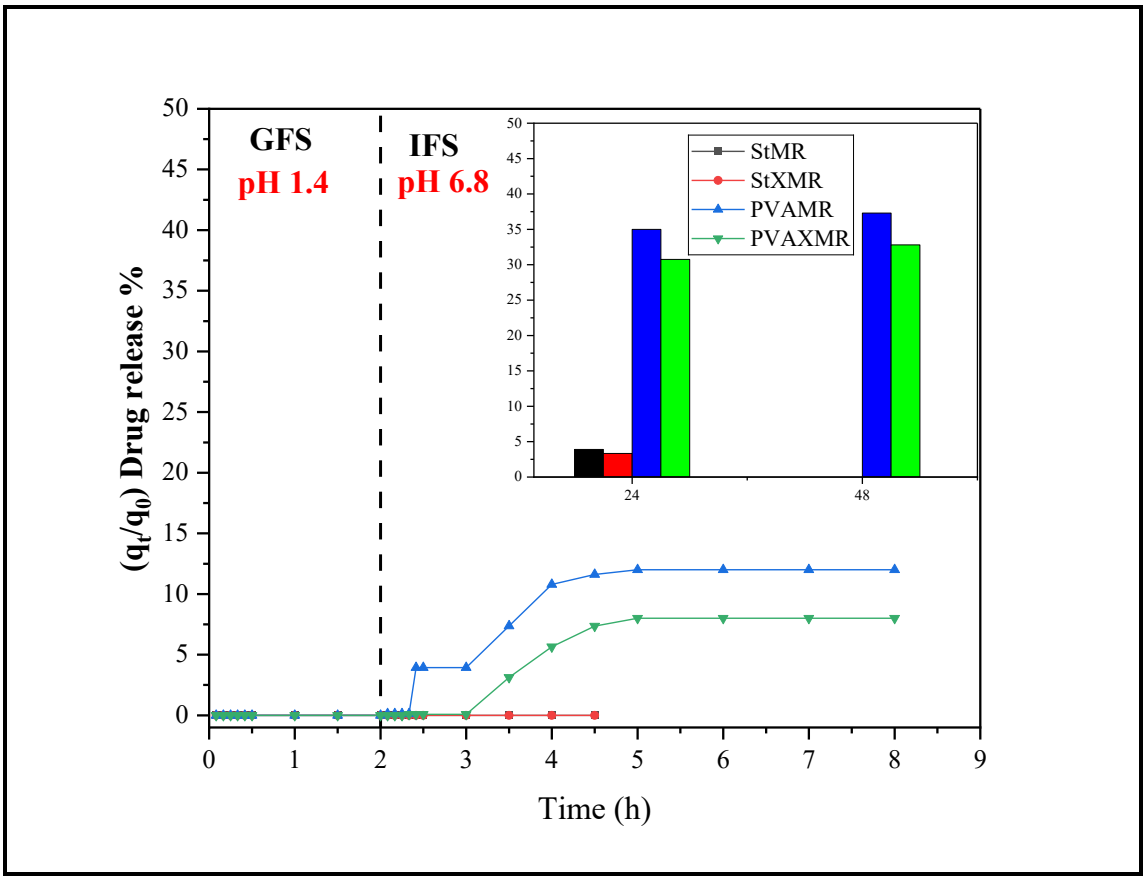

Figure III.3.2.1.2: The Release of encapsulated VC from the biohydrogels in GFS and IFS as a function of time at a temperature of 37°C.

The percentage of drug released, defined as the rate of the amount of drug released at time t q_t to the initially encapsulated drug quantity q_0, was evaluated as a function of time under simulated physiological conditions. The release study was conducted in two

sequential phases to mimic the gastrointestinal environment. During the initial 2 hour period, the hydrogels were exposed to Simulated Gastric Fluid (GFS) at pH 1.4, where no drug release (0%) was observed for all formulations of our hydrogels, indicating effective protection of the drug within the acidic gastric milieu.

Subsequently, from 2 hours onward, the medium was switched to Simulated Intestinal Fluid (IFS) at pH 6.8, replicating the intestinal environment. Under these conditions, the hydrogels PVAMR and PVAXMR exhibited drug release, with PVAMR demonstrating a more rapid release profile, achieving approximately 12% cumulative release by 5 hours, after which the release plateaued. In contrast, PVAXMR showed a slower release rate, reaching about 8% at the same time point. Conversely, the StMR and StXMR hydrogels did not exhibit any appreciable drug release in SIF, maintaining negligible release levels.

Extended-release profiles reveal that at 24 and 48 hours, PVAMR and PVAXMR hydrogels attained significantly higher cumulative drug release, ranging from 34.99% to 37.3% for PVAMR and 30.76% to 32.81% for PVAXMR, respectively. Meanwhile, StMR and StXMR maintained minimal drug release below 5% throughout the extended period. These findings collectively suggest that PVAMR and PVAXMR hydrogels are optimized for delayed and sustained drug release, predominantly occurring in the intestinal environment over prolonged durations.

References

[1] B. M. Baraker et B. Lobo, « Spectroscopic analysis of $CdCl_2$ doped PVA–PVP blend films », *Can. J. Phys.*, vol. 95, n° 8, p. 738-747, 2017, doi: 10.1139/cjp-2016-0848.

[2] Huisuo Huang, Ingolf U. Grün, Mark Ellersieck, et Andrew D. Clarke, « Measurement of Total Sodium Alginate in Restructured Fish Products Using Fourier Transform Infrared Spectroscopy », *EC Nutr.*, vol. 11, n° 1, p. 33-45, 2017.

[3] Odiongenyi, A.O., Essien, N.B., et Ukpe, R.A., « Corn Starch as a Substitute for Commercial Food Starch: FT-IR and Rheological Characterization », *J. Sci. Eng. Res.*, vol. 3, n° 6, p. 494-501.

CONCLUSION

General Conclusion

This study focused on the development and characterization of advanced bio-sourced hydrogels based on poly(vinyl alcohol) (PVA), starch (St) and sodium alginate (SA), cross-linked with calcium chloride ($CaCl_2$), for use as controlled oral delivery systems for pH-sensitive active ingredients, such as Vitamin C (ascorbic acid). Two preparation methods were explored: the conventional method and the freeze-thaw cycle technique.

FTIR, XRD and XRF analysis confirmed the formation of stable cross-linked polymeric networks. The swelling study revealed a significant influence of pH, $CaCl_2$ concentration and synthesis method on hydrogel properties. Hydrogels containing 3% $CaCl_2$ showed increased structural stability and swelling in neutral and basic media. On the other hand, starch-based hydrogels obtained by freeze-thawing exhibited higher swelling in acidic media, probably due to a more porous internal structure.

Functionally, unfilled formulations such as (PVA/SA)Ca3 and (St/SA)Ca1 showed negligible antioxidant activity, prompting the incorporation of Vitamin C. The latter demonstrated excellent antioxidant activity with an IC_{50} of 1.8 µg/mL, and rapid scavenging kinetics, completely achieved in 10 minutes a particularly desirable behavior in a biomedical context.

Two strategies for incorporating Vitamin C were implemented:

The post-synthesis loading method, applied to both St Load and PVA Load formulations, achieved a remarkable loading efficiency for PVA Load (87.23%), compared with 55.92% for St Load.

The direct encapsulation method, involving the introduction of Vitamin C prior to cross-linking, was used for StMR, StXMR, PVAMR and PVAXMR formulations.

In vitro release studies, conducted in gastric medium (pH 1.4) followed by passage through intestinal medium (pH 6.8), revealed a delayed and selective release, highly dependent on formulation.

PVA Load and St Load hydrogels showed no release in the gastric environment. In the small intestine, St Load showed rapid release, while PVA Load showed progressive and sustained release (up to 57.98% at 22 h).

Concerning encapsulated formulations, PVAXMR, prepared without reflux assembly to preserve the thermal stability of Vitamin C, showed a slow and prolonged release in intestinal medium (32.81% at 48 h), with no gastric release.

PVAMR also showed good intestinal release (up to 37.3%), while StMR and StXMR showed very low intestinal releases (below 5%), indicating a need for optimization.

Although the encapsulation efficiency of PVAXMR has not been measured directly, its targeted intestinal release behavior is a promising result.

Complementing the main methods, the PVAXMR and StXMR formulations, developed without reflux assembly, were designed to avoid thermal degradation of Vitamin C. Although introduced in a second experimental phase, these formulations reflect a proactive approach to comparing and optimizing preparation conditions. The PVAXMR formulation, in particular, stands out for its targeted intestinal release behavior, without gastric salting-out, and represents a relevant advance for oral delivery systems of heat-sensitive molecules.

In summary, this study has enabled the development of several effective bio-sourced hydrogels for the controlled oral delivery of Vitamin C. The PVAXMR system appears to be an ideal candidate for prolonged, targeted intestinal release, while PVA Load combines high loading efficiency with sustained intestinal release. These results pave the way for promising biomedical applications in the field of pH-sensitive delivery systems.

These results pave the way for several research perspectives:

- In vivo studies to confirm the biocompatibility, biodegradability and therapeutic efficacy of the formulations developed.
- Optimization of starch-based systems, in particular to improve their encapsulation capacity and intestinal release profile.
- Extending these platforms to other active ingredients sensitive to pH or oxidation, with a view to a variety of biomedical applications.

ANNEXES

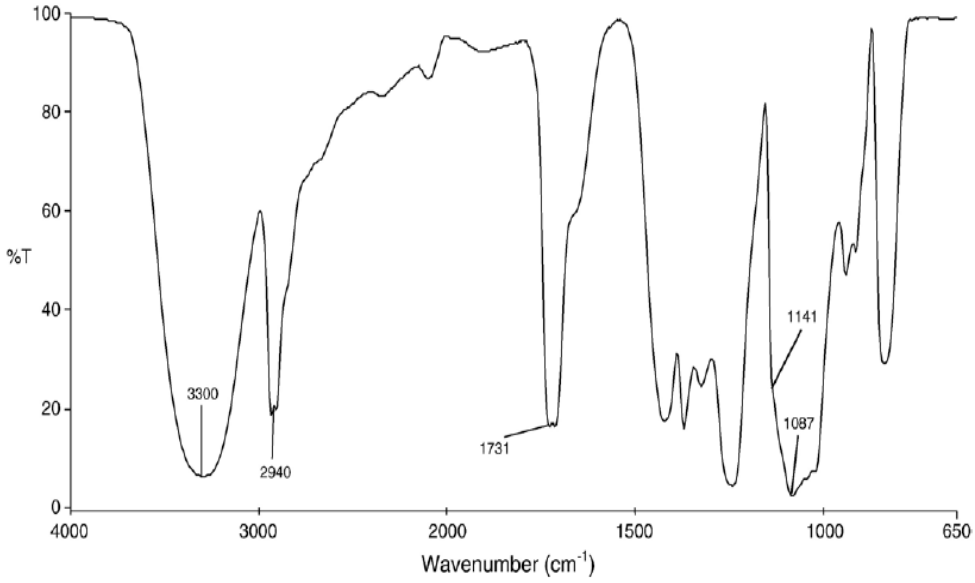

Annex 1: FTIR Spectra of PVA (PVA 87-89 % hydrolyzed)

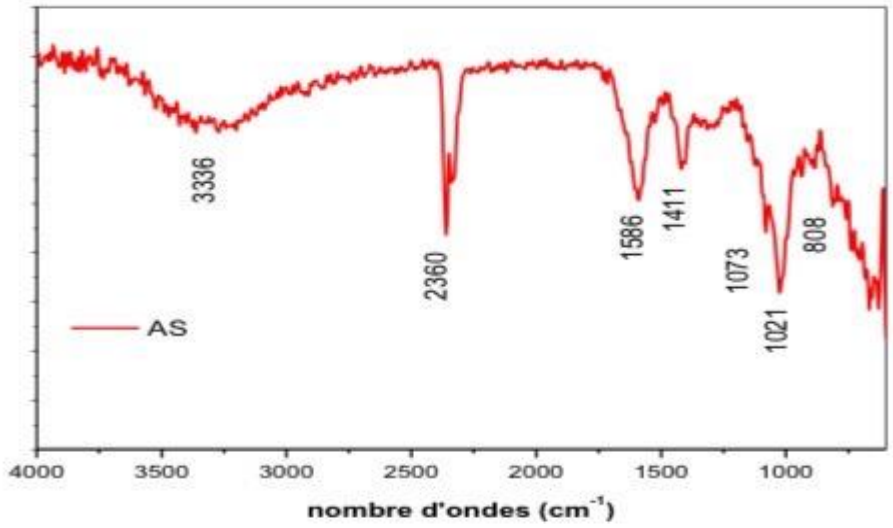

Annex 2: FTIR Spectra of Sodium Alginate

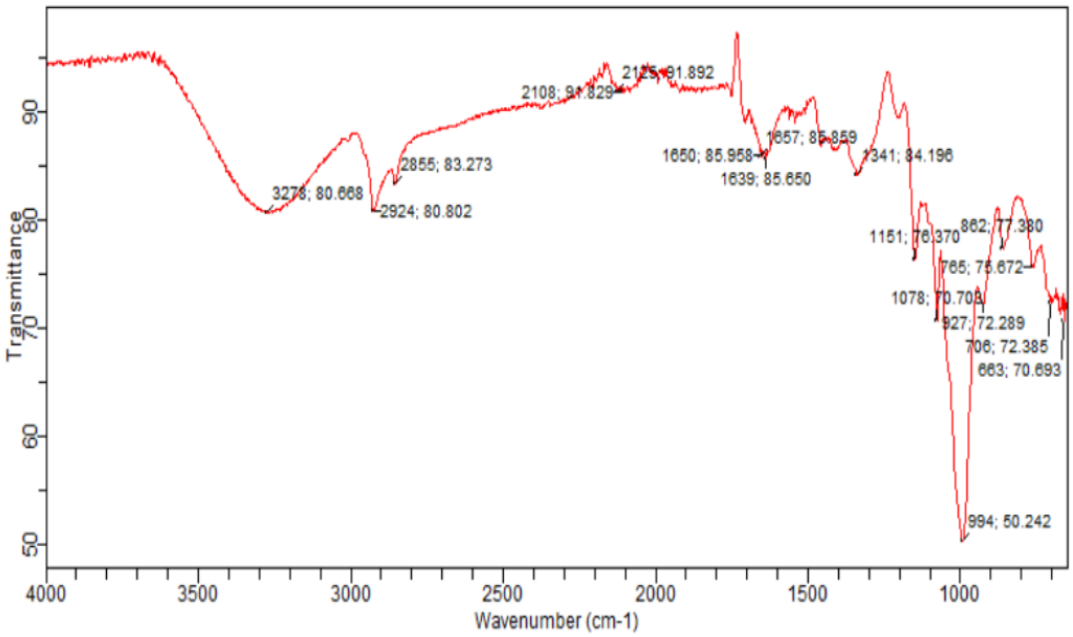

Annex 3: FTIR Spectra of Starch

ملخص:

تكمن أهمية هذه الدراسة في تطوير البولي فينيل الكحول/ألجينات الصوديوم (PVA/SA) والنشا/ألجينات الصوديوم (St/SA) الهلاميات المائية الحيوية المرتبطة بأيونات الكالسيوم (Ca^{2+})، للتطبيقات المحتملة. تم تحضير الهلاميات المائية بطريقتين: طريقة تقليدية بتركيزين من 1% $CaCl_2$ و3%)، وطريقة دورة التجميد/الذوبان المطبقة فقط باستخدام 3٪ $CaCl_2$. تم قياس نسبة التورم لتقييم القدرة على امتصاص الماء، وتم اختبار النشاط المضاد للأكسدة لاثنين من الهلاميات المائية المختارة - (PVA/SA)Ca3 و(St/SA)Ca1 - باستخدام اختبار DPPH، مع استخدام حمض الأسكوربيك كمرجع. لم تظهر النتائج أي نشاط كبير مضاد للأكسدة لأي منهما. ثم تم استكشاف استخدام هذه الهلاميات المائية كنظم لتوصيل فيتامين C باستخدام طريقتين: التحميل المباشر والتغليف. تم تنفيذ التغليف باستخدام بروتوكولين، مع الارتجاع وبدونه. أظهرت النتائج أن بنية الهلام وطريقة تحضيره تؤثر بشدة على قدرة التحميل وسلوك الإطلاق، مما يسلط الضوء على إمكانات هذه الهلاميات المائية الحيوية كنظم إطلاق محكومة.

Abstract :

The importance of this study lies in the development of biohydrogels based on polyvinyl alcohol/sodium alginate (PVA/SA) and starch/sodium alginate (St/SA), crosslinked using calcium ions (Ca^{2+}), for potential applications. The hydrogels were prepared using two synthesis methods: a conventional method with two $CaCl_2$ concentrations (1% and 3%), and a freeze–thaw method applied only with 3% $CaCl_2$. The swelling rate was measured to evaluate water absorption capacity, and the antioxidant activity of two selected biohydrogels((PVA/SA)Ca3 and (St/SA)Ca1)was tested using the DPPH assay, with ascorbic acid as a reference. The results showed no significant antioxidant activity for either. Their use as vitamin C delivery systems was then explored using two approaches: direct loading and encapsulation. Encapsulation was performed using two protocols, with and without reflux. The results showed that the hydrogel structure and preparation method strongly influence loading capacity and release behavior, highlighting the potential of these biohydrogels for controlled release applications.

Résumé :

L’importance de cette étude réside dans le développement de biohydrogels à base de polyalcool vinylique/alginate de sodium (PVA/SA) et d’amidon/alginate de sodium (St/SA), réticulés par des ions calcium (Ca^{2+}), pour des applications potentielles. Les hydrogels ont été préparés selon deux méthodes : une méthode conventionnelle avec deux concentrations de $CaCl_2$ (1% et 3%), et une méthode par cycles de congélation/décongélation appliquée uniquement avec 3% de $CaCl_2$. Le taux de gonflement a été mesuré pour évaluer la capacité d’absorption d’eau, et l’activité antioxydante de deux hydrogels sélectionnés (PVA/SA)Ca3 et (St/SA)Ca1 a été testée à l’aide du test DPPH, avec l’acide ascorbique comme référence. Les résultats n’ont montré aucune activité antioxydante significative pour les deux. L’utilisation de ces hydrogels comme systèmes de libération de la vitamine C a ensuite été explorée à travers deux approches: le chargement direct et l’encapsulation. L’encapsulation a été réalisée selon deux protocoles, avec et sans reflux. Les résultats ont montré que la structure du gel et la méthode de préparation influencent fortement la capacité de chargement et le comportement de libération, soulignant le potentiel de ces biohydrogels en tant que systèmes de libération contrôlée.